6

Energy and Exergy Analyses of Thermal Energy Storage Systems

6.1 Introduction

Thermal energy storage (TES) systems for heating or cooling capacity are often utilized in applications where the occurrence of a demand for energy and that of the economically most favorable supply of energy are not coincident. Thermal storages are an essential element of many energy conservation programs – in industry, commercial building, and solar energy utilization. Numerous reports on TES applications and studies have been published (Hahne, 1986; Kleinbach *et al*., 1993; Dincer *et al*., 1997a, 1997b; Dincer, 1999; Beckman and Gilli, 1984; Bejan, 1982, 1995; Jansen and Sorensen, 1984).

Many types of TES systems exist for storing either heating or cooling capacity. The storage medium often remains in a single phase during the storing cycle (so that only sensible heat is stored), but sometimes undergoes phase change (so that some of the energy is stored as latent heat). Sensible TES systems (e.g., liquid water systems) exhibit changes in temperature in the store as heat is added or removed (Ismail and Stuginsky, 1999; Ismail *et al*., 1997). In latent TES systems (e.g., liquid water/ice systems and eutectic salt systems), the storage temperature remains fixed during the phase-change portion of the storage cycle (Adebiyi *et al*., 1996; Laouadi and Lacroix, 1999; Brousseau and Lacroix, 1999; Costa *et al*., 1998). The storage medium can be located in storage "containers" of various types and sizes, including storage tanks, ponds, caverns, and underground aquifers.

Many researchers have investigated methodologies for TES evaluation and comparison (Rosen, 1991, 1992b, 1999b; Rosen and Dincer, 1999a), and concluded that, while many technically and economically successful thermal storages are in operation, no generally valid basis for comparing the achieved performance of one storage with that of another operating under different conditions has found broad acceptance. The energy efficiency of a TES system, the ratio of the energy recovered from storage to that originally input, is conventionally used to measure TES performance. The energy efficiency, however, is an inadequate measure because it does not take into account all the considerations necessary in TES evaluation (e.g., how nearly the performance of the system approaches the ideal, the storage duration, the temperatures of the supplied and recovered thermal energy and of the surroundings).

Exergy analysis is a thermodynamic analysis technique based on the second law of thermodynamics, which provides an alternative and illuminating means of assessing and comparing TES

Thermal Energy Storage: Systems and Applications, *Second Edition* İbrahim Dinçer and Marc A. Rosen
 ISBN: 978-0-470-74706-3

systems rationally and meaningfully. In particular, exergy analysis yields efficiencies that provide a true measure of how nearly actual performance approaches the ideal and identifies more clearly than energy analysis the causes and locations of thermodynamic losses. Consequently, exergy analysis can assist in improving and optimizing TES designs. Increasing application and recognition of the usefulness of exergy methods by those in industry, government, and academia has been observed in recent years (Moran, 1989, 1990; Kotas, 1995; Edgerton, 1982; Ahern, 1980; Morris *et al*., 1988; Dincer and Rosen, 2007). Some researchers have examined exergy-analysis methodologies (Rosen and Horazak, 1995; Rosen, 1999a) and applied them to industrial systems (Rosen and Scott, 1998; Rosen and Horazak, 1995), countries (Rosen and Dincer, 1997b; Rosen, 1992a), environmental impact assessments (Crane *et al*., 1992; Rosen and Dincer, 1997a, 1999b; Gunnewiek and Rosen, 1998), and TES. To date, however, few exergy analyses of TES systems have been performed (Badar *et al*., 1993; Bascetincelik *et al*., 1998; Bejan, 1978, 1982, 1995; Bjurstrom and Carlsson, 1985; Hahne *et al*., 1989; Krane, 1985, 1987; Krane and Krane, 1991; Mathiprakasam and Beeson, 1983; Moran and Keyhani, 1982; Rosenblad, 1985; Taylor, 1986). Exergy analysis is described extensively elsewhere (Gaggioli, 1983; Maloney and Burton, 1980; Moran and Shapiro, 2000; Rosen, 1999a; Kestin, 1980; Dincer and Rosen, 2007), and background material is provided on energy and exergy analyses that is relevant to applications to TES systems in the next section.

The main objectives of this chapter are to describe how energy and exergy analyses of TES systems are performed and to demonstrate the usefulness of such analyses in providing insights into TES behavior and performance. In the presentation, the thermodynamic considerations and challenges involved in the evaluation of TES systems are discussed, and recent advances in addressing these challenges are described in the hope that standardized exergy-based methodologies can evolve for TES evaluation and comparison.

The topics covered in this chapter can be summarized as follows: First, theoretical and practical aspects of energy and exergy analyses are described (Section 6.2) and general thermodynamic considerations in TES evaluation are discussed (Section 6.3). Then, the use of exergy in evaluating a closed TES system is detailed (Section 6.4), with in-depth discussions of two critical evaluation factors: appropriate TES efficiency measures (Section 6.5) and the importance of temperature in performance evaluations for sensible TES systems (Section 6.6). Next, applications of exergy analysis to a wide range of TES systems are considered, including aquifer TES systems (Section 6.7), thermally stratified storage systems (Section 6.8), and cold TES systems (Section 6.9). Finally, uses of exergy analysis in optimization and design activities are illustrated by examining exergy-based optimal discharge periods for closed TES systems (Section 6.10), and a solar pond is also examined (Section 6.11). Many illustrative examples are given in all the above-listed sections.

6.2 Theory: Energy and Exergy Analyses

This section reviews the aspects of thermodynamics that are most relevant to energy and exergy analyses. Fundamental principles and such related issues as reference environment selection, efficiency definition, and material properties acquisition are discussed. These issues were also discussed by others (Moran and Shapiro, 2000; Moran, 1989, 1990; Kotas, 1995; Gaggioli, 1983; Dincer and Rosen, 2007). General implications of exergy analysis results are discussed, and a step-by-step procedure for energy and exergy analyses is given.

A note on terminology is in order here. A relatively standard terminology and nomenclature has evolved for conventional classical thermodynamics. However, at present, there is no generally agreed-upon terminology and nomenclature for exergy analysis. A diversity of symbols and names exist for basic and derived quantities (Kotas *et al*., 1987; Lucca, 1990). For example, exergy is often called available energy, availability, work capability, essergy, and so on; and exergy consumption is often called irreversibility, lost work, dissipated work, dissipation, and so on. The exergy analysis nomenclature used here follows that proposed by Kotas *et al*. (1987) as a standard exergy analysis nomenclature. For the reader unfamiliar with exergy, a glossary of selected exergy terminology is included (see Appendix at the end of this chapter).

6.2.1 Motivation for Energy and Exergy Analyses

Thermodynamics permits the behavior, performance, and efficiency to be described for systems for the conversion of energy from one form to another. Conventional thermodynamic analysis is based primarily on the first law of thermodynamics, which states the principle of conservation of energy. An energy analysis of an energy-conversion system is essentially an accounting of the energies entering and exiting. The exiting energy can be broken down into products and wastes. Efficiencies are often evaluated as ratios of energy quantities and are often used to assess and compare various systems. Conventional thermal storages, for example, are often compared on the basis of their energy efficiencies.

However, energy efficiencies are often misleading in that they do not always provide a measure of how nearly the performance of a system approaches ideality. Further, the thermodynamic losses that occur within a system (i.e., those factors that cause performance to deviate from ideality) are often not accurately identified and assessed with energy analysis. The results of energy analysis can indicate the main inefficiencies to be within the wrong sections of the system and a state of technological efficiency different than what actually exists.

Exergy analysis helps to overcome many of the shortcomings of energy analysis. Exergy analysis is based on the second law of thermodynamics and is useful in identifying the causes, locations, and magnitudes of process inefficiencies. The exergy associated with an energy quantity is a quantitative assessment of its usefulness or quality. Exergy analysis acknowledges that, although energy cannot be created or destroyed, it can be degraded in quality, eventually reaching a state in which it is in complete equilibrium with the surroundings and hence of no further use for performing tasks. This statement is of particular importance to TES systems in that, from a thermodynamic perspective, one would wish to recover as much thermal energy as is reasonably possible after the input energy is stored, with little or no degradation of temperature toward the environmental state.

For TES systems, exergy analysis allows one to determine the maximum potential associated with the incoming thermal energy. This maximum is retained and recovered only if the thermal energy undergoes processes in a reversible manner. No further useful thermal energy or exergy can be extracted by allowing a system and its environment to interact if they are in equilibrium. Losses in the potential for exergy recovery occur in the real world because actual processes are always irreversible.

The exergy flow rate of a flowing commodity is the maximum rate at which work may be obtained from it as it passes reversibly to the environmental state, exchanging heat and materials only with the surroundings. In essence, exergy analysis states the theoretical limitations imposed upon a TES system, clearly pointing out that no real system can conserve thermal exergy and that only a portion of the input thermal exergy can be recovered. Also, exergy analysis quantitatively specifies practical TES limitations by providing losses in a form in which they are a direct measure of lost thermal exergy.

6.2.2 Conceptual Balance Equations for Mass, Energy, and Entropy

A general balance for a quantity in a system may be written as

$$\text{Input} + \text{Generation} - \text{Output} - \text{Consumption} = \text{Accumulation} \tag{6.1}$$

Input and output refer respectively to quantities entering and exiting through system boundaries. Generation and consumption refer respectively to quantities produced and consumed within the system. Accumulation refers to build-up (either positive or negative) of the quantity within the system.

Versions of the general balance equation above may be written for mass, energy, entropy, and exergy. Mass and energy, being subject to conservation laws (neglecting nuclear reactions), can be

neither generated nor consumed. Consequently, the general balance (Equation 6.1) written for each of these quantities becomes

$$\text{Mass input} - \text{Mass output} = \text{Mass accumulation} \tag{6.2}$$

$$\text{Energy input} - \text{Energy output} = \text{Energy accumulation} \tag{6.3}$$

Before giving the balance equation for exergy, it is useful to examine that for entropy:

$$\text{Entropy input} + \text{Entropy generation} - \text{Entropy output} = \text{Entropy accumulation} \tag{6.4}$$

Entropy is created during a process because of irreversibilities, but cannot be consumed. By combining the conservation law for energy and nonconservation law for entropy, the exergy balance can be obtained as follows:

$$\text{Exergy input} - \text{Exergy output} - \text{Exergy consumption} = \text{Exergy accumulation} \tag{6.5}$$

Exergy is consumed owing to irreversibilities. Exergy consumption is proportional to entropy creation. Equations 6.3 and 6.5 demonstrate an important and main difference between energy and exergy: energy is conserved while exergy, a measure of energy quality or work potential, can be consumed.

These balances describe what is happening in a system between two instants of time. For a complete cyclic process where the initial and final states of the system are identical, the accumulation terms in all the balances are zero.

6.2.3 *Detailed Balance Equations for Mass, Energy, and Entropy*

Two types of systems are normally considered: open (flow) and closed (nonflow). In general, open systems have mass, heat, and work interactions, and closed systems have heat and work interactions. Mass flow "into," heat transfer "into," and work transfer "out of" the system are defined to be positive. Mathematical formulations of the principles of mass and energy conservation and entropy nonconservation can be written for any system, following the general physical interpretations in Equations 6.2–6.4.

Consider a nonsteady flow process in a time interval t_1 to t_2. Balances of mass, energy, and entropy, respectively, can be written for a control volume as

$$\sum_i m_i - \sum_e m_e = m_2 - m_1 \tag{6.2a}$$

$$\sum_i (e + Pv)_i\, m_i - \sum_e (e + Pv)_e m_e + \sum_r (Q_r)_{1,2} - \left(W'\right)_{1,2} = E_2 - E_1 \tag{6.3a}$$

$$\sum_i s_i m_i - \sum_e s_e m_e + \sum_r (Q_r/T_r)_{1,2} + \Pi_{1,2} = S_2 - S_1 \tag{6.4a}$$

Here, m_i and m_e denote respectively the amounts of mass input across port i and exiting across port e; $(Q_r)_{1,2}$ denotes the amount of heat transferred into the control volume across region r on the control surface; $(W')_{1,2}$ denotes the amount of work transferred out of the control volume; $\Pi_{1,2}$ denotes the amount of entropy created in the control volume; m_1, E_1, and S_1 denote respectively the amounts of mass, energy, and entropy in the control volume at time t_1, and m_2, E_2, and S_2 denote respectively the same quantities at time t_2; and e, s, P, T, and v denote specific energy, specific entropy, absolute pressure, absolute temperature, and specific volume, respectively. The total work W' done by a system excludes flow work, and can be written as

$$W' = W + W_x \tag{6.6}$$

where W is the work done by a system owing to change in its volume and W_x is the shaft work done by the system. The term *shaft work* includes all forms of work that can be used to raise a weight (i.e., mechanical work, electrical work, etc.), but excludes work done by a system because of change in its volume. The specific energy e is given by

$$e = u + ke + pe \tag{6.7}$$

where u, ke, and pe denote respectively specific internal, kinetic, and potential (due to conservative force fields) energies. For irreversible processes, $\Pi_{1,2} > 0$, and for reversible processes, $\Pi_{1,2} = 0$.

The left sides of Equations 6.2a, 6.3a, and 6.4a represent the net amounts of mass, energy, and entropy transferred into (and in the case of entropy created within) the control volume, while the right sides represent the amounts of these quantities accumulated within the control volume.

For the mass flow m_j across port j,

$$m_j = \int_{t_1}^{t_2} \left[\int_j (\rho V_n dA)_j \right] dt \tag{6.8}$$

Here, ρ is the density of matter crossing an area element dA on the control surface in time interval t_1 to t_2 and V_n is the velocity component of the matter flow normal to dA. The integration is performed over port j on the control surface. One-dimensional flow (i.e., flow in which the velocity and other intensive properties do not vary with position across the port) is often assumed. Then, the previous equation becomes

$$m_j = \int_{t_1}^{t_2} (\rho V_n A)_j dt \tag{6.8a}$$

It has been assumed that heat transfers occur at discrete regions on the control surface and the temperature across these regions is constant. If the temperature varies across a region of heat transfer,

$$(Q_r)_{1,2} = \int_{t_1}^{t_2} \left[\int_r (q dA)_r \right] dt \tag{6.9}$$

and

$$(Q_r/T_r)_{1,2} = \int_{t_1}^{t_2} \left[\int_r (q/T)_r \, dA_r \right] dt \tag{6.10}$$

where T_r is the temperature at the point on the control surface where the heat flux is q_r. The integral is performed over the surface area of region A_r.

The quantities of mass, energy, and entropy in the control volume (denoted by m, E, and S) on the right sides of Equations 6.2a, 6.3a, and 6.4a, respectively, are given more generally by

$$m = \int \rho dV \tag{6.11}$$

$$E = \int \rho e dV \tag{6.12}$$

$$S = \int \rho s dV \tag{6.13}$$

where the integrals are over the control volume.

For a closed system, $m_i = m_e = 0$ and Equations 6.2a, 6.3a, and 6.4a become

$$0 = m_2 - m_1 \tag{6.2b}$$

$$\sum_r (Q_r)_{1,2} - \left(W'\right)_{1,2} = E_2 - E_1 \tag{6.3b}$$

$$\sum_r (Q_r/T_r)_{1,2} + \Pi_{1,2} = S_2 - S_1 \tag{6.4b}$$

6.2.4 *Basic Quantities for Exergy Analysis*

Several quantities related to the conceptual exergy balance are described here, following the presentations by Moran (1989), Kotas (1995), and Dincer and Rosen (2007).

Exergy of a Closed System

The exergy Ξ of a closed system of mass m, or the nonflow exergy, can be expressed as

$$\Xi = \Xi_{ph} + \Xi_o + \Xi_{kin} + \Xi_{pot} \tag{6.14}$$

where

$$\Xi_{pot} = PE \tag{6.15}$$

$$\Xi_{kin} = KE \tag{6.16}$$

$$\Xi_o = \sum_i (\mu_{io} - \mu_{ioo}) N_i \tag{6.17}$$

$$\Xi_{ph} = (U - U_o) + P_o (V - V_o) - T_o (S - S_o) \tag{6.18}$$

where the system has a temperature T, pressure P, chemical potential μ_i for species i, entropy S, energy E, volume V, and number of moles N_i of species i. The system is within a conceptual environment in an equilibrium state with intensive properties T_o, P_o, and μ_{ioo}. The quantity μ_{io} denotes the value of μ at the environmental state (i.e., at T_o and P_o). The terms on the right side of Equation 6.14 represent respectively physical, chemical, kinetic, and potential components of the nonflow exergy of the system.

The exergy Ξ is a property of the system and conceptual environment combining the extensive properties of the system with the intensive properties of the environment.

Physical nonflow exergy is the maximum work obtainable from a system as it is brought to the environmental state (i.e., to thermal and mechanical equilibrium with the environment), and chemical nonflow exergy is the maximum work obtainable from a system as it is brought from the environmental state to the dead state (i.e., to complete equilibrium with the environment).

Exergy of a Flowing Stream of Matter

The exergy of a flowing stream of matter $\in$ is the sum of nonflow exergy and the exergy associated with the flow work of the stream (with reference to P_o), that is,

$$\in = \Xi + (P - P_o) V \tag{6.19}$$

Alternatively, $\in$ can be expressed following Equation 6.14 in terms of physical, chemical, kinetic, and potential components:

$$\in = \in_{ph} + \in_o + \in_{kin} + \in_{pot} \tag{6.20}$$

where

$$\in_{pot} = PE \tag{6.21}$$

$$\in_{kin} = KE \tag{6.22}$$

$$\in_o = \Xi_o = \sum_i (\mu_{io} - \mu_{ioo}) N_i \tag{6.23}$$

$$\in_{ph} = (H - H_o) - T_o (S - S_o) \tag{6.24}$$

Exergy of Thermal Energy

Consider a control mass, initially at the dead state, being heated or cooled at constant volume in an interaction with some other system. The heat transfer experienced by the control mass is Q. The flow of exergy associated with the heat transfer Q is denoted by X, and can be expressed as

$$X = \int_i^f (1 - T_o/T)\delta Q \tag{6.25}$$

where δQ is an incremental heat transfer, and the integral is from the initial state (i) to the final state (f). This "thermal exergy" is the minimum work required by the combined system of the control mass and the environment in bringing the control mass to the final state from the dead state.

Often, the dimensionless quantity in parentheses in this expression is called the *exergetic temperature factor* and is denoted by τ:

$$\tau = 1 - T_o/T \tag{6.26}$$

The relation between τ and the temperature ratio T/T_o is illustrated in Figure 6.1.

If the temperature T of the control mass is constant, the thermal exergy transfer associated with a heat transfer is

$$X = (1 - T_o/T)\, Q = \tau Q \tag{6.25a}$$

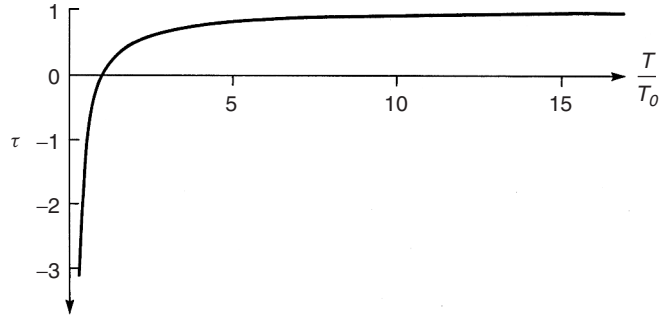

Figure 6.1 The relation between the exergetic temperature factor τ and the absolute temperature ratio T/T_o. The factor τ is equal to zero when $T = T_o$. For heat transfer at above-environment temperatures (i.e., $T > T_o$), $0 < \tau \leq 1$. For heat transfer at subenvironment temperatures (i.e., $T < T_o$), $\tau < 0$, implying that exergy and energy flow in opposite directions in such cases. Note that the magnitude of exergy flow exceeds that of the energy flow when $\tau < -1$, which corresponds to $T < T_o/2$

For heat transfer across a region r on a control surface for which the temperature may vary,

$$X = \int_r \left[q\,(1 - T_o/T)\,dA \right]_r \tag{6.25b}$$

where q_r is the heat flow per unit area at a region on the control surface at which the temperature is T_r.

Exergy of Work and Electricity

Equation 6.6 separates total work W' into two components: W_x and W. The exergy associated with shaft work W_x is by definition W_x. Similarly, the exergy associated with electricity is equal to the energy.

The exergy transfer associated with work done by a system due to volume change is the net usable work due to the volume change, and is denoted by W_{NET}. Thus, for a process in time interval t_1 to t_2,

$$(W_{NET})_{1,2} = W_{1,2} - P_o\,(V_2 - V_1) \tag{6.27}$$

where $W_{1,2}$ is the work done by the system due to volume change $(V_2 - V_1)$. The term $P_o(V_2 - V_1)$ is the displacement work necessary to change the volume against the constant pressure P_o exerted by the environment.

Exergy Consumption

For a process occurring in a system, the difference between the total exergy flows into and out of the system, less the exergy accumulation in the system, is the exergy consumption I, expressible as

$$I = T_o \Pi \tag{6.28}$$

Equation 6.28 points out that exergy consumption is proportional to entropy creation, and is known as the Gouy–Stodola relation.

6.2.5 *Detailed Exergy Balance*

An analogous balance to those given in Equations 6.2a, 6.3a, and 6.4a can be written for exergy, following the physical interpretation of Equation 6.5. For a nonsteady flow process during time interval t_1 to t_2

$$\sum_i \varepsilon_i m_i - \sum_e \varepsilon_e m_e + \sum_r (X_r)_{1,2} - (W_x)_{1,2} - (W_{NET})_{1,2} - I_{1,2} = \Xi_2 - \Xi_1 \tag{6.5a}$$

where $(W_{NET})_{1,2}$ is given by Equation 6.27 and

$$(X_r)_{1,2} = \int_{t_1}^{t_2} \left[\int_r (1 - T_o/T_r)\, q_r\, dA_r \right] dt \tag{6.29}$$

$$I_{1,2} = T_o \Pi_{1,2} \tag{6.30}$$

$$\Xi = \int \rho \xi\, dV \tag{6.31}$$

Here, I and Π respectively denote exergy consumption and entropy creation, Ξ denotes specific nonflow exergy, and the integral for Ξ is performed over the control volume. The first two terms on the left side of Equation 6.5a represent the net input of exergy associated with matter; the third term, the net input of exergy associated with heat; the fourth and fifth terms, the net input of exergy associated with work; and the sixth term the exergy consumption. The right side of Equation 6.5a shows the accumulation of exergy.

For a closed system, Equation 6.5a simplifies to

$$\sum_r (X_r)_{1,2} - (W_x)_{1,2} - (W_{NET})_{1,2} - I_{1,2} = \Xi_2 - \Xi_1 \tag{6.5b}$$

When volume is fixed, $(W_{NET})_{1,2} = 0$ in Equations 6.5a and b. Also, when the initial and final states are identical as in a complete cycle, the right sides of Equations 6.5a and b are zero.

6.2.6 *The Reference Environment*

Exergy is evaluated with respect to a reference environment. The intensive properties of the reference environment determine the exergy of a stream or system. The exergy of the reference environment is zero. The exergy of a stream or system is zero when it is in equilibrium with the reference environment. The reference environment is in stable equilibrium, with all parts at rest relative to one another. No chemical reactions can occur between the environmental components. The reference environment acts as an infinite system, and is a sink and source for heat and materials. It experiences only internal reversible processes in which its intensive state remains unaltered (i.e., its temperature T_o, pressure P_o, and the chemical potentials μ_{ioo} for each of the i components present remain constant).

The natural environment does not have the theoretical characteristics of a reference environment. The natural environment is not in equilibrium and its intensive properties exhibit spatial and temporal variations. Many chemical reactions in the natural environment are blocked because the transport mechanisms necessary to reach equilibrium are too slow at ambient conditions. Thus, the exergy of the natural environment is not zero; work could be obtained if it were to come to equilibrium. Consequently, models for the reference environment are used that try to achieve a compromise between the theoretical requirements of the reference environment and the actual behavior of the natural environment.

One important class of the reference-environment model is the natural-environment-subsystem type. These models attempt to simulate realistic subsystems of the natural environment. One such model consisting of saturated moist air and liquid water in phase equilibrium was proposed by Baehr and Schmidt (1963). An extension of the above model, which allowed sulphur-containing materials to be analyzed, was proposed by Gaggioli and Petit (1977) and Rodriguez (1980). The temperature and pressure of this reference environment (see Table 6.1) is normally taken to be 25 °C and 1 atm, respectively, and the chemical composition is taken to consist of air saturated with water vapor, and the following condensed phases at 25 °C and 1 atm: water (H_2O), gypsum ($CaSO_4 \cdot 2H_2O$), and limestone ($CaCO_3$). The stable configurations of C, O, and N, respectively, are taken to be those of CO_2, O_2, and N_2 as they exist in air saturated with liquid water at T_o and P_o; of hydrogen is taken to be in the liquid phase of water saturated with air at T_o and P_o; and of S and Ca, respectively, are taken to be those of $CaSO_4 \cdot 2H_2O$; and $CaCO_3$ at T_o and P_o.

The analyses in this chapter use the natural-environment-subsystem model described in Table 6.1, but with a temperature modified to reflect the approximate mean ambient temperature of the location of the TES for the time period under consideration (e.g., annual, seasonal, monthly). Other classes of reference-environment models have been proposed.

- **Reference-substance models.** These are models in which a "reference substance" is selected and assigned a zero exergy for every chemical element. One such model in which the reference

Table 6.1 A reference-environment model

Temperature: $T_o = 298.15\,\text{K}$
Pressure: $P_o = 1\,\text{atm}$
Composition: (i) Atmospheric air saturated with H_2O at T_o and P_o having the following composition:

Air constituents	Mole fraction
N_2	0.7567
O_2	0.2035
H_2O	0.0303
Ar	0.0091
CO_2	0.0003
H_2	0.0001

(ii) Condensed phases at T_o and P_o:
Water (H_2O)
Limestone ($CaCO_3$)
Gypsum ($CaSO_4 \cdot 2H_2O$)

Source: Adapted from Gaggioli and Petit (1977).

substances were selected as the most valueless substances found in abundance in the natural environment was proposed by Szargut (1967). The criteria for selecting such reference substances are consistent with the notion of simulating the natural environment, but are primarily economic in nature, and are vague and arbitrary with respect to the selection of reference substances. Part of this environment is the composition of moist air, including N_2, O_2, CO_2, H_2O and the noble gases, gypsum (for sulphur), and limestone (for calcium). Another model in this class, in which reference substances are selected arbitrarily, was proposed by Sussman (1980, 1981). This model is not similar to the natural environment, consequently absolute exergies evaluated with this model do not relate to the natural environment, and cannot be used rationally to evaluate efficiencies. Since exergy-consumption values are independent of the choice of reference substances, they can be rationally used in analyses.

- **Equilibrium models.** A model in which all the materials present in the atmosphere, oceans, and a layer of the crust of the earth are pooled together and an equilibrium composition is calculated for a given temperature was proposed by Ahrendts (1980). The selection of the thickness of crust considered is subjective, and is intended to include all materials accessible to technical processes. Ahrendts considered thicknesses varying from 1 m to 1000 m, and a temperature of 25 °C. For all thicknesses, Ahrendts found that the model differed significantly from the natural environment. Exergy values obtained using these environments are significantly dependent on the thickness of crust considered, and represent the absolute maximum amount of work obtainable from a material. Since there is no technical process available that can obtain this work from materials, Ahrendts' equilibrium model does not give meaningful exergy values when applied to the analysis of real processes.
- **Constrained-equilibrium models.** Ahrendts (1980) also proposed a modified version of his equilibrium environment in which the calculation of an equilibrium composition excludes the possibility of the formation of nitric acid (HNO_3) and its compounds. That is, all chemical reactions in which these substances are formed are in constrained equilibrium, and all other reactions are in unconstrained equilibrium. When a thickness of crust of 1 m and temperature of 25 °C were used, the model was similar to the natural environment.
- **Process-dependent models.** A model which contains only components that participate in the process being examined in a stable equilibrium composition at the temperature and total pressure of the natural environment was proposed by Bosnjakovic (1963). This model is dependent on the process examined, and is not general. Exergies evaluated for a specific process-dependent model

are relevant only to the process; they cannot rationally be compared with exergies evaluated for other process-dependent models.

Many researchers have examined the characteristics of and models for reference environments (Wepfer and Gaggioli, 1980; Sussman, 1981; Ahrendts, 1980), and the sensitivities of exergy values to different reference-environment models (Rosen and Scott, 1987).

6.2.7 *Efficiencies*

General Efficiency Concepts

Efficiency has always been an important consideration in decision making regarding resource utilization. Efficiency is defined as "the ability to produce a desired effect without waste of, or with minimum use of, energy, time, resources, and so on," and is used by people to refer to the effectiveness with which something is used to produce something else, or the degree to which the ideal is approached in performing a task.

For general engineering systems, nondimensional ratios of quantities are typically used to determine efficiencies. Ratios of energy are conventionally used to determine efficiencies of engineering systems whose primary purpose is the transformation of energy. These efficiencies are based on the first law of thermodynamics. A process has maximum efficiency according to the first law if energy input equals recoverable energy output (i.e., if no "energy losses" occur). However, efficiencies determined using energy are misleading, because, in general, they are not measures of "an approach to an ideal."

To determine more meaningful efficiencies, a quantity is required for which ratios can be established that do provide a measure of an approach to an ideal. Thus, the second law must be involved, as this law states that maximum efficiency is attained (i.e., ideality is achieved) for a reversible process. However, the second law must be quantified before efficiencies can be defined.

The "increase of entropy principle," which states that entropy is created because of irreversibilities, quantifies the second law. From the viewpoint of entropy, maximum efficiency is attained for a process in which entropy is conserved. Entropy is created for nonideal processes. The magnitude of entropy creation is a measure of the nonideality or irreversibility of a process. In general, however, ratios of entropy do not provide a measure of an approach to an ideal.

A quantity that has been discussed in the context of meaningful measures of efficiency is negentropy (Hafele, 1981). Negentropy is defined such that the negentropy consumption due to irreversibilities is equal to the entropy creation due to irreversibilities. As a consequence of the "increase of entropy principle," maximum efficiency is attained from the viewpoint of negentropy for a process in which negentropy is conserved. Negentropy is consumed for nonideal processes. Negentropy is a measure of order. Consumptions of negentropy are therefore equivalent to degradations of order. Since the abstract property of order is what is valued and useful, it is logical to attempt to use negentropy in developing efficiencies. However, general efficiencies cannot be determined based on negentropy because its absolute magnitude is not defined.

Negentropy can be further quantified through the ability to perform work. Then, a maximum efficiency is attainable only if, at the completion of a process, the sum of all energy involved has an ability to do work equal to the sum before the process occurred. Exergy is a measure of the ability to perform work and, from the viewpoint of exergy, maximum efficiency is attained for a process in which exergy is conserved. Efficiencies determined using ratios of exergy do provide a measure of an approach to an ideal. Exergy efficiencies are often more intuitively rational than energy efficiencies, because efficiencies between 0 and 100% are always obtained. Measures that can be greater than 100% when energy is considered, such as coefficient of performance, are normally between 0 and 100% when exergy is considered. In fact, some researchers (Gaggioli, 1983) call exergy efficiencies "real" or "true" efficiencies, while calling energy efficiencies "approximations to real" efficiencies.

Energy and Exergy Efficiencies

Many researchers (Sussman, 1981; Hevert and Hevert, 1980; Alefeld, 1990) have examined efficiencies and other measures of performance. Different efficiency definitions generally answer different questions.

Energy (η) and exergy (ψ) efficiencies are often written for steady-state processes occurring in systems as

$$\eta = \frac{\text{Energy in product outputs}}{\text{Energy in inputs}} = 1 - \frac{\text{Energy loss}}{\text{Energy in inputs}} \tag{6.32}$$

$$\psi = \frac{\text{Exergy in product outputs}}{\text{Exergy in inputs}} = 1 - \frac{\text{Exergy loss plus consumption}}{\text{Exergy in inputs}} \tag{6.33}$$

Two other common exergy-based efficiencies for steady-state devices are as follows:

$$\text{Rational efficiency} = \frac{\text{Total exergy output}}{\text{Total exergy input}} = 1 - \frac{\text{Exergy consumption}}{\text{Total exergy input}} \tag{6.34}$$

$$\text{Task efficiency} = \frac{\text{Theoretical minimum exergy input required}}{\text{Actual exergy input}} \tag{6.35}$$

Exergy efficiencies often give more illuminating insights into process performance than energy efficiencies because (i) they weigh energy flows according to their exergy contents, and (ii) they separate inefficiencies into those associated with effluent losses and those due to irreversibilities. In general, exergy efficiencies provide a measure of potential for improvement.

6.2.8 Properties for Energy and Exergy Analyses

Many material properties are needed for energy and exergy analyses of processes. Sources of conventional property data are abundant for many substances, for example, steam, air and combustion gases (Keenan *et al*., 1992), and chemical substances (Chase *et al*., 1985).

Energy values of heat and work flows are absolute, while the energy values of material flows are relative. Enthalpies are evaluated relative to a reference level. Since energy analyses are typically concerned only with energy differences, the reference level used for enthalpy calculations can be arbitrary. For the determination of some energy efficiencies, however, the enthalpies must be evaluated relative to specific reference levels (e.g., for energy-conversion processes, the reference level is often selected so that the enthalpy of a material equals its higher heating value (*HHV*).

If, however, the results from energy and exergy analyses are to be compared, it is necessary to specify the reference levels for enthalpy calculations such that the enthalpy of a compound is evaluated relative to the stable components of the reference environment. Thus, a compound that exists as a stable component of the reference environment is defined to have an enthalpy of zero at T_o and P_o. Enthalpies calculated with respect to such conditions are referred to as *base enthalpies* (Rodriguez, 1980). The base enthalpy is similar to the enthalpy of formation. While the latter is the enthalpy of a compound (at T_o and P_o) relative to the elements (at T_o and P_o) from which it would be formed, the former is the enthalpy of a component (at T_o and P_o) relative to the stable components of the environment (at T_o and P_o). For many environment models, the base enthalpies of material fuels are equal to their *HHV* s.

The base enthalpies for many substances, corresponding to the reference-environment model in Table 6.1, are listed in Table 6.2 (Rodriguez, 1980). It is required to determine chemical exergy values for exergy analysis. Many researchers have developed methods and tabulated values for evaluating chemical exergies (Rodriguez, 1980; Szargut, 1967; Sussman, 1980). Included are methods for evaluating the chemical exergies of solids, liquids, and gases. For complex materials (e.g., coal, tar, and ash), approximation methods have been developed. By considering environmental air

Table 6.2 Base enthalpy and chemical exergy values of selected species

Species	Specific base enthalpy (kJ/g-mol)	Specific chemical exergy[a] (kJ/g-mol)
Ammonia (NH_3)	382.585	$2.478907 \ln y + 337.861$
Carbon (graphite) (C)	393.505	410.535
Carbon dioxide (CO_2)	0.000	$2.478907 \ln y + 20.108$
Carbon monoxide (CO)	282.964	$2.478907 \ln y + 275.224$
Ethane (C_2H_6)	1564.080	$2.478907 \ln y + 1484.952$
Hydrogen (H_2)	285.851	$2.478907 \ln y + 235.153$
Methane (CH_4)	890.359	$2.478907 \ln y + 830.212$
Nitrogen (N_2)	0.000	$2.478907 \ln y + 0.693$
Oxygen (O_2)	0.000	$2.478907 \ln y + 3.948$
Sulphur (rhombic) (S)	636.052	608.967
Sulphur dioxide (SO_2)	339.155	$2.478907 \ln y + 295.736$
Water (H_2O)	44.001	$2.478907 \ln y + 8.595$

[a] y represents the molal fraction for each of the respective species.
Source: Compiled from data in Rodriguez (1980) and Gaggioli and Petit (1977).

and gaseous process streams as ideal gas mixtures, chemical exergy can be calculated for gaseous streams using component chemical exergy values, that is, values of $(\mu_{io} - \mu_{ioo})$ listed in Table 6.2.

6.2.9 *Implications of Results of Exergy Analyses*

The results of exergy analyses of TES systems have direct implications on application decisions and on research and development (R&D) directions.

Further, exergy analyses provide insights into the "best" directions for R&D effort more than energy analyses. Here, "best" is loosely taken to mean "most promising for significant efficiency gains." There are two main reasons for this statement:

- Exergy losses represent true losses of the potential that exists to generate the desired product (recovered thermal energy with little temperature degradation, here) from the given driving input (input thermal energy and electricity, here). In general, this is not true for energy losses. Thus, if the objective is to increase TES efficiency while accounting for temperature degradation, focusing on exergy losses permits R&D to focus on reducing losses that will affect the objective.
- Exergy efficiencies always provide a measure of how nearly the operation of a system approaches the ideal or theoretical upper limit. In general, this is not true for energy efficiencies. By focusing R&D effort on those plant sections or processes with the lowest exergy efficiencies, the effort is being directed to those areas that inherently have the largest margins for efficiency improvement. By focusing on energy efficiencies, on the other hand, one can expend R&D effort on topics for which small margins for improvement, even theoretically, exist.

Exergy analysis results typically suggest that R&D efforts should concentrate more on internal rather than external exergy losses, based on thermodynamic considerations, with a higher priority for the processes having larger exergy losses. Although this statement suggests focusing on those areas for which margins for improvement are greatest, it does not indicate that R&D should not be devoted to those processes having low exergy losses, as simple and cost-effective ways to increase efficiency by reducing small exergy losses should certainly be considered when identified.

More generally, it is noted that application and R&D allocation decisions should not be based exclusively on the results of energy and exergy analyses, even though these results provide useful

information to assist in such decision making. Other factors must also be considered, such as economics, environmental impact, safety, and social and political implications.

6.2.10 Steps for Energy and Exergy Analyses

A simple procedure for performing energy and exergy analyses involves the following steps:

- Subdivide the process under consideration into as many sections as desired, depending on the depth of detail and understanding desired from the analysis.
- Perform conventional mass and energy balances on the process, and determine all basic quantities (e.g., work, heat) and properties (e.g., temperature, pressure) (Section 6.2.3).
- Based on the nature of the process, the acceptable degree of analysis complexity and accuracy, and the questions for which answers are sought, select a reference-environment model (Section 6.2.6).
- Evaluate energy and exergy values, relative to the selected reference-environment model (Sections 6.2.4 and 6.2.8).
- Perform exergy balances, including the determination of exergy consumptions (Section 6.2.5).
- Select efficiency definitions depending on the measures of merit desired, and evaluate values for the efficiencies (Section 6.2.7).
- Interpret the results and draw appropriate conclusions and recommendations relating to such issues as design changes, retrofit plant modifications, and so on. (Section 6.2.9).

6.3 Thermodynamic Considerations in TES Evaluation

Several of the more important thermodynamic factors to be considered during the evaluation and comparison of TES systems are discussed in this section (Rosen and Dincer, 1999a).

6.3.1 Determining Important Analysis Quantities

The two most significant quantities to consider when evaluating TES systems are energy and exergy. Exergy analysis involves the examination of the exergy at different points in a series of energy-conversion steps, and the determination of meaningful efficiencies and of the steps having the largest losses (i.e., the largest margin for improvement). The authors and others feel that the use of exergy analysis circumvents many of the problems associated with conventional TES evaluation and comparison methodologies by providing a more rational basis.

Exergy analysis permits more rational and convenient evaluation than energy analysis of TES systems for cooling capacity as well as heating capacity. Exergy analysis applies equally well to systems for storing thermal energy at temperatures above and below the temperature of the environment, because the exergy associated with such energy is always greater than or equal to zero. Energy analysis is more difficult to apply to such storage systems because efficiency definitions have to be carefully modified when cooling capacity, instead of heating capacity, is stored, or when both warm and cool reservoirs are included.

6.3.2 Obtaining Appropriate Measures of Efficiency

The evaluation of a TES system requires a measure of performance that is rational, meaningful, and practical. The conventional energy storage efficiency, as pointed out earlier, is an inadequate measure. A more perceptive basis for comparison is apparently needed if the true usefulness of thermal storages is to be assessed, and so permit maximization of their economic benefit. Efficiencies

based on ratios of exergy do provide rational measures of performance, since they can measure the approach of the performance of a system to the ideal.

That the energy efficiency is an inappropriate measure of thermal storage performance can best be appreciated through a simple example. Consider a perfectly insulated thermal storage containing 1000 kg of water, initially at 40 °C. The ambient temperature is 20 °C.

A quantity of 4200 kJ of heat is transferred to the storage through a heat exchanger from an external body of 100 kg of water cooling from 100 °C to 90 °C (i.e., using Equation 6.168, (100 kg)(4.2 kJ/kg K)(100 – 90) °C = 4200 kJ). This heat addition raises the storage temperature from 1.0 °C to 41 °C (i.e., with Equation 6.181, (4200 kJ)/((1000 kg)(4.2 kJ/kg K)) = 1.0 °C). After a period of storage, 4200 kJ of heat are recovered from the storage through a heat exchanger that delivers it to an external body of 100 kg of water, raising the temperature of that water from 20 °C to 30 °C (i.e., with Equation 6.168, $\Delta T = (4200\,\text{kJ})/((100\,\text{kg})(4.2\,\text{kJ/kg K})) = 10$ °C). The storage is returned to its initial state at 40 °C.

For this storage cycle, the energy efficiency, the ratio of the heat recovered from the storage to the heat injected, is 4200 kJ/4200 kJ = 1, or 100%. But, the recovered heat is at only 30 °C, and of little use, having been degraded even though the storage energy efficiency was 100%. With Equation 6.170a, the exergy recovered in this example is evaluated as (100 kg)(4.2 kJ/kg K)[(30 – 20) °C – (293 K) ln (303/293)] = 70 kJ, and the exergy supplied as (100 kg)(4.2 kJ/kg K)[(100 – 90) °C – (293 K) ln (373/363)] = 856 kJ. Thus the exergy efficiency, the ratio of the thermal exergy recovered from storage to that injected, is 70/856 = 0.082, or 8.2%, a much more meaningful expression of the achieved performance of the storage cycle.

In most TES investigations, the energy and exergy efficiency definitions in Equations 6.32 and 6.33 are used. These efficiency definitions are dependent on what quantities are considered to be products and inputs. Two possible sets of efficiency definitions are presented in Table 6.3. The energy or exergy initially in the store is neglected in the first definition, and considered to be an "input" in the second definition. Depending on the particular circumstances, the energy efficiency definitions in Table 6.3 can yield values that are identical or radically different. The same statement can be made for the exergy efficiencies. Regardless of definition, however, the authors feel that the use of exergy analysis is necessary for evaluating TES systems.

6.3.3 Pinpointing Losses

With energy analysis, all losses are attributable to energy releases across system boundaries. With exergy analysis, losses are divided into two types: those associated with releases of exergy from the system and those associated with internal consumptions of exergy (Alefeld, 1990). For a TES system, the total exergy loss is the sum of the exergy associated with heat loss to the surroundings and the exergy loss due to internal exergy consumptions, such as by reductions in availability of the stored heat through mixing of warm and cool fluids. The division of losses associated with exergy analysis allows the causes of inefficiencies to be more accurately identified than does energy analysis, and R&D effort to be more effectively allocated. The analysis of the heat flows from

Table 6.3 Two overall energy (η) and exergy (ψ) TES efficiencies

Efficiency	Definition 1	Definition 2
η	$\frac{\text{Energy recovered from TES}}{\text{Energy input to TES}}$	$\frac{\text{Energy recovered from and remaining in TES}}{\text{Energy input to and originally in TES}}$
ψ	$\frac{\text{Exergy recovered from TES}}{\text{Exergy input to TES}}$	$\frac{\text{Exergy recovered from and remaining in TES}}{\text{Exergy input to and originally in TES}}$

or into TES systems is often investigated (Rosen, 1990, 1998a, 1998b), and is discussed in the first chapter.

6.3.4 Assessing the Effects of Stratification

Water tanks are one of the most economic devices for TES. For many TES applications, performance is strongly dependent on the temperature required to meet the thermal energy demand, and stratification within the tank can play a significant role (Yoo *et al*., 1998; Homan *et al*., 1996; Mavros *et al*., 1994; Nelson *et al*., 1999; Gretarsson *et al*., 1994). In practice, in most cases, a vertical cylindrical tank with a hot water inlet (outlet) at the top and a cold water inlet (outlet) at the bottom is used. The hot and cold water in the tank are usually stratified initially into two layers, with a mixing layer in between. The degree of stratification is dependent on the volume and configuration of the tank, the size, location, and design of the inlets and outlets, the flow rates of the entering and exiting streams, and the durations of the charging, storing, and discharging periods.

Four primary factors contribute to the loss of stratification and hence the degradation of the stored energy:

- heat losses to (or leakages from) the surrounding environment;
- heat conduction from the hot portions of the storage fluid to the colder portions;
- vertical conduction in the tank wall; and
- mixing during charging and discharging periods.

Among these, the last item generally is the major cause of loss of stratification, with particularly significant mixing losses occurring during lengthy storing periods. Improving stratification often leads to substantial improvement in TES efficiency relative to a system incorporating a thermally mixed-storage tank.

TES evaluation methodologies must quantitatively and clearly assess the effects of stratification on system performance. The effects of stratification are more clearly assessed with exergy analysis than with energy analysis because of the internal spatial temperature variations that stratified storages exhibit (Hahne *et al*., 1989; Krane and Krane, 1991; Rosen and Tang, 1997). Through carefully managing the injection, recovery, and holding of heat (or cold) during a storage cycle so that temperature degradation is minimized, better storage-cycle performance can be achieved (as measured by better thermal energy recovery and temperature retention). This improved performance is accounted for explicitly with exergy analysis through increased exergy efficiencies. Some relatively simple approaches for stratified TES evaluation have been developed (Hooper *et al*., 1988; Rosen and Hooper, 1991a, 1991b, 1992, 1994), which take into consideration the second-law concerns, and which assess the performance of real stratified storages with an accuracy acceptable for most purposes, and certainly superior to that from assessments based only on the first law.

6.3.5 Accounting for Time Duration of Storage

Rational measures of merit for the evaluation and comparison of TES systems must account for the length of time thermal energy is in storage. The length of time that thermal energy is retained in a TES does not enter into the expressions for thermal efficiency and exergy efficiency for thermal storages, although it is clearly a dominant consideration in the overall effectiveness for such systems. The authors have examined the relation between the length of time thermal energy is held in storage and storage effectiveness, and have developed an approach for comparing TES systems using a time parameter (Barbaris *et al*., 1988).

6.3.6 Accounting for Variations in Reference-Environment Temperature

Over the time periods involved in some TES cycles (up to six months for seasonal systems), the value of the reference-environment temperature T_o varies with time. The value of T_o also varies with location. Since the results of TES evaluations based on energy and exergy analyses depend on the value of T_o, the temporal and spatial dependencies must be considered in such evaluations.

The value of $T_o(t)$ can often be assumed to be the same as the ambient temperature variation with time, $T_{amb}(t)$. On an annual basis, the ambient temperature varies approximately sinusoidally with time t about the annual mean:

$$T_{amb}(t) = \overline{T}_{amb} + \Delta T_{amb}\left[\sin\frac{2\pi t}{\text{period}} + (\text{phase shift})\right] \tag{6.36}$$

where $\overline{T}_{amb}$ is the mean annual ambient temperature and ΔT_{amb} is the maximum temperature deviation from the annual mean. The values of the parameters in Equation 6.36 vary spatially and the period is one year.

In evaluating the performance of most storages (particularly of long-term storages), a constant value of T_o can be assumed. Some possible values for T_o are:

- the appropriate seasonal mean value of the temperature of the atmosphere;
- the appropriate annual mean value of the temperature of the atmosphere;
- the temperature of soil far enough below the surface that the temperature remains approximately constant throughout the year, that is, near the water table (this temperature is usually near to that specified in the previous point); and
- the lowest value of the atmosphere temperature during the year, for heat storage processes, and the highest value of the atmosphere temperature during the year, for cooling capacity storage processes.

6.3.7 Closure

The factors discussed here that significantly impacts on the evaluation and comparison of TES systems are summarized in Table 6.4.

6.4 Exergy Evaluation of a Closed TES System

The use of exergy analysis in the evaluation of a specific TES system (a simple closed tank storage with heat transfers by heat exchanger) is described in this section, following an earlier report (Rosen *et al*., 1988). A complete storing cycle, as well as the individual charging, storing, and discharging

Table 6.4 Some exergy-related thermodynamic considerations in TES system evaluations

- Determining important analysis quantities.
- Evaluating storages for cooling as well as heating capacity.
- Obtaining appropriate measures of efficiency.
- Pinpointing losses.
- Assessing the effects of stratification.
- Assessing the performance of subprocesses.
- Accounting for temporal and spatial variations in T_o.
- Accounting for the time duration of storage.

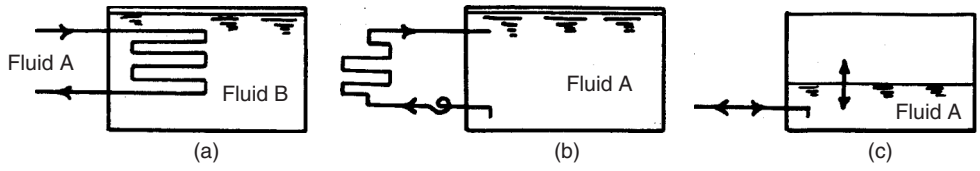

Figure 6.2 Three basic types of thermal storage. (a) A closed system in which heat transfer occurs between the transport fluid A and the storage fluid B. (b) An open system of constant mass in which the same fluid is used for both transport and storage of heat. (c) An open system of variable mass

periods, is considered. A numerical example for a simple case is given (see Section 6.4.6). This application highlights the fact that, although energy is conserved in an adiabatic system, mixing of the high- and low-temperature portions of the storage medium causes a consumption (or destruction) of exergy, which is conserved only in fully reversible processes.

A clear understanding of the TES type under consideration and a clear declaration of the assumptions used are important in establishing a consistent basis for TES analysis and comparison. Three basic sensible heat storage types are shown in Figure 6.2. The first type, which is considered here, represents a closed system storing heat in a fixed amount of storage fluid B, to or from which heat is transferred through a heat exchanger by means of a heat transport fluid A. The second type is also of fixed mass, but is open, and the transport and storage fluids are of the same substance. No heat exchanger is involved. The third type uses an open system storing a variable amount of the combined heat transport and storage fluid. For each of these storage types, further characteristics can yield additional cases and conditions (e.g., adiabatic or nonadiabatic boundaries, complete or incomplete cycles, fully mixed or stratified storage fluid, steady or intermittent fluid flows, steady or variable ambient conditions, short or long storage periods, constant or variable physical properties, and one-, two-, or three-dimensional heat flows).

6.4.1 Description of the Case Considered

A specific, simple case is considered in which a TES system undergoes a complete storage cycle, ending with the final state identical to the initial state. Figure 6.3 illustrates the three periods in the overall storage process considered. The TES may be stratified. Other characteristics of the considered case are:

- nonadiabatic storage boundaries;
- finite charging, storing, and discharging time periods;
- surroundings at constant temperature and pressure;
- constant storage volume;
- negligible work interactions (e.g., pump work); and
- negligible kinetic and potential energy terms.

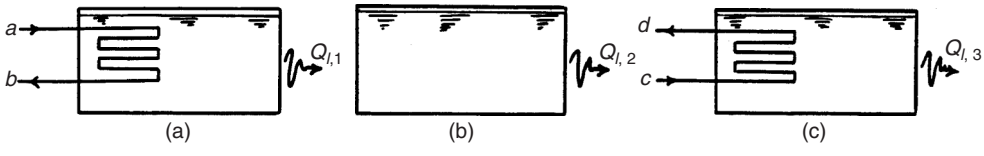

Figure 6.3 The three stages in a simple heat storage process: charging period (a), storing period (b), and discharging period (c)

The operation of the heat exchangers is simplified by assuming that there are no heat losses to the surrounding environment from the charging and discharging fluids. That is, it is assumed for the charging period that all heat removed from the charging fluid is added to the storage medium, and for the discharging period that all heat added to the discharging fluid originated in the storage medium. This assumption is valid if heat losses from the charging and discharging fluids are small compared with heat losses from the storage medium. This assumption can be extended by lumping actual heat losses from the charging and discharging fluids together with heat losses from the TES. Also, as is often done for practical systems, the charging- and discharging-fluid flows are considered steady and with time-independent properties, and modeled as one-dimensional.

6.4.2 Analysis of the Overall Process

For the cases considered (Figure 6.3), energy and exergy balances and efficiencies are provided for the overall process.

Overall Energy Balance

Following Equations 6.3 and 6.3a, an energy balance for the overall storage process can be written as

$$\text{Energy input} - (\text{Energy recovered} + \text{Energy loss}) = \text{Energy accumulation} \tag{6.37}$$

or

$$(H_a - H_b) - [(H_d - H_c) + Q_l] = \Delta E \tag{6.37a}$$

where H_a, H_b, H_c, and H_d are the total enthalpies of the flows at states a, b, c, and d, respectively; Q_l denotes the heat losses during the process and ΔE the accumulation of energy in the TES. In Equation 6.37a, $(H_a - H_b)$ represents the net heat delivered to the TES and $(H_d - H_c)$ the net heat recovered from the TES. The quantity in square brackets represents the net energy output from the system. The terms ΔE and Q_l are given by

$$\Delta E = E_f - E_i \tag{6.38}$$

$$Q_l = \sum_{j=1}^{3} Q_{l,j} \tag{6.39}$$

Here E_i and E_f denote the initial and final energy contents of the storage, and $Q_{l,j}$ denotes the heat losses during the period j, where $j = 1, 2, 3$ corresponds to the charging, storing, and discharging periods, respectively. In the case of identical initial and final states, $\Delta E = 0$, and the overall energy balance simplifies.

Overall Exergy Balance

Following Equations 6.5 and 6.5a, an overall exergy balance can be written as

$$\begin{aligned}&\text{Exergy input} - (\text{Exergy recovered} + \text{Exergy loss}) - \text{Exergy consumption}\\ &\quad = \text{Exergy accumulation}\end{aligned} \tag{6.40}$$

or

$$(\in_a - \in_b) - [(\in_d - \in_c) + X_l] - I = \Delta \Xi \tag{6.40a}$$

where $\in_a, \in_b, \in_c$, and $\in_d$ are the exergies of the flows at states a, b, c, and d, respectively; and X_l denotes the exergy loss associated with Q_l; I is the exergy consumption; and $\Delta\Xi$ is the exergy accumulation. In Equation 6.40a, $(\in_a - \in_b)$ represents the net exergy input and $(\in_d - \in_c)$ is the net exergy recovered. The quantity in square brackets represents the net exergy output from the system. The terms I, X_l, and $\Delta\Xi$ are given respectively by

$$I = \sum_{j=1}^{3} I_j \tag{6.41}$$

$$X_l = \sum_{j=1}^{3} X_{l,j} \tag{6.42}$$

$$\Delta\Xi = \Xi_f - \Xi_i \tag{6.43}$$

Here, I_1, I_2, and I_3 denote respectively the consumptions of exergy during the charging, storing, and discharging periods; $X_{l,1}$, $X_{l,2}$, and $X_{l,3}$ denote the exergy losses associated with heat losses during the same periods; and Ξ_i and Ξ_f denote the initial and final exergy contents of the storage. When the initial and final states are identical, $\Delta\Xi = 0$.

The exergy content of the flow at the states $k = a, b, c, d$ is evaluated as

$$\in_k = (H_k - H_o) - T_o\,(S_k - S_o) \tag{6.44}$$

where $\in_k$, H_k, and S_k denote the exergy, enthalpy, and entropy of state k, respectively, and H_o and S_o the enthalpy and the entropy at the temperature T_o and pressure P_o of the reference environment. The exergy expression in Equation 6.44 only includes physical (or thermomechanical) exergy. Potential and kinetic exergy components are, as pointed out earlier, considered negligible for the devices under consideration. The chemical component of exergy is neglected because it does not contribute to the exergy flows for sensible TES systems. Thus, the exergy differences between the inlet and outlet for the charging and discharging periods are, respectively:

$$\in_a - \in_b = (H_a - H_b) - T_o\,(S_a - S_b) \tag{6.45}$$

and

$$\in_d - \in_c = (H_d - H_c) - T_o\,(S_d - S_c) \tag{6.46}$$

Here it has been assumed that T_o and P_o are constant, so that H_o and S_o are constant at states a and b, and at states c and d.

For a fully mixed tank, the exergy losses associated with heat losses to the surroundings are evaluated following Equation 6.25 as

$$X_{l,j} = \int_i^f \left(1 - \frac{T_o}{T_j}\right) dQ_{l,j} \text{ for } j = 1, 2, 3 \tag{6.47}$$

where j represents the particular period. If T_1, T_2, and T_3 are constant during the respective charging, storing, and discharging periods, then $X_{l,j}$ may be written with Equation 6.25a as follows:

$$X_{l,j} = \left(1 - \frac{T_o}{T_j}\right) Q_{l,j} \tag{6.47a}$$

Sometimes when applying Equation 6.47a to TES systems, T_j represents a mean temperature within the tank for period j.

Overall Energy and Exergy Efficiencies

Following Equations 6.32 and 6.33, the energy efficiency η can be defined as

$$\eta = \frac{\text{Energy recovered from TES during discharging}}{\text{Energy input to TES during charging}} = \frac{H_d - H_c}{H_a - H_b} = 1 - \frac{Q_l}{H_a - H_b} \tag{6.48}$$

and the exergy efficiency ψ as

$$\psi = \frac{\text{Exergy recovered from TES during discharging}}{\text{Exergy input to during charging}} = \frac{\in_d - \in_c}{\in_a - \in_b} = 1 - \frac{X_l + I}{\in_a - \in_b} \tag{6.49}$$

The efficiency expressions in Equations 6.48 and 6.49 do not depend on the initial energy and exergy contents of the TES.

If the TES is adiabatic, $Q_{l,j} = X_{l,j} = 0$ for all j. Then, the energy efficiency is fixed at unity and the exergy efficiency simplifies to

$$\psi = 1 - \frac{I}{\in_a - \in_b} \tag{6.49a}$$

emphasizing the point that even when TES boundaries are adiabatic and there are therefore no energy losses, the exergy efficiency is less than unity due to internal irreversibilities.

6.4.3 *Analysis of Subprocesses*

Many different efficiencies based on energy and exergy can be defined for the charging, storing, and discharging periods (as discussed in Section 6.5). In the present analysis of the subprocesses (see Figure 6.3), only one set of efficiencies is considered.

Analysis of Charging Period

An energy balance for the charging period can be written as follows:

$$\text{Energy input} - \text{Energy loss} = \text{Energy accumulation} \tag{6.50}$$

$$(H_a - H_b) - Q_{l,1} = \Delta E_1 \tag{6.50a}$$

Here,

$$\Delta E_1 = E_{f,1} - E_{i,1} \tag{6.51}$$

and $E_{i,1}$ and $E_{f,1}$ denote the initial and the final energy of the TES for the charging period. Note that $E_{i,1} \equiv E_i$ (see Equation 6.38). A charging-period energy efficiency can be defined as

$$\eta_1 = \frac{\text{Energy accumulation in TES during charging}}{\text{Energy input to TES during charging}} = \frac{\Delta E_1}{H_a - H_b} \tag{6.52}$$

An exergy balance for the charging period can be written as

$$\text{Exergy input} - \text{Exergy loss} - \text{Exergy consumption} = \text{Exergy accumulation} \tag{6.53}$$

$$(\in_a - \in_b) - X_{l,1} - I_1 = \Delta \Xi_1 \tag{6.53a}$$

Here,

$$\Delta \Xi_1 = \Xi_{f,1} - \Xi_{i,1} \tag{6.54}$$

and $\Xi_{i,1}$ and $\Xi_{f,1}$ are the initial and the final exergy of the TES for the charging period. Note that $\Xi_{i,1} \equiv \Xi_i$ (see Equation 6.43). A charging-period exergy efficiency can be defined as

$$\psi_1 = \frac{\text{Exergy accumulation in TES during charging}}{\text{Exergy input to TES during charging}} = \frac{\Delta \Xi_1}{\epsilon_a - \epsilon_b} \tag{6.55}$$

The charging efficiencies in Equations 6.52 and 6.55 indicate the fraction of the input energy/exergy that is accumulated in the store during the charging period.

Analysis of Storing Period

An energy balance for the storing period can be written as

$$-\text{Energy loss} = \text{Energy accumulation} \tag{6.56}$$

$$-Q_{l,2} = \Delta E_2 \tag{6.56a}$$

Here,

$$\Delta E_2 = E_{f,2} - E_{i,2} \tag{6.57}$$

and $E_{i,2}(\equiv E_{f,1})$ and $E_{f,2}$ denote the initial and final energy contents of the TES for the storing period. An energy efficiency for the storing period can be defined as

$$\eta_2 = \frac{\text{Energy accumulation in TES during charging and storing}}{\text{Energy accumulation in TES during charging}} = \frac{\Delta E_1 + \Delta E_2}{\Delta E_1} \tag{6.58}$$

Using Equation 6.56a, the energy efficiency can be rewritten as

$$\eta_2 = \frac{\Delta E_1 - Q_{l,2}}{\Delta E_1} \tag{6.58a}$$

An exergy balance for the storing period can be written as

$$-\text{Energy loss} - \text{Exergy consumption} = \text{Exergy accumulation} \tag{6.59}$$

$$-X_{l,2} - I_2 = \Delta \Xi_2 \tag{6.59a}$$

Here,

$$\Delta \Xi_2 = \Xi_{f,2} - \Xi_{i,2} \tag{6.60}$$

and $\Xi_{i,2}(\equiv \Xi_{f,1})$ and $\Xi_{f,2}$ denote the initial and the final exergies of the system for the storing period. An exergy efficiency for the storing period can be defined as

$$\psi_2 = \frac{\text{Exergy accumulation in TES during charging and storing}}{\text{Exergy accumulation in TES during charging}} = \frac{\Delta \Xi_1 + \Delta \Xi_2}{\Delta \Xi_1} \tag{6.61}$$

Using Equation 6.59a, the exergy efficiency can be rewritten as

$$\psi_2 = \frac{\Delta \Xi_1 - \left(X_{l,2} + I_2\right)}{\Delta \Xi_1} \tag{6.61a}$$

The storing efficiencies in Equations 6.58 and 6.61 indicate the fraction of the energy/exergy accumulated during charging that is still retained in the store at the end of the storing period.

Analysis of Discharging Period

An energy balance for the discharging period can be written as

$$-(\textit{Energy recovered} + \textit{Energy loss}) = \textit{Energy accumulation} \tag{6.62}$$

$$-\left[(H_d - H_c) + Q_{l,3}\right] = \Delta E_3 \tag{6.62a}$$

Here,

$$\Delta E_3 = E_{f,3} - E_{i,3} \tag{6.63}$$

and $E_{i,3}(= E_{f,2})$ and $E_{f,3}$ $(= E_f$ in Equation 6.38) denote the initial and final energies of the store for the discharging period. The quantity in square brackets represents the energy output during discharging. An energy efficiency for the discharging period can be defined as

$$\eta_3 = \frac{\text{Energy recovered from TES during discharging}}{\text{Energy accumulation in TES during charging and storing}} = \frac{H_d - H_c}{\Delta E_1 + \Delta E_2} \tag{6.64}$$

Using Equation 6.56a, the energy efficiency can be rewritten as

$$\eta_3 = \frac{H_d - H_c}{\Delta E_1 - Q_{1,2}} \tag{6.64a}$$

An exergy balance for the discharging period can be written as follows:

$$-(\textit{Exergy recovered} + \textit{Exergy loss}) - \textit{Exergy consumption} = \textit{Exergy accumulation} \tag{6.65}$$

$$-[(\epsilon_d - \epsilon_c) + X_{l,3}] - I_3 = \Delta \Xi_3 \tag{6.65a}$$

Here,

$$\Delta \Xi_3 = \Xi_{f,3} - \Xi_{i,3} \tag{6.66}$$

and $\Xi_{i,3}(= \Xi_{f,2})$ and $\Xi_{f,3}$ $(= \Xi_f$ in Equation 6.43) denote the initial and final exergies of the store for the discharging period. The quantity in square brackets represents the exergy output during discharging. An exergy efficiency for the discharging period can be defined as

$$\psi_3 = \frac{\text{Exergy recovered from TES during discharging}}{\text{Exergy accumulation in TES during charging and storing}} = \frac{\epsilon_d - \epsilon_c}{\Delta \Xi_1 + \Delta \Xi_2} \tag{6.67}$$

Using Equation 6.59a, the exergy efficiency can be rewritten as

$$\psi_3 = \frac{\epsilon_d - \epsilon_c}{\Delta \Xi_1 - (X_{l,2} + I_2)} \tag{6.67a}$$

The discharging efficiencies in Equations 6.64 and 6.67 indicate the fraction of the energy/exergy input during charging and still retained at the end of storing that is recovered during discharging.

6.4.4 Alternative Formulations of Subprocess Efficiencies

Several alternative subprocess efficiency formulations, which can be useful depending upon the inclination of the analyst and the application addressed, are given here.

In the expressions for the subprocess energy and exergy efficiencies, that is, in Equations 6.52, 6.55, 6.58a, 6.61a, 6.64a, and 6.67a, the terms ΔE_1 and $\Delta \Xi_1$ can be eliminated using Equations

6.50a and 6.53a, respectively. After substitutions for ΔE_1 and $\Delta \Xi_1$ and minor rearrangement of the equations, the following are obtained:

$$\eta_1 = \frac{(H_a - H_b) - Q_{1,1}}{(H_a - H_b)} = 1 - \frac{Q_{l,1}}{H_a - H_b} \tag{6.52a}$$

$$\psi_1 = \frac{(\in_a - \in_b) - (X_{l,1} + I_1)}{(\in_a - \in_b)} = 1 - \frac{X_{l,1} + I_1}{\in_a - \in_b} \tag{6.55a}$$

$$\eta_2 = \frac{\left[(H_a - H_b) - Q_{l,1}\right] - Q_{l,2}}{(H_a - H_b) - Q_{l,1}} = \frac{(H_a - H_b) - \sum_{j=1}^{2} Q_{l,j}}{(H_a - H_b) - Q_{l,1}} = 1 - \frac{Q_{l,2}}{(H_a - H_b) - Q_{l,1}} \tag{6.58b}$$

$$\psi_2 = \frac{\left[(\in_a - \in_b) - (X_{l,1} + I_1)\right] - \left[X_{l,2} + I_2\right]}{(\in_a - \in_b) - (X_{l,1} + I_1)} = \frac{(\in_a - \in_b) - \sum_{j=1}^{2} (X_{l,j} + I_j)}{(\in_a - \in_b) - (X_{l,1} + I_1)}$$
$$= 1 - \frac{X_{l,2} + I_2}{(\in_a - \in_b) - (X_{l,1} + I_1)} \tag{6.61b}$$

$$\eta_3 = \frac{H_d - H_c}{[(H_a - H_b) - Q_{l,1}] - Q_{l,2}} = \frac{H_d - H_c}{(H_a - H_b) - \sum_{j=1}^{2} Q_{l,j}} \tag{6.64b}$$

$$\psi_3 = \frac{\in_d - \in_c}{[(\in_a - \in_b) - (X_{l,1} + I_1)] - (X_{l,2} + I_2)} = \frac{\in_d - \in_c}{(\in_a - \in_b) - \sum_{j=1}^{2} (X_{l,j} + I_j)} \tag{6.67b}$$

The above equations for η_3 and ψ_3 can be further modified if the terms in the numerators are eliminated using Equations 6.37a and 6.40a with $\Delta E = \Delta \Xi = 0$. Then,

$$\eta_3 = \frac{(H_a - H_b) - Q_l}{(H_a - H_b) - \sum_{j=1}^{2} Q_{l,j}} = \frac{(H_a - H_b) - \sum_{j=1}^{3} Q_{l,j}}{(H_a - H_b) - \sum_{j=1}^{2} Q_{l,j}} = 1 - \frac{Q_{l,3}}{(H_a - H_b) - \sum_{j=1}^{2} Q_{l,j}} \tag{6.64c}$$

$$\psi_3 = \frac{(\in_a - \in_b) - (X_l + I)}{(\in_a - \in_b) - \sum_{j=1}^{2} (X_{l,j} + I_j)} = \frac{(\in_a - \in_b) - \sum_{j=1}^{3} (X_{l,j} + I_j)}{(\in_a - \in_b) - \sum_{j=1}^{2} (X_{l,j} + I_j)}$$
$$= 1 - \frac{X_{l,3} + I_3}{(\in_a - \in_b) - \sum_{j=1}^{2} (X_{l,j} + I_j)} \tag{6.67c}$$

6.4.5 *Relations between Performance of Subprocesses and Overall Process*

The total energy and exergy efficiencies can be written as the products of the energy and exergy efficiencies of the charging, storing, and discharging periods. That is,

$$\eta = \prod_{j=1}^{3} \eta_j \tag{6.68}$$

$$\psi = \prod_{j=1}^{3} \psi_j \tag{6.69}$$

The energy efficiency relationship can be verified by multiplying together Equations 6.52, 6.58a, and 6.64a and comparing the result to Equation 6.48. Similarly, the exergy efficiency relationship can be verified by comparing the product of Equations 6.55, 6.61a, and 6.67a to Equation 6.49a. Equations 6.68 and 6.69 can also be shown to hold when using the alternative formulations of the subprocess efficiencies.

In addition, it can be shown that the summations of the energy or exergy balance equations, respectively, for the three subprocesses give the energy or exergy balance equations for the overall process. This statement can be verified by noting that,

$$\sum_{j=1}^{3} \Delta E_j = E_{3,f} - E_{1,i} = E_f - E_i = \Delta E \tag{6.70}$$

$$\sum_{j=1}^{3} \Delta \Xi_j = \Xi_{3,f} - \Xi_{l,i} = \Xi_f - \Xi_i = \Delta \Xi \tag{6.71}$$

and by comparing the sum of Equations 6.50a, 6.56a, and 6.62a with Equation 6.37a for energy, and by comparing the sum of Equations 6.53a, 6.59a, and 6.65a with Equation 6.40a for exergy. In writing Equations 6.70 and 6.71, it has been noted that for period j,

$$\Delta E_j = E_{f,j} - E_{i,j} \tag{6.72}$$

$$\Delta \Xi_j = \Xi_{f,j} - \Xi_{i,j} \tag{6.73}$$

and that $E_{i,1} = E_i$, $E_{f,3} = E_f$, and $E_{i,j+1} = E_{f,j}$ for $j = 1, 2$, while analogous expressions hold for the Ξ terms.

6.4.6 *Example*

Consider two different thermal storages, each of which undergoes a similar charging process. In each charging operation, heat is transferred to a closed thermal storage from a stream of 1000 kg of water that enters at 85 °C and leaves at 25 °C (see Figure 6.4). Consider Cases A and B, representing two different modes of operation. For Case A, heat is recovered from the storage after 1 day by a stream of 5000 kg of water entering at 25 °C and leaving at 35 °C. For Case B, heat is recovered from the storage after 100 days by a stream of 1000 kg of water entering at 25 °C and leaving at 75 °C.

Energy and exergy analyses of the overall processes are performed for both cases using superscripts A and B to denote Cases A and B, respectively. In both cases, the temperature of the surroundings remains constant at 20 °C, and the final state of the storage is the same as the initial state. Water is taken to be an incompressible fluid having a specific heat at constant pressure of $c_p = 4.18$ kJ/kg K, and heat exchanges during charging and discharging are assumed to occur at constant pressure.

The numerical values used in the example were selected to illustrate the concepts discussed in this section, and to resemble values for possible practical system configurations. Several physical implications of the selected numerical values are as follows. First, the inlet and outlet temperatures for the charging and discharging fluids imply that a stratified temperature profile exists in the TES after charging. Secondly, the higher discharging-fluid temperature for Case B implies that a greater degree of stratification is maintained during the storing period for Case B (or that greater internal mixing occurs for Case A). Thirdly, the quantities of discharging fluid and the associated temperatures imply that the discharging fluid is circulated through the TES at a greater rate for Case A than for Case B.

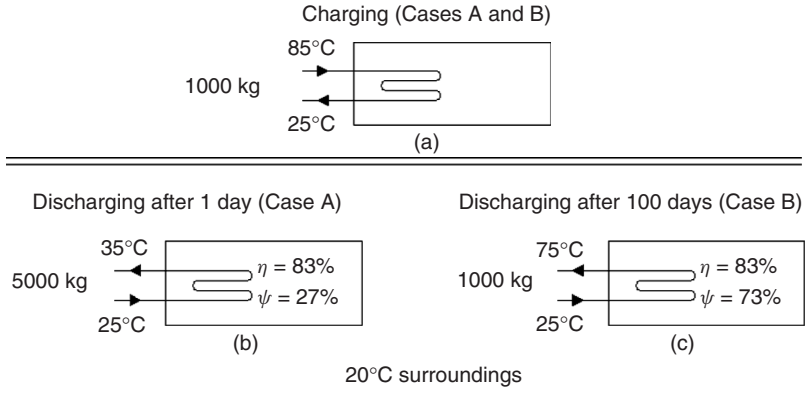

Figure 6.4 An example in which two cases are considered. Shown are the charging process, which is identical for Cases A and B (a), the discharging process for Case A (b), and the discharging process for Case B (c)

Energy Analysis for the Overall Process

The net heat input to the storage during the charging period for each case is

$$H_a - H_b = m_1 c_p (T_a - T_b) = 1000\,\text{kg} \times 4.18\,\text{kJ/kg K} \times (85 - 25)\,\text{K} = 250{,}800\,\text{kJ}$$

For Case A, the heat recovered during the discharging period is

$$(H_d - H_c)^A = 5000\,\text{kg} \times 4.18\,\text{kJ/kg K} \times (35 - 25)\,\text{K} = 209{,}000\,\text{kJ}$$

The energy efficiency of storage is (see Equation 6.48)

$$\eta^A = \frac{\text{Heat recovered}}{\text{Heat input}} = \frac{(H_d - H_c)^A}{H_a - H_b} = \frac{209{,}000\,\text{kJ}}{250{,}800\,\text{kJ}} = 0.833$$

The heat lost to the surroundings during storage is (see Equation 6.37a with $\Delta E = 0$)

$$Q_l^A = (H_a - H_b) - (H_c - H_d)^A = 250{,}000\,\text{kJ} - 209{,}000\,\text{kJ} = 41{,}800\,\text{kJ}$$

For Case B, the heat recovered during discharging, the energy efficiency, and the heat lost to the surroundings can be evaluated similarly:

$$(H_d - H_c)^B = 1000\,\text{kg} \times 4.18\,\text{kJ/kg K} \times (75 - 25)\,\text{K} = 209{,}000\,\text{kJ}$$

$$\eta^B = \frac{209{,}000\,\text{kJ}}{250{,}800\,\text{kJ}} = 0.833$$

$$Q_l^B = 250{,}800\,\text{kJ} - 209{,}000\,\text{kJ} = 41{,}800\,\text{kJ}$$

The values of the three parameters evaluated above for Case B are the same as the corresponding values for Case A.

Exergy Analysis for the Overall Process

The net exergy input during the charging period ($\in_a - \in_b$) can be evaluated with Equation 6.45. In that expression, the quantity ($H_a - H_b$) represents the net energy input to the store during charging,

evaluated as 250,800 kJ in the previous subsection. Noting that the difference in specific entropy can be written assuming incompressible substances having a constant specific heat as

$$s_a - s_b = c_p \ln \frac{T_a}{T_b} = 4.18 \frac{\text{kJ}}{\text{kg K}} \times \ln \frac{358\,\text{K}}{298\,\text{K}} = 0.7667 \frac{\text{kJ}}{\text{kg K}}$$

the quantity $T_o(S_a - S_b)$, which represents the unavailable part of the input heat, is

$$T_o(S_a - S_b) = T_o m_1 (s_a - s_b) = 293\,\text{K} \times 1000\,\text{kg} \times 0.7667\,\text{kJ/kg K} = 224{,}643\,\text{kJ}$$

where m_1 denotes the mass of the transport fluid cooled during the charging period. Then, the net exergy input is

$$\in_a - \in_b = 250{,}800\,\text{kJ} - 224{,}643\,\text{kJ} = 26{,}157\,\text{kJ}$$

The net exergy output during the discharging period $(\in_d - \in_c)$ can be evaluated using Equation 6.46 and denoting the mass of the transport fluid circulated during the discharging period as m_3, in a similar three-step fashion for Cases A and B. For Case A,

$$(s_d - s_c)^A = c_p \ln \frac{T_d^A}{T_c^A} = 4.18 \frac{\text{kJ}}{\text{kg K}} \times \ln \frac{308\,\text{K}}{298\,\text{K}} = 0.1379 \frac{\text{kJ}}{\text{kg K}}$$

$$T_o(S_d - S_c)^A = T_o m_3^A (s_d - s_c)^A = 293\,\text{K} \times 5000\,\text{kg} \times 0.1379\,\text{kJ/kg K} = 202{,}023\,\text{kJ}$$

$$(\in_d - \in_c)^A = 209{,}000\,\text{kJ} - 202{,}023\,\text{kJ} = 6977\,\text{kJ}$$

For Case B,

$$(s_d - s_c)^B = c_p \ln \frac{T_d^B}{T_c^B} = 4.18 \frac{\text{kJ}}{\text{kg K}} \times \ln \frac{348\ \text{K}}{298\ \text{K}} = 0.6483 \frac{\text{kJ}}{\text{kg K}}$$

$$T_o(S_d - S_c)^B = T_o m_3^B (s_d - s_c)^B = 293\,\text{K} \times 1000\,\text{kg} \times 0.6483\,\text{kJ/kg K} = 189{,}950\,\text{kJ}$$

$$(\in_d - \in_c)^B = 209{,}000\,\text{kJ} - 189{,}950\,\text{kJ} = 19{,}050\,\text{kJ}$$

Thus, the exergy efficiency (see Equation 6.49) for Case A is

$$\psi^A = \frac{(\in_d - \in_c)^A}{\in_a - \in_b} = \frac{6977\ \text{kJ}}{26{,}157\ \text{kJ}} = 0.267$$

and for Case B

$$\psi^B = \frac{(\in_d - \in_c)^B}{\in_a - \in_b} = \frac{19{,}050\ \text{kJ}}{26{,}157\ \text{kJ}} = 0.728$$

which is considerably higher than for Case A.

The exergy losses (total) can be evaluated with Equation 6.40a (with $\Delta \Xi = 0$) as the sum of the exergy loss associated with heat loss to the surroundings and the exergy loss due to internal exergy consumptions:

$$(X_l + I)^A = (\in_a - \in_b) - (\in_d - \in_c)^A = 26{,}157\,\text{kJ} - 6977\,\text{kJ} = 19{,}180\,\text{kJ}$$

$$(X_l + I)^B = (\in_a - \in_b) - (\in_d - \in_c)^B = 26{,}157\,\text{kJ} - 19{,}050\,\text{kJ} = 7107\,\text{kJ}$$

Here, no attempt has been made to evaluate the individual values of the two exergy loss parameters. If it is assumed that heat is transferred at T_o to the surroundings, then $X_l^A = X_l^B = 0$, and all the exergy losses are internal consumptions.

Table 6.5 Comparison of the performance of a TES for two cases

	Case A	Case B
General parameters		
Storing period (days)	1	100
Charging-fluid temperatures (in/out) (°C)	85/25	85/25
Discharging-fluid temperatures (in/out) (°C)	25/35	25/75
Energy parameters		
Energy input (kJ)	250,800	250,800
Energy recovered (kJ)	209,000	209,000
Energy loss (kJ)	41,800	41,800
Energy efficiency (%)	83.3	83.3
Exergy parameters		
Exergy input (kJ)	26,157	26,157
Exergy recovered (kJ)	6,977	19,050
Exergy loss (kJ)	19,180	7,107
Exergy efficiency (%)	26.7	72.8

Comparative Summary

The two cases are summarized and compared in Table 6.5. Although the same quantity of energy is discharged for Cases A and B, a greater quantity of exergy is discharged for Case B. In addition, Case B stores the energy and exergy for a greater duration of time.

6.4.7 Closure

This section demonstrates the application of exergy analysis to closed TES systems. The use of exergy analysis clearly takes into account the external and temperature losses in TES operations, and hence it more correctly reflects their thermodynamic behavior. Exergy and energy analyses do not quantitatively assess the value associated with the length of time the heat is held in storage, so this factor must be considered separately. Other TES types are considered in subsequent sections.

6.5 Appropriate Efficiency Measures for Closed TES Systems

Generally accepted standards have not been established for TES evaluation and comparison for at least two reasons. First, many different but valid efficiency measures can be defined. As shown in Table 6.3, for example, TES energy efficiency can be defined as the ratio of energy recovered to energy input, or as the ratio of energy recovered and remaining in a TES to energy input and originally in the TES; both definitions are reasonable but can yield different values in some circumstances. Secondly, while most TES efficiency definitions are based on energy, more meaningful efficiencies can be defined based on exergy, which takes into account temperature level (and hence quality) of the energy transferred.

In this section, several categories of TES energy and exergy efficiencies are discussed, following an earlier analysis (Rosen, 1992b). The overall storage process and the charging, storing, and discharging subprocesses are considered. An illustrative example is presented. This section is an extension of the previous one where a limited set of TES efficiencies are considered and helps determine which efficiencies are most appropriate in different circumstances.

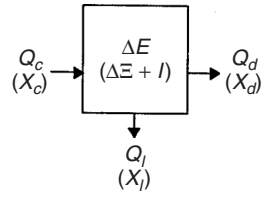

Figure 6.5 The overall heat storage process, showing energy parameters (terms not in parentheses) and exergy parameters (terms in parentheses)

6.5.1 TES Model Considered

As in Section 6.4, a simple TES model is considered, which undergoes a storage process (Figure 6.5) involving distinct charging, storing, and discharging periods (Figure 6.6). The model is described in Section 6.4.1. Heat is transferred at specified temperatures to and from the TES. For simplicity, only the net thermal energy and thermal exergy transfers associated with material flows are considered here, rather than the energy and exergy values of the material flows themselves.

6.5.2 Energy and Exergy Balances

Energy and exergy balances for the overall storage process (Figure 6.5) can be expressed, following Equations 6.37 and 6.40, respectively, as

$$Q_c - (Q_d + Q_l) = \Delta E \tag{6.74}$$

$$X_c - (X_d + X_l) - I = \Delta\Xi \tag{6.75}$$

where Q_c, Q_d, and Q_l denote respectively the heat input during charging, recovered during discharging, and lost during the entire process; and X_c, X_d, and X_l denote respectively the exergy transfers associated with Q_c, Q_d, and Q_l. For the case of a complete cycle (i.e., a process with identical initial and final states), $\Delta E = \Delta\Xi = 0$. The exergy Ξ can be written with Equation 6.18 which, for a tank of constant volume and a working fluid that behaves ideally, becomes

$$\Xi = mc_v[(T - T_o) - T_o \ln(T/T_o)] \tag{6.76}$$

where T, c_v, and m respectively denote for the TES temperature, specific heat at constant volume, and mass. The terms Q_l, X_l, I, ΔE, and $\Delta\Xi$ can be written in terms of subprocess values as in Equations 6.39, 6.42, 6.70, and 6.71, respectively.

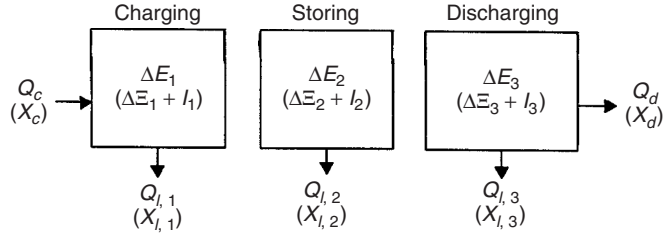

Figure 6.6 The three periods in the overall heat storage process (charging, storing, and discharging), showing energy parameters (not in parentheses) and the exergy parameters (in parentheses)

Energy and exergy balances, respectively, can be written for the charging period as in Equations 6.50a (with Q_c replacing $H_a - H_b$) and 6.53 (with X_c replacing $\in_a - \in_b$), for the storing period as in Equations 6.56a and 6.59a, and for the discharging period as in Equations 6.62a (with Q_d replacing $H_d - H_c$) and 6.65a (with X_d replacing $\in_d - \in_c$).

By introducing the definition $E' \equiv E - E_o$, where E' represents the TES energy content, Equations 6.70 and 6.72 can be written as

$$\Delta E = (E_f - E_o) - (E_i - E_o) = E'_f - E'_i \tag{6.70a}$$

$$\Delta E_j = (E_{f,j} - E_o) - (E_{i,j} - E_o) = E'_{f,j} - E'_{i,j} \tag{6.72a}$$

The terms Ξ and E' are analogous (e.g., both are equal to zero at the dead state, i.e., $\Xi_o = E'_o = 0$).

6.5.3 Energy and Exergy Efficiencies

Since several quantities can be considered to be products and inputs for TES systems, various efficiency definitions are possible. For each subprocess and the overall storage process, energy and exergy efficiencies are evaluated here based on the quantities of heat transferred to and from a TES, the temperatures at which the heat transfers occur, and the initial and final TES states. Furthermore, for each energy and exergy efficiency, four cases are considered (where possible). The initial energy or exergy in the store is neglected in Cases *A* and *B*, and accounted for in Cases *C* and *D*, while the net accumulation of energy or exergy in the store is treated as a loss for Cases *A* and *C*, and as a product for Cases *B* and *D*. Here, efficiency cases are denoted by superscripts and, following the notation introduced earlier, efficiencies with subscripts denote period efficiencies while efficiencies without subscripts denote overall efficiencies. Other efficiency cases are possible but not considered here.

6.5.4 Overall Efficiencies

The following four overall energy efficiency η definitions are considered:

$$\eta^A = \frac{\text{Energy recovered}}{\text{Energy input}} = 1 - \frac{\text{Energy loss} + \text{Energy accumulation}}{\text{Energy input}}$$

$$\eta^A = \frac{Q_d}{Q_c} = 1 - \frac{Q_l + \Delta E}{Q_c} \tag{6.77}$$

$$\eta^B = \frac{\text{Energy recovered} + \text{Energy accumulation}}{\text{Energy input}} = 1 - \frac{\text{Energy loss}}{\text{Energy input}}$$

$$\eta^B = \frac{Q_d + \Delta E}{Q_c} = 1 - \frac{Q_l}{Q_c} \tag{6.77a}$$

$$\eta^C = \frac{\text{Energy recovered}}{\text{Energy input} + \text{Initial energy in store}} = 1 - \frac{\text{Energy loss} + \text{Final energy in store}}{\text{Energy input} + \text{Initial energy in store}}$$

$$\eta^C = \frac{Q_d}{Q_c + E'_i} = 1 - \frac{Q_l + E'_f}{Q_c + E'_i} \tag{6.77b}$$

$$\eta^D = \frac{\text{Energy recovered} + \text{Final energy in store}}{\text{Energy input} + \text{Initial energy in store}} = 1 - \frac{\text{Energy loss}}{\text{Energy input} + \text{Initial energy in store}}$$

$$\eta^D = \frac{Q_d + E'_f}{Q_c + E'_i} = 1 - \frac{Q_l}{Q_c + E'_i} \tag{6.77c}$$

Four overall exergy efficiencies, analogous to those in Equations 6.77–6.77c, respectively, are defined:

$$\psi^A = \frac{X_d}{X_c} = 1 - \frac{X_l + I + \Delta\Xi}{X_c} \tag{6.78}$$

$$\psi^B = \frac{X_d + \Delta\Xi}{X_c} = 1 - \frac{X_l + I}{X_c} \tag{6.78a}$$

$$\psi^C = \frac{X_d}{X_c + \Xi_i} = 1 - \frac{X_l + I + \Xi_f}{X_c + \Xi_i} \tag{6.78b}$$

$$\psi^D = \frac{X_d + \Xi_f}{X_c + \Xi_i} = 1 - \frac{X_l + I}{X_c + \Xi_i} \tag{6.78c}$$

Note that $\eta^A = \eta^B = \eta^C = \eta^D$ if $E_i' = E_f' = 0$, and $\psi^A = \psi^B = \psi^C = \psi^D$ if $\Xi_i = \Xi_f = 0$, while $\eta^A = \eta^B$ if $\Delta E = 0$, and $\psi^A = \psi^B$ if $\Delta\Xi = 0$. Also, if $\Delta E < 0$ and $\Delta\Xi < 0$, the definitions for Cases *A* and *B* do not provide rational measures of performance for normal applications, while those for Cases *C* and *D* do. Furthermore, if the store is adiabatic, $Q_{l,j} = X_{l,j} = 0$, and all the efficiencies simplify (e.g., the energy efficiencies in Equations 6.77a and c become 100%).

6.5.5 Charging-Period Efficiencies

The following two energy efficiency definitions for the charging period are considered:

$$\eta_1^B = \frac{\text{Energy accumulation}}{\text{Energy input}} = 1 - \frac{\text{Energy loss}}{\text{Energy input}}$$

$$\eta_1^B = \frac{\Delta E_1}{Q_c} = 1 - \frac{Q_{l,1}}{Q_c} \tag{6.79}$$

$$\eta_1^D = \frac{\text{Final energy in store}}{\text{Energy input} + \text{Initial energy in store}} = 1 - \frac{\text{Energy loss}}{\text{Energy input} + \text{Initial energy in store}}$$

$$\eta_1^D = \frac{E_{f,1}'}{Q_c + E_{i,1}'} = 1 - \frac{Q_{l,1}}{Q_c + E_{i,1}'} \tag{6.79a}$$

Two analagous exergy efficiencies are defined:

$$\psi_1^B = \frac{\Delta\Xi_1}{X_c} = 1 - \frac{X_{l,1} + I_1}{X_c} \tag{6.80}$$

$$\psi_1^D = \frac{\Xi_{F,1}}{X_c + \Xi_{I,1}} = 1 - \frac{X_{L,1} + I_1}{X_c + \Xi_{I,1}} \tag{6.80a}$$

Meaningful charging-period efficiencies cannot be defined for Cases *A* and *C*, since accumulations are treated as losses for these cases, resulting in the efficiencies reducing to zero.

6.5.6 Storing-Period Efficiencies

As for the charging period, only two sets of storing-period efficiencies can be defined. The two energy efficiencies are

$$\eta_2^B = \frac{\text{Energy accumulation during charging and storing}}{\text{Energy accumulation during charging}}$$

$$= 1 - \frac{\text{Energy loss during storing}}{\text{Energy accumulation during charging}}$$

$$\eta_2^B = \frac{\Delta E_1 + \Delta E_2}{\Delta E_1} = 1 - \frac{Q_{l,2}}{\Delta E_1} \tag{6.81}$$

$$\eta_2^D = \frac{\text{Final energy in store}}{\text{Initial energy in store}} = 1 - \frac{\text{Energy loss during storing}}{\text{Initial energy in store}}$$

$$\eta_2^D = \frac{E'_{f,2}}{E'_{i,2}} = 1 - \frac{Q_{l,2}}{E'_{i,2}} \tag{6.81a}$$

and the two corresponding exergy efficiencies are

$$\psi_2^B = \frac{\Delta \Xi_1 + \Delta \Xi_2}{\Delta \Xi_1} = 1 - \frac{X_{l,2} + I_2}{\Delta \Xi_1} \tag{6.82}$$

$$\psi_2^D = \frac{\Xi_{f,2}}{\Xi_{i,2}} = 1 - \frac{X_{l,2} + I_2}{\Xi_{i,2}} \tag{6.82a}$$

It can be shown that $\eta_2^B = \eta_2^D$ if $E'_{i,1} = 0$, and $\psi_2^B = \psi_2^D$ if $\Xi_{i,1} = 0$.

6.5.7 Discharging-Period Efficiencies

Four discharging-period energy efficiencies are considered:

$$\eta_3^A = \frac{Q_d}{\Delta E_1 + \Delta E_2} = 1 - \frac{\Delta E + Q_{l,3}}{\Delta E_1 + \Delta E_2} \tag{6.83}$$

where Q_d is energy recovered, ΔE_1 and ΔE_2 are energy accumulation during charging and storing, ΔE is overall energy accumulation, and $Q_{l,3}$ is energy loss.

$$\eta_3^B = \frac{Q_d + \Delta E}{\Delta E_1 + \Delta E_2} = 1 - \frac{Q_{l,3}}{\Delta E_1 + \Delta E_2} \tag{6.83a}$$

where Q_d is energy recovered, ΔE_1 and ΔE_2 are energy accumulation during charging and storing, ΔE is overall energy accumulation, and $Q_{l,3}$ is energy loss.

$$\eta_3^C = \frac{\text{Energy recovered}}{\text{Initial energy in store}} = 1 - \frac{\text{Final energy in store} + \text{Energy loss}}{\text{Initial energy in store}}$$

$$\eta_3^C = \frac{Q_d}{E'_{i,3}} = 1 - \frac{E'_{f,3} + Q_{l,3}}{E'_{i,3}} \tag{6.83b}$$

$$\eta_3^D = \frac{\text{Energy recovered} + \text{Final energy in store}}{\text{Initial energy in store}} = 1 - \frac{\text{Energy loss}}{\text{Initial energy in store}}$$

$$\eta_3^D = \frac{Q_d + E'_{f,3}}{E'_{i,3}} = 1 - \frac{Q_{l,3}}{E'_{i,3}} \tag{6.83c}$$

Four analogous exergy efficiencies are defined:

$$\psi_3^A = \frac{X_d}{\Delta \Xi_1 + \Delta \Xi_2} = 1 - \frac{\Delta \Xi + X_{l,3} + I_3}{\Delta \Xi_1 + \Delta \Xi_2} \tag{6.84}$$

$$\psi_3^B = \frac{X_d + \Delta \Xi}{\Delta \Xi_1 + \Delta \Xi_2} = 1 - \frac{X_{l,3} + I_3}{\Delta \Xi_1 + \Delta \Xi_2} \tag{6.84a}$$

$$\psi_3^C = \frac{X_d}{\Xi_{i,3}} = 1 - \frac{X_{l,3} + I_3 + \Xi_{f,3}}{\Xi_{i,3}} \tag{6.84b}$$

$$\psi_3^D = \frac{X_d + \Xi_{f,3}}{\Xi_{i,3}} = 1 - \frac{X_{l,3} + I_3}{\Xi_{i,3}} \tag{6.84c}$$

6.5.8 Summary of Efficiency Definitions

The efficiency definitions in the four preceding subsections are summarized in Table 6.6. Although all the efficiencies are useful in specific applications, the choice of definition depends on the specific application and the aspect of performance considered critical. Many of the efficiencies discussed here are applied in practice and some are used in Section 6.4, but with Q_c (or X_c) given as the difference between the total enthalpy (or exergy) of the fluid passing into and out of the store during charging, and Q_d (or X_d) as the corresponding difference during discharging.

For the assumptions considered in this section, it can be shown for Cases B and D that the overall efficiency is the product of the three corresponding subprocess efficiencies, that is,

$$\eta^B = \prod_{j=1}^{3} \eta_j^B \tag{6.85}$$

$$\eta^D = \prod_{j=1}^{3} \eta_j^D \tag{6.86}$$

$$\psi^B = \prod_{j=1}^{3} \psi_j^B \tag{6.87}$$

$$\psi^D = \prod_{j=1}^{3} \psi_j^D \tag{6.88}$$

Table 6.6 Summary of possible efficiency definitions for closed TES systems[a]

	Energy Efficiency, η			
Period	Case A	Case B	Case C	Case D
Overall	$\frac{Q_d}{Q_c}$	$\frac{Q_d + \Delta E}{Q_c}$	$\frac{Q_d}{Q_c + E_i'}$	$\frac{Q_d + E_f'}{Q_c + E_i'}$
Charging (1)	–	$\frac{\Delta E + 1}{Q_c}$	–	$\frac{E_{f,1}'}{Q_c + E_{i,1}'}$
Storing (2)	–	$\frac{\Delta E_1 + \Delta E_2}{\Delta E_1}$	–	$\frac{E_{f,2}'}{E_{i,2}'}$
Discharging (3)	$\frac{Q_d}{\Delta E_1 + \Delta E_2}$	$\frac{Q_d + \Delta E}{\Delta E_1 + \Delta E_2}$	$\frac{Q_d}{E_{i,3}'}$	$\frac{Q_d + E_{f,3}'}{E_{i,3}'}$
	Exergy Efficiency, ψ			
Period	Case A	Case B	Case C	Case D
Overall	$\frac{X_d}{X_c}$	$\frac{X_d + \Delta \Xi}{X_c}$	$\frac{X_d}{X_c + \Xi_i}$	$\frac{X_d + \Xi_f}{X_c + \Xi_i}$
Charging (1)	–	$\frac{\Delta \Xi_1}{X_c}$	–	$\frac{\Xi_{f,1}}{X_c + \Xi_{i,1}}$
Storing (2)	–	$\frac{\Delta \Xi_1 + \Delta \Xi_2}{\Delta \Xi_1}$	–	$\frac{\Xi_{f,2}}{\Xi_{i,2}}$
Discharging (3)	$\frac{X_d}{\Delta \Xi_1 + \Delta \Xi_2}$	$\frac{X_d + \Delta \Xi}{\Delta \Xi_1 + \Delta \Xi_2}$	$\frac{X_d}{\Xi_{i,3}}$	$\frac{X_d + \Xi_{f,3}}{\Xi_{i,3}}$

[a]Charging and storing efficiencies are not defined for Cases A and C. The cases listed across the top are denoted by superscripts, and the periods along the left side by subscripts (e.g., the lower left entry corresponds to η_3^A and the upper right entry to ψ^D).

By noting the similarities between Cases A and B and between Cases C and D, it can also be shown that

$$\eta^A = \eta_1^B \eta_2^B \eta_3^A \tag{6.89}$$

$$\eta^C = \eta_1^D \eta_2^D \eta_3^C \tag{6.90}$$

$$\psi^A = \psi_1^B \psi_2^B \psi_3^A \tag{6.91}$$

$$\psi^C = \psi_1^D \psi_2^D \psi_3^C \tag{6.92}$$

6.5.9 *Illustrative Example*

Problem Statement

A TES that undergoes discrete charging, storing, and discharging processes is considered. Three modes of operation are considered and defined according to the sign of the energy and exergy accumulations during the overall storing process:

I. $\Delta E > 0$ and $\Delta \Xi > 0$;
II. $\Delta E = \Delta E \Xi = 0$, that is, a complete storage cycle; and
III. $\Delta E < 0$ and $\Delta \Xi < 0$.

For all modes of operation, and with values in kilojoules, $Q_c = 100$, $Q_{l,1} = Q_{l,3} = 5$, $Q_{l,2} = 10$, $E'_{i,1} = 20$, $X_{l,j} = 0$ for all j, $\Xi_{i,1} = 1$, $I_1 = 4$, and $I_2 = I_3 = 1$. For modes I, II, and III, respectively, Q_d is 60, 80, and 100 kJ. Also, $X_c = 0.1 \times Q_c$ and $X_d = 0.05 \times Q_d$. Note that the specification of the exergy parameters involves assumptions regarding the temperatures associated with the heat transfers Q_c, Q_d, and $Q_{l,j}$ (e.g., the fact that $X_{l,j} = 0$ and $Q_{l,j} \neq 0$ for all j, implies that heat transfers $Q_{l,j}$ occur at the environmental temperature T_o). The specified parameter values are chosen so as to represent a realistic but simple case.

Results and Discussion

Unknown parameter values are evaluated using the previously specified values and energy and exergy balances. Following the format of Figure 6.6, all relevant values are summarized illustratively in Figure 6.7 for energy parameters and in Figure 6.8 for exergy parameters. Since the charging and storing processes are identical for all three modes of operation, they are illustrated only once, while the discharging process is shown for each operation mode. Values for ΔE and $\Delta \Xi$ are not shown in Figures 6.7 and 6.8, but by substituting subprocess values for ΔE_j and $\Delta \Xi_j$ from Figures 6.7 and 6.8 into Equations 6.70 and 6.71, can be shown to be (in kJ) as follows: $\Delta E = 20$ and $\Delta \Xi = 1$ for mode of operation I, $\Delta E = \Delta \Xi = 0$ for mode II, and $\Delta E = -20$ and $\Delta \Xi = -1$ for mode III. The exergy values associated with all heat transfers in Figure 6.8 are significantly less than the corresponding energy values in Figure 6.7, reflecting the fact that for most TES applications, the temperatures associated with all heat transfers are relatively low (between T_o and $2T_o$). These values indicate that the usefulness of thermal energy transferred at a practical temperature is significantly less than an equal quantity of any work-equivalent energy form.

Efficiencies are evaluated according to the expressions in Table 6.6, and tabulated in the same format in the top, middle, and bottom sections of Table 6.7 for operation modes I, II, and III, respectively. The corresponding efficiencies for modes I to III are the same for charging and storing since these processes are independent of mode of operation. Several points are demonstrated in Table 6.7. First, all exergy efficiency values are less than the corresponding energy efficiency values, due to the degradation of temperature as heat is transferred and stored. Since this degradation is reflected in efficiencies based on exergy and not in those based on energy, exergy efficiencies are

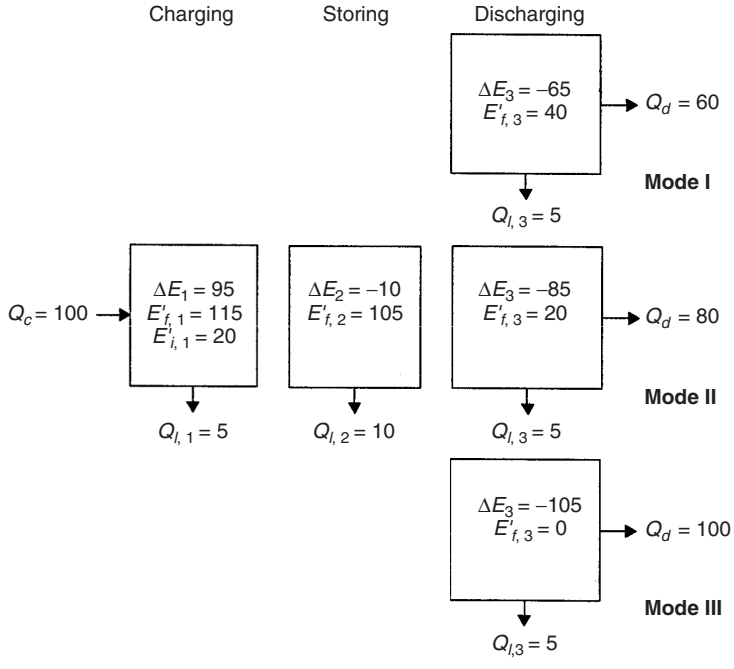

Figure 6.7 Energy values (in kJ) for the example, showing the three modes of operation (I, II, and III) and the three storing periods (charging, storing, and discharging)

considered more meaningful. Second, for energy and exergy efficiencies for all periods, the values of the calculated efficiencies are different for Cases *A* to *D*. The achievement of consistent comparisons and evaluations of performance requires that care be exercised in selecting efficiency definitions. Third, some efficiency values are not meaningful because they are not based on rational measures of performance for the operation mode considered. For example, consider, for Case A and operation mode III, the overall energy efficiency ($\eta^A = 100\%$), the discharging energy efficiency ($\eta_3^A = 118\%$), and the discharging exergy efficiency ($\psi_3^A = 100\%$). These efficiency values consider the percentage of the input energy or exergy that is discharged, but are not rational measures because they do not account for the fact that part of the discharged energy and exergy is attributable to energy and exergy in the TES before the charging process began. Thus, the efficiency definitions presented for Cases *B* to *D* are more meaningful for mode of operation III.

Several generalizations can be made for each of the three modes of operation with respect to the validity and meaningfulness of the efficiency definitions for the different cases. For mode I, the definitions for Cases *B* and *D* are preferred. The definitions for Cases *A* and *C*, although valid, can be misleading because they neglect the fact that some of the charging energy or exergy increases the internal energy or exergy of the TES. For mode II (the complete storage cycle), the definitions for all cases are valid and meaningful. For mode III, the definitions for Cases *B* and *D* are preferred. As discussed in the previous paragraph, the definition for Case *A* is not rational for mode III, while that for Case *C*, although valid, can be misleading.

6.5.10 Closure

Several key points are discussed in this section. First, many valid and meaningful TES efficiency definitions exist. Differences in definitions normally depend on which quantities are considered to

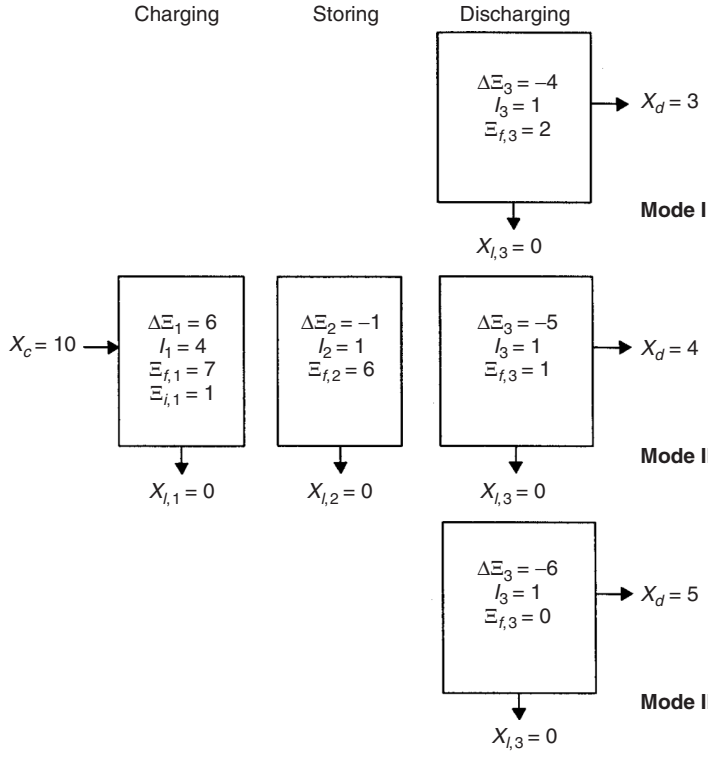

Figure 6.8 Exergy values (in kJ) for the example, showing the three modes of operation and the three storing periods

Table 6.7 Efficiency values (in %) for the illustrative example

	Energy efficiency, η				Exergy efficiency, ψ			
Period	A	B	C	D	A	B	C	D
Mode of operation I								
Overall	60	80	50	83	30	40	27	45
Charging (1)	–	95	–	96	–	60	–	64
Storing (2)	–	89	–	91	–	83	–	86
Discharging (3)	71	94	57	95	60	80	50	83
Mode of operation II								
Overall	80	80	67	83	40	40	36	45
Charging (1)	–	95	–	96	–	60	–	64
Storing (2)	–	89	–	91	–	83	–	86
Discharging (3)	94	94	76	95	80	80	67	83
Mode of operation III								
Overall	100	80	83	83	50	40	45	45
Charging (1)	–	95	–	96	–	60	–	64
Storing (2)	–	89	–	91	–	83	–	86
Discharging (3)	118	94	95	95	100	80	83	83

be products and inputs. Second, different efficiency definitions are appropriate in different situations and when different aspects of performance are being evaluated. Of course, efficiency comparisons for different TES systems are logical only if the efficiencies are based on common definitions. Third, exergy efficiencies, because they measure how nearly a system approaches ideal performance and account for the loss of temperature in TES systems, are generally more meaningful and illuminating than energy efficiencies, and may prove useful in establishing standards for TES evaluation and comparison.

6.6 Importance of Temperature in Performance Evaluations for Sensible TES Systems

Being energy-based, most existing TES evaluation measures disregard the temperatures associated with the heat injected into and recovered from a TES. Examining energy efficiencies alone can result in misleading conclusions because such efficiencies weight all thermal energy equally. Exergy efficiencies acknowledge that the usefulness of thermal energy depends on its quality, which is related to its temperature level, and are therefore more suitable for determining how advantageous is one TES relative to another.

This section discusses the importance of temperature in TES performance evaluations, following an earlier report (Rosen, 1991). The energy and exergy efficiencies for a simple sensible TES system are compared and the differences between them highlighted. It is demonstrated that exergy analysis weights the usefulness of thermal energy appropriately, while energy analysis tends to present overly optimistic views of TES performance by neglecting the temperature levels associated with thermal energy flows. The concepts are illustrated by examining several TES systems.

6.6.1 Energy, Entropy, and Exergy Balances for the TES System

Consider a process involving only heat interactions and occurring in a closed system for which the state is the same at the beginning and end of the process. Balances of energy and exergy, respectively, can be written for the system using Equations 6.3b and 6.5b as follows:

$$\sum_r Q_r = 0 \tag{6.93}$$

$$\sum_r X_r - I = 0 \tag{6.94}$$

where I denotes the exergy consumption, and X_r denotes the exergy associated with Q_r, the heat transferred into the system across region r at temperature T_r. Note that the exergetic temperature factor τ is illustrated as a function of the temperature ratio T/T_o in Figure 6.1, and these parameters are compared with the temperature T in Table 6.8 for above-environmental temperatures (i.e., for $T \geq T_o$), the temperature range of interest for most heat storages.

6.6.2 TES System Model Considered

Consider the overall storage process for the general TES system shown in Figure 6.9. Heat Q_c is injected into the system at a constant temperature T_c during a charging period. After a storing period, heat Q_d is recovered at a constant temperature T_d during a discharging period. During all periods, heat Q_l leaks from the system at a constant temperature T_l and is lost to the surroundings.

For normal heating applications, the temperatures T_c, T_d, and T_l exceed the environment temperature T_o, but the discharging temperature cannot exceed the charging temperature. Hence, the exergetic temperature factors for the charged and discharged heat are subject to the constraint $0 \leq \tau_d \leq \tau_c \leq 1$.

Table 6.8 Relation between several temperature parameters for above-environment temperatures[a]

T/T_o	T (K)	τ
1.00	283	0.00
1.25	354	0.20
1.50	425	0.33
2.00	566	0.50
3.00	849	0.67
5.00	1415	0.80
10.00	2830	0.90
100.00	28,300	0.99
Infinity	Infinity	1.00

[a]The reference-environment temperature is $T_o = 10\ ^\circ\text{C} = 283\ \text{K}$.

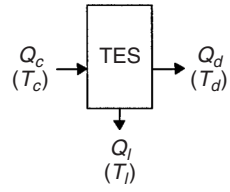

Figure 6.9 The overall heat storage process for a general TES system. Shown are heat flows and associated temperatures at the TES boundary (terms in parentheses). The corresponding energy and exergy parameters are shown for this system in Figure 6.5

6.6.3 *Analysis*

The energy and exergy balances in Equations 6.93 and 6.94, respectively, can be written for the modeled system as

$$Q_c = Q_d + Q_l \tag{6.93a}$$

and

$$X_c = X_d + X_l + I \tag{6.94a}$$

With Equation 6.25a, the exergy balance can be expressed as

$$Q_c\tau_c = Q_d\tau_d + Q_l\tau_l + I \tag{6.94b}$$

Following the general energy and exergy efficiency statements in Equations 6.32 and 6.33, the energy efficiency can be written for the modeled system as

$$\eta = \frac{Q_d}{Q_c} \tag{6.95}$$

and the exergy efficiency (with Equations 6.25a and 6.95) as

$$\psi = \frac{X_d}{X_c} = \frac{Q_d\tau_d}{Q_c\tau_c} = \frac{\tau_d}{\tau_c}\eta \tag{6.96}$$

6.6.4 Comparison of Energy and Exergy Efficiencies

An illuminating parameter for comparing the efficiencies is the ratio ψ/η. For the general TES system above, Equation 6.96 implies that the energy-efficiency-to-exergy-efficiency ratio can be expressed as

$$\frac{\psi}{\eta} = \frac{\tau_d}{\tau_c} \tag{6.97}$$

With Equation 6.25a, Equation 6.97 can be alternatively expressed as

$$\frac{\psi}{\eta} = \frac{(T_d - T_o)T_c}{(T_c - T_o)T_d} \tag{6.97a}$$

The ratio ψ/η is plotted against τ_d for several values of τ_c in Figure 6.10. It is seen that ψ/η varies linearly with τ_d for a given value of τ_c. Also, if the product heat is delivered at the charging temperature (i.e., $\tau_d = \tau_c$), $\psi = \eta$, while if the product heat is delivered at the temperature of the environment (i.e., $\tau_d = 0$), $\psi = 0$ regardless of the charging temperature. In the first case, there is no loss of temperature during the entire storage process, while in the second there is complete loss of temperature. The largest deviation between values of ψ and η occurs in the second case.

The deviation between ψ and η is significant for most present day TES systems. This can be seen by noting that (i) most TES systems operate between charging temperatures as high as $T_c = 130$ °C and discharging temperatures as low as $T_d = 40$ °C, and (ii) a difference of about 30°C between charging and discharging temperatures is utilized in most TES systems (i.e., $T_c - T_d = 30$°C). With Equation 6.26 and $T_o = 10$°C, the first condition can be shown to imply for most present day systems that $0.1 \leq \tau_d \leq \tau_c \leq 0.3$. Since it can be shown with Equation 6.26 that

$$\tau_c - \tau_d = \frac{(T_c - T_d)T_o}{T_c T_d} \tag{6.98}$$

the difference in exergetic temperature factor varies roughly between 0.06 and 0.08. Then the value of the exergy efficiency is nearly 50–80% of that of the energy efficiency.

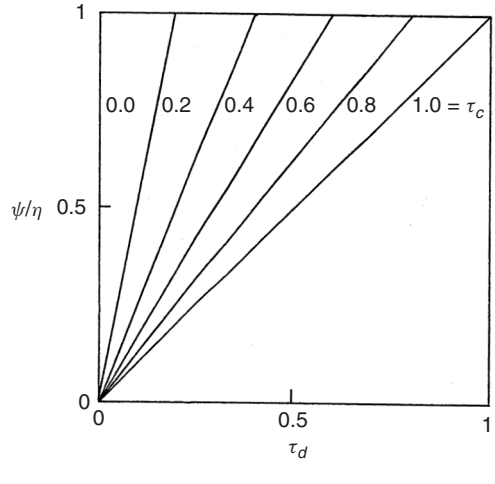

Figure 6.10 Energy-efficiency-to-exergy-efficiency ratio, ψ/η, as a function of the discharging exergetic temperature factor τ_d, for several values of the charging exergetic temperature factor τ_c

Table 6.9 Values of the ratio ψ/η for a range of practical values for T_d and T_c[a]

Discharging temperature,	Charging temperature, T_c (°C)			
T_d(°C)	40	70	100	130
40	1.00	0.55	0.40	0.32
70	–	1.00	0.72	0.59
100	–	–	1.00	0.81
130	–	–	–	1.00

[a]The reference-environment temperature is $T_o = 10\ ^\circ\text{C} = 283\ \text{K}$.

6.6.5 *Illustration*

The ratio ψ/η is illustrated in Table 6.9 for a simple TES having charging and discharging temperatures ranging between 40 °C and 130 °C, and a reference-environment temperature of $T_o = 10^\circ\text{C}$. The energy and exergy efficiencies differ (with the exergy efficiency always being the lesser of the two) when $T_d < T_c$, and the difference becomes more significant as the difference between T_c and T_d increases. The efficiencies are equal only when the charging and discharging temperatures are equal (i.e., $T_d = T_c$), and no values of the ratio ψ/η are reported for the cases when $T_c < T_d$, since such situations are not physically possible. Unlike the exergy efficiencies, the energy efficiencies tend to appear overly optimistic, in that they only account for losses attributable to heat leakages but ignore temperature degradation.

6.6.6 *Closure*

This section demonstrates the importance of temperature in TES performance evaluations. Exergy efficiencies are seen to be more illuminating than energy efficiencies because they weight heat flows appropriately, being sensitive to both the fraction of the heat injected into a TES that is recovered and the temperature at which heat is recovered relative to the temperature at which it is injected. Energy efficiencies are only sensitive to the first of the above factors. TES energy efficiencies are good approximations to exergy efficiencies when there is little temperature degradation, as thermal energy quantities then have similar qualities. In most practical situations, however, thermal energy is injected and recovered at significantly different temperatures, making energy efficiencies both poor approximations to exergy efficiencies and prone to lead to erroneous interpretations and conclusions.

6.7 Exergy Analysis of Aquifer TES Systems

Underground aquifers are the storage type considered in this section (Jenne, 1992). The storage medium in many aquifer thermal energy storage (ATES) systems remains in a single phase during the storing cycle, so that temperature changes are exhibited in the store as thermal energy is added or removed. To assess ATES systems and to integrate them into larger thermal systems properly, their characteristics must be accurately expressed. As for TES systems, standards have not been established for evaluating and comparing the performance of different ATES systems, and conventional energy-based performance measures are often misleading. Exergy methods are advantageous in this regard.

In this section, the application of exergy analysis to ATES systems is described, following a previous assessment (Rosen, 1999b). For an elementary ATES model, expressions are presented for the

injected and recovered quantities of energy and exergy and for efficiencies. The impact is examined of introducing a threshold temperature below which residual heat remaining in the aquifer water is not considered worth recovering. ATES exergy efficiencies are demonstrated to be more useful and meaningful than energy efficiencies because the former account for the temperatures associated with thermal energy transfers and consequently assess how nearly ATES systems approach ideal thermodynamic performance. ATES energy efficiencies do not provide a measure of approach to ideal performance and, in fact, are often misleadingly high because some of the thermal energy can be recovered at temperatures too low for useful purposes. A case study using realistic ATES parameter values is presented.

6.7.1 ATES Model

Charging of the ATES occurs over a finite time period t_c and after a holding interval discharging occurs over a period t_d. The working fluid is water, having a constant specific heat c, and assumed incompressible. The temperature of the aquifer and its surroundings prior to heat injection is T_o, the reference-environment temperature. Only heat stored at temperatures above T_o is considered, and pump work is neglected.

Charging and Discharging

During charging, heated water at a constant temperature T_c is injected at a constant mass flow rate $\dot{m}_c$ into the ATES. Then, after a storing period, discharging occurs, during which water is extracted from the ATES at a constant mass flow rate $\dot{m}_d$. The fluid discharge temperature is taken to be a function of time, that is, $T_d = T_d(t)$. The discharge temperature after an infinite time is taken to be the temperature of the reference-environment, that is, $T_d(\infty) = T_o$, and the initial discharge temperature is taken to be between the charging and reference-environment temperatures, that is, $T_o \le T_d(0) \le T_c$.

Many discharge temperature–time profiles are possible. The discharge temperature may be taken to decrease linearly with time from an initial value $T_d(0)$ to a final value T_o. The final temperature is reached at a time t_f and remains fixed at T_o for all subsequent times, that is,

$$T_d(t) = \begin{cases} T_d(0) - (T_d(0) - T_o t/t_f, & 0 \le t \le t_f \\ T_0, & t_f \le t \le \infty \end{cases} \tag{6.99}$$

Alternatively, the discharge temperature can be expressed as

$$T_d(t) = T_o + (T_d(0) - T_o)e^{-\alpha t} \tag{6.99a}$$

Here, the discharge temperature decreases with time asymptotically toward the environment temperature T_o, at a rate controlled by the arbitrary constant α. Of course, these and other models of discharging temperature–time profiles are simply elementary representations of events that are often more complicated in actual devices.

The simple linear discharge temperature–time profile (Equation 6.99) is used here because, for the purposes of this section, most of the other possible discharge temperature–time profiles are inconveniently complex mathematically. The linear profile is sufficiently realistic and simple to illustrate the importance of using exergy analysis in ATES evaluation and comparison, without obscuring the central ideas of the section. The temperature–time profiles considered in the present model for the fluid flows during the charging and discharging periods are summarized in Figure 6.11.

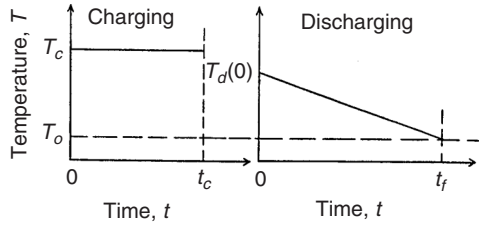

Figure 6.11 Temperature–time profiles assumed for the charging and discharging periods in the ATES model considered

Thermodynamic Losses

The two main types of thermodynamic losses that occur in ATES systems are accounted for in the model:

- **Energy losses.** Energy injected into an ATES that is not recovered is considered lost. Thus, energy losses include energy remaining in the ATES at a point where it could still be recovered if pumping were continued, and energy injected into the ATES that is convected in a water flow or is transferred by conduction far enough from the discharge point that it is unrecoverable, regardless of how much or how long water is pumped out of the ATES. The effect of energy losses is that less than 100% of the injected energy is recoverable after storage.
- **Mixing losses.** As heated water is pumped into an ATES, it mixes with the water already present (which is usually cooler), resulting in the recovered water being at a lower temperature than the injected water. In the present model, this loss results in the discharge temperature T_d being at all times less than or equal to the charging temperature T_c, but not below the reference-environment temperature T_o(i.e., $T_o \leq T_d(t) \leq T_c$ for $0 \leq t \leq \infty$).

6.7.2 *Energy and Exergy Analyses*

To perform energy and exergy analyses of ATES systems, the quantities of energy and exergy injected during charging and recovered during discharging must be evaluated. The energy flow associated with a flow of liquid at a constant mass flow rate$\dot{m}$,for an arbitrary period of time with T a function of t, is

$$E = \int_t \dot{E}(t)dt \tag{6.100}$$

where the integration is performed over the time period, and the energy flow rate at time t is

$$\dot{E}(t) = \dot{m}c(T(t) - T_o) \tag{6.101}$$

Here c denotes the specific heat of the liquid. Combining Equations 6.100 and 6.101 for constant $\dot{m}$, c, and T_o,

$$E = \dot{m}c \int_t (T(t) - T_o)dt \tag{6.100a}$$

The corresponding exergy flow is

$$\in = \int_t \dot{\in}(t)dt \tag{6.102}$$

where the exergy flow rate at time t is

$$\dot{\in}(t) = \dot{m}c[(T(t) - T_o) - T_o \ln(T(t)/T_o)] \tag{6.103}$$

Combining Equations 6.102 and 6.103, and utilizing Equation 6.100a,

$$\in = \dot{m}c \int_t [(T(t) - T_o) - T_o \ln(T(t)/T_o)]dt = E - \dot{m}cT_o \int_t \ln(T(t)/T_o)dt \tag{6.102a}$$

Charging

The energy input to the ATES during charging, for a constant water injection rate $\dot{m}_c$ and over a time period beginning at zero and ending at t_c, is expressed by Equation 6.100a with $T(t) = T_c$. That is,

$$E_c = \dot{m}_c c \int_{t=0}^{t_c} (T_c - T_o)dt = \dot{m}_c c t_c (T_c - T_o) \tag{6.104}$$

The corresponding exergy input is expressed by Equation 6.102a, with the same conditions as for E_c. Thus, after integration,

$$\in_c = \dot{m}_c c t_c [(T_c - T_o) - T_o \ln(T_c/T_o)] = E_c - \dot{m}_c c t_c T_o \ln(T_c/T_o) \tag{6.105}$$

Discharging

The energy recovered from the ATES during discharging, for a constant water recovery rate $\dot{m}_d$ and for a time period starting at zero and ending at t_d, is expressed by Equation 6.100a with $T(t)$ as in Equation 6.99. Thus,

$$E_d = \dot{m}_d c \int_{t=0}^{t_d} (T_d(t) - T_o)dt = \dot{m}_d c[T_d(0) - T_o]\theta(2t_f - \theta)/(2t_f) \tag{6.106}$$

where

$$\theta = \begin{cases} t_d, & 0 \le t_d \le t_f \\ t_f, & t_f \le t_d \le \infty \end{cases} \tag{6.107}$$

The corresponding exergy recovered is expressed by Equation 6.102a, with the same conditions as for E_d. Thus,

$$\in_d = \dot{m}_d c \int_{t=0}^{t_d} [(T_d(t) - T_o) - T_o \ln(T_d(t)/T_o)]dt = E_d - \dot{m}_d c T_o \int_{t=0}^{t_d} \ln(T_d(t)/T_o)dt \tag{6.108}$$

Here,

$$\int_{t=0}^{t_d} \ln(T_d(t)/T_o)\, dt = \int_{t=0}^{t_d} \ln(at + b)dt = [(a\theta + b)/a]\ln(a\theta + b) - \theta - (b/a)\ln b \tag{6.109}$$

where

$$a = [T_o - T_d(0)]/(T_o t_f) \tag{6.110}$$

$$b = T_d(0)/T_o \tag{6.111}$$

When $t_d \geq t_f$, the expression for the integral in Equation 6.109 reduces to

$$\int_{t=0}^{t_d} \ln(T_d(t)/T_o)dt = t_f \left[\frac{T_d(0)}{T_d(0) - T_o} \ln \frac{T_d(0)}{T_o} - 1 \right] \tag{6.109a}$$

Energy and Exergy Balances

An ATES energy balance taken over a complete charging–discharging cycle states that the energy injected is either recovered or lost. A corresponding exergy balance states that the exergy injected is either recovered or lost, where lost exergy is associated with both waste exergy emissions and internal exergy consumptions due to irreversibilities.

If f is defined as the fraction of injected energy E_c that can be recovered if the length of the discharge period approaches infinity (i.e., water is extracted until all recoverable energy has been recovered), then

$$E_d(t_d \to \infty) = fE_c \tag{6.112}$$

It follows from the energy balance that $(1 - f)E_c$ is the energy irreversibly lost from the ATES. Clearly, f varies between zero for a thermodynamically worthless ATES and unity for an ATES having no energy losses during an infinite discharge period. (Note that even if $f = 1$, the ATES can still have mixing losses that reduce the temperature of the recovered water and consequently cause exergy losses.) Since E_c is given by Equation 6.104 and $E_d(t_d \to \infty)$ by Equation 6.106 with $\theta = t_f$, Equation 6.112 may be rewritten as

$$\dot{m}_d c(T_d(0) - T_o)t_f/2 = f\dot{m}_c c(T_c - T_o)t_c \tag{6.112a}$$

or, after rearranging,

$$f = \frac{t_f \dot{m}_d (T_d(0) - T_o)}{2t_c \dot{m}_c (T_c - T_o)} \tag{6.112b}$$

Since $T_d(0)$ can vary from T_o to T_c, the temperature-related term $(T_d(0) - T_o)/(T_c - T_o)$, like f, varies between zero and unity. The time ratio t_f/t_c and mass flow rate ratio $\dot{m}_d/\dot{m}_c$ can both take on any positive values, subject to the above equality.

Efficiencies and Losses

For either energy or exergy, efficiency is defined as the fraction, taken over a complete cycle, of the quantity input during charging that is recovered during discharging, while loss is the difference between input and recovered amounts of the quantity. Hence, the energy loss as a function of the discharge time period is given by $[E_c - E_d(t_d)]$, while the corresponding exergy loss is given by $[\in_c - \in_d (t_d)]$. It is emphasized that energy losses do not reflect the temperature degradation associated with mixing, while exergy losses do.

The energy efficiency η for an ATES, as a function of the discharge time period, is

$$\eta(t_d) = \frac{E_d(t_d)}{E_c} = \frac{\dot{m}_d (T_d(0) - T_o)}{\dot{m}_c (T_c - T_o)} \frac{\theta(2t_f - \theta)}{2t_f t_c} \tag{6.113}$$

and the corresponding exergy efficiency ψ by

$$\psi(t_d) = \in_d (t_d)/ \in_c \tag{6.114}$$

Note that the energy efficiency in Equation 6.113 simplifies when the discharge period t_d exceeds t_f, that is, $\eta(t_d \geq t_f) = f$. Thus, for an ATES in which all injected energy is recoverable during an infinite discharge period, that is, $f = 1$, the energy efficiency can reach 100% if the discharge period t_d is made long enough. The corresponding exergy efficiency, however, remains less than 100% because due to mixing losses, much of the heat is recovered at near-environmental temperatures. Only a thermodynamically reversible storage, which would never be an objective since such other factors as economics must be considered, would permit the achievement of an exergy efficiency of 100%.

6.7.3 *Effect of a Threshold Temperature*

In practice, it is not economically feasible to continue the discharge period until as much recoverable heat as possible is recovered. As the discharge period increases, water is recovered from an ATES at ever-decreasing temperatures (ultimately approaching the reference-environment temperature T_o), and the energy in the recovered water is of decreasing usefulness. Exergy analysis reflects this phenomenon, as the magnitude of the recovered exergy decreases as the recovery temperature decreases. To determine the appropriate discharge period, a threshold temperature T_t is often introduced, below which the residual energy in the aquifer water is not considered worth recovering from an ATES. For the linear temperature–time relation used here (see Equation 6.99), it is clear that no thermal energy could be recovered over a cycle if the threshold temperature exceeds the initial discharge temperature, while the appropriate discharge period can be evaluated using Equation 6.99 with T_t replacing $T_d(t)$ for the case where $T_o \leq T_t \leq T_d(0)$. Thus,

$$t_d = \begin{cases} \dfrac{T_d(0) - T_t}{T_d(0) - T_o} t_f, & T_o \leq T_t \leq T_d(0) \\ 0, & T_d(0) \leq T \end{cases} \tag{6.115}$$

The effect of a threshold temperature in practice, therefore, is to place an upper limit on the allowable discharge time period. Utilizing a threshold temperature usually has the effect of decreasing the difference between the corresponding energy and exergy efficiencies.

6.7.4 *Case Study*

Background

In this case study, experimental data are used from the first of four short-term ATES test cycles, using the Upper Cambrian Franconia–Ironton–Galesville confined aquifer. The test cycles were performed at the University of Minnesota's St. Paul campus from November 1982 to December 1983 (Hoyer *et al.*, 1985). During the test, water was pumped from the source well, heated in a heat exchanger, and returned to the aquifer through the storage well. After storage, energy was recovered by pumping the stored water through a heat exchanger and returning it to the supply well. The storage and supply wells are located 255 m apart.

For the test cycle considered here, the water temperature and volumetric flow rate vary with time during the injection and recovery processes as shown in Figure 6.12. The storage period duration (13 days) is also shown. Charging occurred during 5.24 days over a 17-day period. The water temperature and volumetric flow rate were approximately constant during charging, and had mean values of 89.4 °C and 18.4 l/s, respectively. Discharging also occurred over 5.24 days, approximately with a constant volumetric flow rate of water and linearly decreasing temperature with time. The mean volumetric flow rate during discharging was 18.1 l/s, and the initial discharge temperature was 77 °C, while the temperature after 5.24 days was 38 °C. The ambient temperature was reported to be 11 °C.

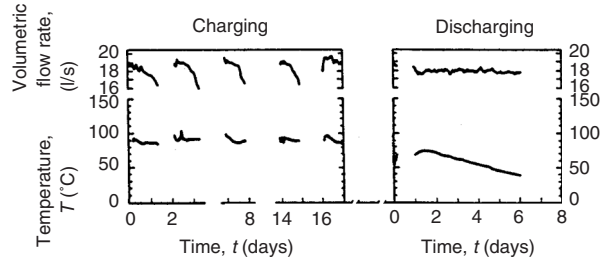

Figure 6.12 Observed values for the temperature and volumetric flow rate of water, as a function of time during the charging and discharging periods, for the experimental test cycles used in the ATES case study

Assumptions and Simplifications

In subsequent calculations, mean values for volumetric flow rates and charging temperature are used. Also, the specific heat and density of water are both taken to be fixed, at 4.2 kJ/kg K and 1000 kg/m^3, respectively. Since the volumetric flow rate (in L/s) is equal to the mass flow rate (in kg/s) when the density is 1000 kg/m^3, $\dot{m}_c = 18.4$ kg/s and $\dot{m}_d = 18.1$ kg/s. Also, the reference-environment temperature is fixed at the ambient temperature, that is, $T_o = 11°\text{C} = 284$ K.

Analysis and Results

During charging, it can be shown using Equations 6.104 and 6.105, with $t_c = 5.24$ d $= 453{,}000$ s and $T_c = 89.4\,°\text{C} = 362.4$ K, that

$$E_c = (18.4\,\text{kg/s})(4.2\,\text{kJ/kg K})(453{,}000\,\text{s})(89.4\,°\text{C} - 11\,°\text{C}) = 2.74 \times 10^9\,\text{kJ}$$

and

$$\begin{aligned}\in_c &= 2.74 \times 10^9\,\text{kJ} - (18.4\,\text{kg/s})(4.2\,\text{kJ/kg K})(453{,}000\,\text{s})(284\,\text{K})\ln(362.4\,\text{K}/284\,\text{K}) \\ &= 0.32 \times 10^9\,\text{kJ}\end{aligned}$$

During discharging, the value of the time t_f is evaluated using the linear temperature–time relation of the present model and the observations that $T_d(t = 5.24\text{ d}) = 38\,°\text{C}$ and $T_d(0) = 77\,°\text{C} = 350$ K. Then, using Equation 6.99 with $t = 5.24$ d,

$$38\,°\text{C} = 77\,°\text{C} - (77\,°\text{C} - 11\,°\text{C})(5.24\,\text{d}/t_f)$$

which can be solved to show that $t_f = 8.87$ d. Thus, with the present linear model, the discharge water temperature would reach T_o if the discharge period was lengthened to almost 9 days. In reality, the rate of temperature decline would likely decrease, and the discharge temperature would asymptotically approach T_o.

The value of the fraction f can be evaluated with Equation 6.112b as

$$f = \frac{(8.87\,\text{d})(18.1\,\text{kg/s})(77\,°\text{C} - 11\,°\text{C})}{2(5.24\,\text{d})(18.4\,\text{kg/s})(89.4\,°\text{C} - 11\,°\text{C})} = 0.701$$

Thus, the maximum energy efficiency achievable is approximately 70%. With these values and Equations 6.110 and 6.111, it can be shown that

$$a = (11\,°\text{C} - 77\,°\text{C})/(284\,\text{K} \times 8.87\,\text{d}) = -0.0262/\text{d} \text{ and } b = (350\,\text{K})/(284\,\text{K}) = 1.232$$

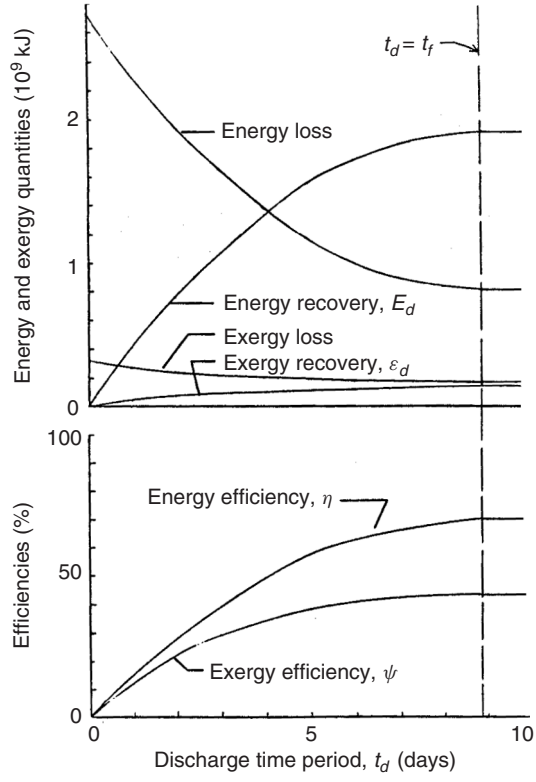

Figure 6.13 Variation of several calculated energy and exergy quantities and efficiencies, as a function of discharge time period, for the ATES case study

Consequently, expressions dependent on discharge time period t_d can be written and plotted (see Figure 6.13) for E_d, $\in_d$, η, and ψ using Equations 6.106–6.111, 6.113, and 6.114, and for the energy loss $(E_c - E_d)$ and exergy loss $(\in_c - \in_d)$.

Discussion

Both energy and exergy efficiencies in Figure 6.13 increase from zero to maximum values as t_d increases. Further, the difference between the two efficiencies increases with increasing t_d. This latter point demonstrates that the exergy efficiency gives less weight than the energy efficiency to the energy recovered at higher t_d values, since it is recovered at temperatures nearer to the reference-environment temperature.

Several other points in Figure 6.13 are worth noting. First, for the conditions specified, all parameters level off as t_d approaches t_f, and remain constant for $t_d \geq t_f$. Second, as t_d increases toward t_f, the energy recovered increases from zero to a maximum value, while the energy loss decreases from a maximum of all the input energy to a minimum (but nonzero) value. The exergy recovery and exergy loss functions behave similarly qualitatively, but exhibit much lower magnitudes.

Importance of Temperature The difference between energy and exergy efficiencies is due to temperature differences between the charging- and discharging-fluid flows. As the discharging time increases, the deviation between these two efficiencies increases (Figure 6.13) because the

temperature of recovered heat decreases (Figure 6.12). In this case, the energy efficiency reaches approximately 70% and the exergy efficiency 40% by the completion of the discharge period, even though the efficiencies are both 0% when discharging commences.

To further illustrate the importance of temperature, a hypothetical modification of the present case study is considered. In the modified case, all details are as in the original case except that the temperature of the injection flow during the charging period is increased from 89.4 °C to 200 °C (473 K), while the duration of the charging period is decreased from its initial value of 5.24 days (453,000 s) so that the energy injected does not change. By equating the energy injected during charging for the original and modified cases, the modified charging-period duration t_c' can be evaluated as a function of the new injection flow temperature T_c' as follows:

$$t_c' = t_c \frac{T_c - T_o}{T_c' - T_o} = (453{,}000\,\text{s}) \frac{(89.4\,^\circ\text{C} - 11\,^\circ\text{C})}{(200\,^\circ\text{C} - 11\,^\circ\text{C})} = 188{,}000\text{s}$$

The modified exergy input during charging can then be evaluated as

$$\begin{aligned} \in_c' &= 2.74 \times 10^9\,\text{kJ} - (18.4\,\text{kg/s})(4.2\,\text{kJ/kg K})(188{,}000\,\text{s})(284\,\text{K}) \ln(473\,\text{K}/284\,\text{K}) \\ &= 0.64 \times 10^9\,\text{kJ} \end{aligned}$$

This value is double the exergy input during charging for the original case, so, since the discharging process remains unchanged in the modified case, the exergy efficiency (for any discharging time period) is half that for the original case. The altered value of exergy efficiency is entirely attributable to the new injection temperature, and occurs despite the fact that the energy efficiency remains unchanged.

Effect of Threshold Temperature If a threshold temperature is introduced and arbitrarily set at 38 °C (the actual temperature at the end of the experimental discharge period of 5.24 days), then the data in Figure 6.13 for $t_d = 5.24$ d apply, and one can see that:

- the exergy recovered (0.127×10^9 kJ) is almost all (91%) of the exergy recoverable in infinite time (0.139×10^9 kJ), while the energy recovered (1.60×10^9 kJ) is not as great a portion (83%) of the ultimate energy recoverable (1.92×10^9 kJ);
- the exergy loss (0.19×10^9 kJ) exceeds the exergy loss in infinite time (0.18×10^9 kJ) slightly (by 5.5%), while the energy loss (1.14×10^9 kJ) exceeds the energy loss in infinite time (0.82×10^9 kJ) substantially (by 39%); and
- the exergy efficiency (40%) has almost attained the exergy efficiency attainable in infinite time (43.5%), while the energy efficiency (58%) is still substantially below the ultimate energy efficiency attainable (70%).

Verification of Results To gain confidence in the model and the results, some of the quantities calculated using the linear model can be compared with the same quantities as reported in the experimental paper (Hoyer *et al*., 1985):

(i) the previously calculated value for the energy injection during charging of 2.74×10^9 kJ is 1.1% less than the reported value of 2.77×10^9 kJ;
(ii) the energy recovered at the end of the experimental discharge period of $t_d = 5.24$ d can be evaluated with Equation 6.106 as

$$\begin{aligned} E_d(5.24\text{d}) &= (18.1)(4.2)(77 - 11)[5.24(2 \times 8.87 - 5.24)/(2 \times 8.87)](86{,}400\,\text{s/d}) \\ &= 1.60 \times 10^9\,\text{kJ} \end{aligned}$$

which is 1.8% less than the reported value of 1.63×10^9 kJ; and

(iii) the energy efficiency at $t_d = 5.24$ d can be evaluated with Equation 6.113 as

$$\eta(5.24\,\mathrm{d}) = (1.60 \times 10^9\,\mathrm{kJ})(2.74 \times 10^9\,\mathrm{kJ}) = 0.584$$

which is 1.0% less than the reported value of 0.59 (referred to as the *energy recovery factor*).

6.7.5 Closure

Although energy-based performance measures are normally used in ATES assessments, it can be seen using an elementary ATES model that ATES performance measures based on exergy are more useful and meaningful than those based on energy. Exergy efficiencies account for the temperatures associated with energy transfers to and from an ATES, as well as the quantities of energy transferred, and consequently provide a measure of how nearly ATES systems approach ideal performance. Energy efficiencies account only for quantities of energy transferred and can often be misleadingly high, for example, in cases where heat is recovered at temperatures too low to be useful. The use of an appropriate threshold recovery temperature can partially avoid the most misleading characteristics of ATES energy efficiencies. The analysis presented here for a simple ATES cycle can be extended to more complex systems, and is applicable to a wide range of ATES designs.

6.8 Exergy Analysis of Thermally Stratified Storages

Two key advantages of exergy analysis over energy analysis in TES applications are that exergy analysis recognizes differences in storage temperature, even for storages containing equivalent energy quantities, and evaluates quantitatively losses due to degradation of storage temperature toward the environment temperature (i.e., the cooling of heat storages and the heating of cold storages) and due to mixing of fluids at different temperatures. These advantages of the exergy method are particularly important for stratified storages because of the internal spatial temperature variations they exhibit. Since thermodynamic losses are incurred when storage fluids at different temperatures mix, the inhibition of mixing through appropriate temperature stratification is advantageous. By carefully managing the injection, recovery, and holding of heat (or cold) during a storage cycle so that temperature degradation is minimized, better storage cycle performance can be achieved (as measured by better thermal energy recovery and temperature retention and accounted for explicitly through exergy efficiencies) (Hahne *et al*., 1989; Krane and Krane, 1991).

This section focuses on the energy and exergy contents of stratified storages, which are usually evaluated numerically for arbitrary temperature distributions. Since numerical methods can be effort consuming and often do not provide practical insights into the physical systems, the temperature distributions may alternatively be modeled so that the corresponding TES energy and exergy values can be evaluated analytically. However, accurate mathematical expressions are usually too complex to permit closed-form solutions, and their solutions again normally necessitate the use of computational techniques. As analytical expressions are usually more convenient and provide greater physical insights, temperature-distribution models that achieve an optimal balance between the needs for accuracy, convenience, and physical insight when evaluating storage energy and exergy contents are desirable. Such models can be particularly useful in economic design activities that are greatly simplified and enhanced if analytical expressions for storage energy and exergy contents are available.

In the first part of this section, which follows earlier reports (Rosen and Hooper, 1991b, 1992, 1994; Rosen *et al*., 1991), several models are presented for the temperature distributions in vertically stratified thermal storages, which are sufficiently accurate, realistic, and flexible for use in engineering design and analysis, yet simple enough to be convenient, and which provide useful physical insights. One-dimensional gravitational temperature stratification is considered, and temperature is expressed as a function of height for each model. To reduce effort, only distributions for

which energy and exergy data can be obtained analytically are considered. Expressions are derived for TES energy and exergy contents in accordance with the models, which are discussed, compared, and illustrated.

In the second part of this section, following previous studies (Rosen and Tang, 1997; Rosen and Dincer, 1999a), the increase in exergy-storage capacity resulting from stratification is described.

6.8.1 General Stratified TES Energy and Exergy Expressions

The energy E and exergy Ξ in a TES can be found, following Equations 6.12 and 6.31, by integrating over the entire storage-fluid mass m within the TES as follows:

$$E = \int_m e\, dm \tag{6.116}$$

$$\Xi = \int_m \zeta\, dm \tag{6.117}$$

where e denotes specific energy and ξ specific exergy. For an ideal liquid, the e and ξ are functions only of temperature T, and can be expressed as follows:

$$e(T) = c(T - T_o) \tag{6.118}$$

$$\zeta(T) = c[(T - T_o) - T_o \ln(T/T_o)] = e(T) - cT_o \ln(T/T_o) \tag{6.119}$$

Both the storage-fluid specific heat c and reference-environment temperature T_o are assumed constant here.

Consider now a TES of height H, which has only one-dimensional stratification, that is, temperature varies only with height h in the vertical direction. The horizontal cross-sectional area of the TES is assumed constant. A horizontal element of mass dm can then be adequately approximated as

$$dm = \frac{m}{H} dh \tag{6.120}$$

Since temperature is a function of height only (i.e., $T = T(h)$), the expressions for e and ξ in Equations 6.118 and 6.119, respectively, can be written as

$$e(h) = c(T(h) - T_o) \tag{6.118a}$$

$$\zeta(h) = e(h) - cT_o \ln(T(h)/T_o) \tag{6.119a}$$

With Equation 6.120, the expressions for E and Ξ in Equations 6.116 and 6.117, respectively, can be written as

$$E = \frac{m}{H} \int_0^H e(h) dh \tag{6.116a}$$

$$\Xi = \frac{m}{H} \int_0^H \zeta(h) dh \tag{6.117a}$$

With Equation 6.118a, the expression for E in Equation 6.116a can be written as

$$E = mc\,(T_m - T_o) \tag{6.116b}$$

where

$$T_m \equiv \frac{1}{H}\int_0^H T(h)dh \tag{6.121}$$

Physically, T_m represents the temperature of the TES fluid when it is fully mixed. This observation can be seen by noting that the energy of a fully mixed tank E_m at a uniform temperature T_m can be expressed, using Equation 6.118 with constant temperature and Equation 6.116, as

$$E_m = mc(T_m - T_o) \tag{6.122}$$

and that the energy of a fully mixed tank E_m is by the principle of conservation of energy the same as the energy of the stratified tank E:

$$E = E_m \tag{6.123}$$

Comparing Equations 6.116b, 6.122, and 6.123 confirms that T_m represents the temperature of the mixed TES fluid.

With Equation 6.119a, the expression for Ξ in Equation 6.117a can be written as

$$\Xi = E - mcT_o \ln(T_e/T_o) \tag{6.117b}$$

where

$$T_e \equiv \exp\left[\frac{1}{H}\int_0^H \ln T(h)dh\right] \tag{6.124}$$

Physically, T_e represents the equivalent temperature of a mixed TES that has the same exergy as the stratified TES. In general, $T_e \neq T_m$, since T_e is dependent on the degree of stratification present in the TES, while T_m is independent of the degree of stratification. In fact, $T_e = T_m$ is the limit condition reached when the TES is fully mixed. This can be seen by noting (with Equations 6.117, 6.117b, 6.122, and 6.123) that the exergy in the fully mixed TES, Ξ_m, is

$$\Xi_m = E_m - mcT_o \ln(T_m/T_o) \tag{6.125}$$

The difference in TES exergy between the stratified and fully mixed (i.e., at a constant temperature T_m) cases can be expressed with Equations 6.117b and 6.125 as

$$\Xi - \Xi_m = mcT_o \ln(T_m/T_e) \tag{6.126}$$

The change given in Equation 6.126 can be shown to be always negative. That is, the exergy consumption associated with mixing fluids at different temperatures, or the minimum work required for creating temperature differences, is always positive.

It is noted that when the temperature distribution is symmetric about the center of the TES such that

$$\frac{T(h) + T(H-h)}{2} = T(H/2) \tag{6.127}$$

the mixed temperature T_m is always equal to the mean of the temperatures at the top and bottom of the TES.

6.8.2 Temperature-Distribution Models and Relevant Expressions

Six stratified temperature-distribution models are considered: linear (denoted by a superscript L), stepped (S), continuous-linear (C), general-linear (G), basic three-zone (B), and general three-zone (T). For each model, the temperature distribution as a function of height is given, and expressions for T_m and T_e are derived. The distributions considered are simple enough in form to permit energy and exergy values to be obtained analytically, but complex enough to be relatively realistic. Although other temperature distributions are, of course, possible, these are chosen because closed-form analytical solutions can readily be obtained for the integrals for T_m in Equation 6.121 and T_e in Equation 6.124.

Linear Temperature-Distribution Model

The linear temperature-distribution model (see Figure 6.14) varies linearly with height h from T_b, the temperature at the bottom of the TES (i.e., at $h = 0$), to T_t, the temperature at the top (i.e., at $h = H$), and can be expressed as

$$T^L(h) = \frac{T_t - T_b}{H} h + T_b \tag{6.128}$$

By substituting Equation 6.128 into Equations 6.121 and 6.124, it can be shown that

$$T_m^L = \frac{T_t + T_b}{2} \tag{6.129}$$

which is the mean of the temperatures at the top and bottom of the TES, and that

$$T_e^L = \exp\left[\frac{T_t(\ln T_t - 1) - T_b(\ln T_b - 1)}{T_t - T_b}\right] \tag{6.130}$$

Stepped Temperature-Distribution Model

The stepped temperature-distribution model (see Figure 6.15) consists of k horizontal zones, each of which is at a constant temperature, and can be expressed as

$$T^S(h) = \begin{cases} T_1, & h_0 \le h \le h_1 \\ T_2, & h_1 < h \le h_2 \\ \cdots & \\ T_k, & h_{k-1} < h \le h_k \end{cases} \tag{6.131}$$

where the heights are constrained as follows:

$$0 = h_0 \le h_1 \le h_2 \ldots \le h_k = H \tag{6.132}$$

It is convenient to introduce here x_j, the mass fraction for zone j:

$$x_j \equiv \frac{m_j}{m} \tag{6.133}$$

Since the TES-fluid density ρ and the horizontal TES cross-sectional area A are assumed constant here, but the vertical thickness of zone j, $h_j - h_{j-1}$, can vary from zone to zone,

$$m_j = \rho V_j = \rho A(h_j - h_{j-1}) \tag{6.134}$$

and

$$m = \rho V = \rho A H \tag{6.135}$$

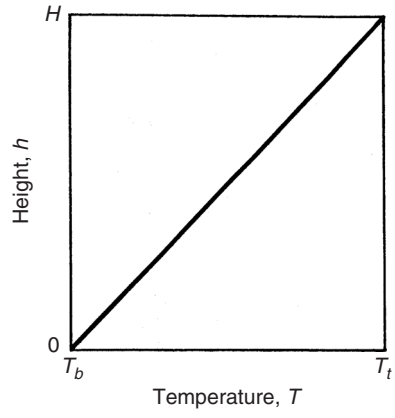

Figure 6.14 A vertically stratified storage having a linear temperature distribution

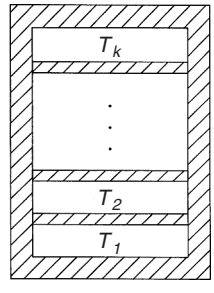

Figure 6.15 A vertically stratified storage having a stepped temperature distribution

where V_j and V denote the volumes of zone j and of the entire TES, respectively. Substitution of Equations 6.134 and 6.135 into Equation 6.133 yields

$$x_j = \frac{h_j - h_{j-1}}{H} \tag{6.133a}$$

With Equations 6.121, 6.124, 6.131, and 6.133a, it can be shown that

$$T_m^s = \sum_{j=1}^{k} x_j T_j \tag{6.136}$$

which is the weighted mean of the zone temperatures, where the weighting factor is the mass fraction of the zone, and that

$$T_e^S = \exp\left[\sum_{j=1}^{k} x_j \ln T_j\right]$$

$$= \prod_{j=1}^{k} T_j^{x_j} \tag{6.137}$$

Continuous-Linear Temperature-Distribution Model

The continuous-linear temperature distribution consists of k horizontal zones, in each of which the temperature varies linearly from the bottom to the top, and can be expressed as

$$T^C(h) = \begin{cases} \phi_1^C(h), & h_0 \le h \le h_1 \\ \phi_2^C(h), & h_1 < h \le h_2 \\ \cdots \\ \phi_k^C(h), & h_{k-1} < h \le h_k \end{cases} \tag{6.138}$$

where $\phi_j^C(h)$ represents the linear temperature distribution in zone j.

$$\phi_j^C(h) = \frac{T_j - T_{j-1}}{h_j - h_{j-1}} h + \frac{h_j T_{j-1} - h_{j-1} T_j}{h_j - h_{j-1}} \tag{6.139}$$

The zone height constraints in Equation 6.132 apply here. The temperature varies continuously between zones.

With Equations 6.121, 6.124, 6.133a, 6.138, and 6.139, it can be shown that

$$T_m^C = \sum_{j=1}^{k} x_j (T_m)_j \tag{6.140}$$

where $(T_m)_j$ is the mean temperature in zone j, that is,

$$(T_m)_j = \frac{T_j + T_{j-1}}{2} \tag{6.141}$$

and that

$$\begin{aligned} T_e^C &= \exp\left[\sum_{j=1}^{k} x_j \ln(T_e)_j\right] \\ &= \prod_{j=1}^{k} (T_e)_j^{x_j} \end{aligned} \tag{6.142}$$

where $(T_e)_j$ is the equivalent temperature in zone j, that is,

$$(T_e)_j = \begin{cases} \exp\left[\dfrac{T_j(\ln T_j - 1) - T_{j-1}(\ln T_{j-1} - 1)}{T_j - T_{j-1}}\right], & \text{if } T_j \ne T_{j-1} \\ T_j, & \text{if } T_j = T_{j-1} \end{cases} \tag{6.143}$$

General-Linear Temperature-Distribution Model

For the general-linear model, there are k horizontal zones, in each of which the temperature varies linearly. The temperature does not necessarily vary continuously between zones. That is,

$$T^G(h) = \begin{cases} \phi_1^G(h), & h_0 \le h \le h_1 \\ \phi_2^G(h), & h_1 < h \le h_2 \\ \cdots \\ \phi_k^G(h), & h_{k-1} < h \le h_k \end{cases} \tag{6.144}$$

where the zone height constraints in Equation 6.132 apply, and $\phi_j^G(h)$ represents the temperature distribution (linear) in zone j:

$$\phi_j^G(h) = \frac{(T_t)_j - (T_b)_j}{h_j - h_{j-1}} h + \frac{h_j (T_b)_j - h_{j-1}(T_t)_j}{h_j - h_{j-1}} \tag{6.145}$$

Here, $(T_t)_j$ and $(T_b)_j$ denote respectively the temperatures at the top and bottom of zone j, and h_j and h_{j-1} the heights at the top and bottom of zone j (relative to the bottom of the TES).

For the general-linear temperature-distribution model,

$$T_m^G = \sum_{j=1}^{k} x_j (T_m^G)_j \tag{6.146}$$

$$T_e^G = \exp\left[\sum_{j=1}^{k} x_j \ln(T_e^G)_j\right] = \prod_{j=1}^{k} (T_e^G)_j^{x_j} \tag{6.147}$$

where

$$(T_m^G)_j = \frac{(T_t)_j + (T_b)_j}{2} \tag{6.148}$$

$$\left(T_e^G\right)_j = \begin{cases} \exp\left[\dfrac{(T_t)_j(\ln(T_t)_j - 1) - (T_b)_j(\ln(T_b)_j - 1)}{(T_t)_j - (T_b)_j}\right] & \text{if } (T_t)_j \neq (T_b)_j \\ (T_t)_j, & \text{if } (T_t)_j = (T_b)_j \end{cases} \tag{6.149}$$

General Three-Zone Temperature-Distribution Model

Two three-zone temperature-distribution models are considered in this and the next subsection: general and basic. Both of the three-zone models are subsets of the continuous-linear model in which there are only three horizontal zones (i.e., $k = 3$). The temperature varies linearly within each zone and continuously across each zone.

The temperature distribution for the general three-zone model is illustrated in Figure 6.16(a), and can be expressed as follows:

$$T^T(h) = \begin{cases} \phi_1^C(h), & h_0 \le h \le h_1 \\ \phi_2^C(h), & h_1 < h \le h_2 \\ \quad \cdots & \\ \phi_3^C(h), & h_2 < h \le h_k \end{cases} \tag{6.150}$$

where $\phi_j^C(h)$ represents the temperature distribution (linear) in zone j (see Equation 6.139), and where the heights are constrained as in Equation 6.132 with $k = 3$.

Expressions for the temperatures T_m and T_e can be obtained for the general three-zone model with Equations 6.121, 6.124, and 6.150 (or from the expressions for T_m and T_e for the continuous-linear model with $k = 3$):

$$T_m^T = \sum_{j=1}^{3} x_j (T_m^C)_j \tag{6.151}$$

$$T_e^T = \exp\left[\sum_{j=1}^{3} x_j \ln(T_e^C)_j\right] = \prod_{j=1}^{3} (T_e^C)_j^{x_j} \tag{6.152}$$

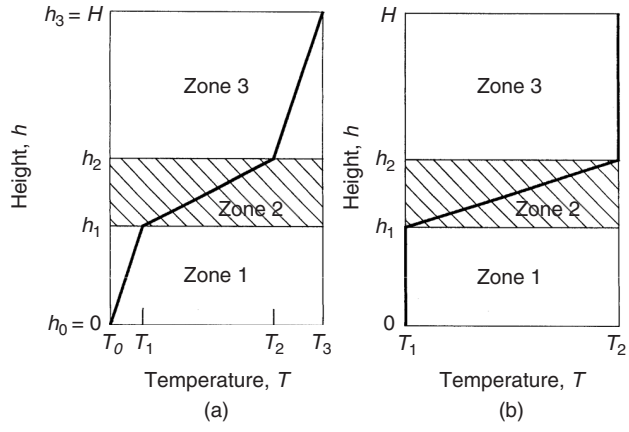

Figure 6.16 The three-zone temperature-distribution models. (a) General (b) basic

where

$$(T_m^C)_j = \frac{T_j + T_{j-1}}{2} \tag{6.153}$$

$$(T_e^C)_j = \begin{cases} \exp\left[\dfrac{T_j(\ln T_j - 1) - T_{j-1}(\ln T_{j-1} - 1)}{T_j - T_{j-1}}\right], & \text{if } T_j \neq T_{j-1} \\ T_j, & \text{if } T_j = T_{j-1} \end{cases} \tag{6.154}$$

Basic Three-Zone Temperature-Distribution Model

The basic three-zone temperature-distribution model (B) is a subset of the general three-zone model. In the top and bottom zones, the temperatures are constant at T_2 and T_1, respectively, and in the middle zone, the temperature varies linearly between T_2 and T_1. The temperature distribution for this model is illustrated in Figure 6.16(b), and can be expressed as

$$T^B(h) = \begin{cases} T_1, & 0 \le h \le h_1 \\ \dfrac{T_2 - T_1}{h_2 - h_1}h + \dfrac{h_2 T_1 - h_1 T_2}{h_2 - h_1}, & h_1 \le h \le h_2 \\ T_2, & h_2 \le h \le H \end{cases} \tag{6.155}$$

where $0 \le h_1 \le h_2 \le H$.

By extension of the general three-zone model, it can be shown that

$$T_m^B = x_1 T_1 + x_2 \frac{T_1 + T_2}{2} + x_3 T_2 = f T_1 + (1 - f) T_2 \tag{6.156}$$

where f represents the mean height fraction in zone 2, expressible as

$$f \equiv \frac{h_1 + h_2}{2H} \tag{6.157}$$

It can also be shown that

$$T_e^B = \exp\left[x_1 \ln T_1 + x_2 \frac{T_2(\ln T_2 - 1) - T_1(\ln T_1 - 1)}{T_2 - T_1} + x_3 \ln T_2\right] \tag{6.158}$$

6.8.3 Discussion and Comparison of Models

Each of the six stratified temperature-distribution models has advantages and disadvantages, particularly with respect to ease of utilization and flexibility to approximate accurately different actual temperature distributions. The linear temperature-distribution model is simple to utilize but not flexible enough to fit the wide range of actual temperature distributions possible, while the stepped, continuous-linear, and general-linear distribution models are flexible and, if the zones are made small enough, can accurately fit any actual temperature distribution. However, the latter models are relatively complex to utilize when the number of zones is large. Although the continuous and general-linear models involve the more complex equations, they usually require fewer zones than the stepped model to achieve similar accuracy in results.

For most normal situations, the three-zone temperature-distribution models may be optimal in terms of achieving an appropriate compromise between such factors as result accuracy, computational convenience, physical insight, and so on. Both the three-zone models are relatively easy to utilize, yet are flexible enough to simulate well the stratification distribution in most actual TES fluids, which possess lower and upper zones of slightly varying or approximately constant temperature, and a middle zone (the thermocline region) in which temperature varies substantially. The intermediate zone, which grows as thermal diffusion occurs in the tank being modeled, accounts for the irreversible effects of thermal mixing. The basic three-zone model is simpler while the general three-zone model is more accurate.

It is noted that simplified forms of the expressions for T_m and T_e can be written for the multizone temperature-distribution models when all zone vertical thicknesses are the same, since in this special case, the mass fractions for each of the k zones are the same (i.e., $x_j = 1/k$ for all j). Also, several relations exist between the model temperature distributions beyond those described earlier:

- The general-linear temperature distribution reduces to (i) the stepped distribution when $(T_t)_j = (T_b)_j$ for all j; (ii) the continuous-linear distribution when $(T_t)_j = (T_b)_{j+1}$ for $j = 1, 2, \ldots k-1$; and (iii) the linear distribution when $k = 1$.
- The continuous-linear model with $k = 1$ reduces to the linear model.

6.8.4 Illustrative Example: The Exergy-Based Advantage of Stratification

This example illustrates the advantage of stratification by showing that the exergy of a stratified storage is greater than the exergy for the same tank when it is fully mixed, even though the energy content does not change. The case considered is a perfectly insulated, rigid tank of volume V, divided by an adiabatic partition into two equal-size compartments. The tank is filled with an incompressible fluid. The temperatures of the fluids in each compartment (T_1 and T_2) are initially different.

The partition is removed and a new equilibrium state is attained. No chemical reactions occur. Clearly, the initial state corresponds to a stratified tank with a stepped temperature distribution, and the final state to a fully mixed tank containing an identical quantity of energy. Thus, the TES energy and exergy contents can be expressed with Equations 6.116b and 6.117b for the initial state (denoted by subscript i) and Equations 6.122 and 6.125 for the final state (f), using the stepped temperature-distribution expressions for T_m^S and T_e^S (Equations 6.136 and 6.137) with $k = 2$ and $x_1 = x_2 = 0.5$.

Since neither work nor heat interactions occur, the total internal energy of the storage fluid does not change, that is, $E_f - E_i = 0$. The exergy change of the fluid can be expressed with Equation 6.126 as

$$\Xi_f - \Xi_i = -T_o mc \ln \frac{T_m}{T_e} \tag{6.159}$$

Equation 6.136 can be used to show that the final temperature of the store after adiabatic mixing is $T_m = (T_1 + T_2)/2$. Also, from Equation 6.137, $T_e = \sqrt{T_1 T_2}$. Equation 6.159 therefore simplifies for this case as follows:

$$\Xi_f - \Xi_i = -T_o m c_v \ln \frac{T_1 + T_2}{2\sqrt{T_1 T_2}} = -T_o m c_v \ln \frac{\sqrt{r} + \sqrt{1/r}}{2} \tag{6.159a}$$

where $r = T_1/T_2$, a positive quantity. The above expression can be further simplified by noting that, since the mixed temperature is given by the mean of the initial temperatures, the initial temperatures can be written as $T_1 = T_m + \Delta T$ and $T_2 = T_m - \Delta T$, where ΔT is an arbitrary temperature increment. Then,

$$\Xi_f - \Xi_i = T_o m c_v \ln \sqrt{1 - \alpha^2} \tag{6.159b}$$

where $\alpha \equiv \Delta T / T_m$ and $0 \le \alpha \le 1$. Note that if $T_m = T_o$, the temperature of the store after mixing is T_o and the total exergy content of the store can be shown with Equation 6.116b to be zero. Noting that $\sqrt{r} + \sqrt{1/r} \ge 2$ and $\sqrt{1 - \alpha^2} \le 1$, that the natural logarithm of a quantity greater than one is always positive and less than one is always negative, and that the other terms in Equations 6.159a and b are positive, it can be seen that $\Xi_f - \Xi_i$ is zero for $r = 1$ and $\alpha = 1$, and negative for all other possible values of r and α.

Thus, while the total energy contained in the store (the sum of the energy in each of the two sections) before and after mixing is equal, the total exergy contained in the store (the sum of the exergy in each of the two sections) before mixing is greater than that contained in the store after mixing. A corollory to this point is that to reverse the mixing process, no net energy need be added to the tank, while some net exergy must be added. The exergy change is zero only if $T_1 = T_2$ (i.e., there are no exergy consumptions due to irreversibilities if fluids of the same temperature are mixed).

6.8.5 *Illustrative Example: Evaluating Stratified TES Energy and Exergy*

Problem Statement

Several energy and exergy quantities are determined for a realistic stratified temperature distribution, which was assembled by the authors based on many temperature observations for actual storages, using the linear, stepped, continuous-linear, general-linear, and general three-zone temperature-distribution models to approximate the actual distribution. For comparative purposes, the exact values for these quantities are determined by numerical integration of the integrals in Equations 6.121 and 6.124 for the actual temperature distribution. Three-stepped distribution cases are considered, each with a different numbers of zones. The actual distribution is shown in Figure 6.17, with most of the model distributions.

The TES fluid is taken to be water. Specified general data are listed in Table 6.10, and additional data specific to the temperature-distribution models are shown in Figure 6.17 and summarized below:

- **Continuous-linear.** $k = 3$, $h_1 = 1.8$ m, $h_2 = 2.2$ m, $T_1 = 318$ K, $T_2 = 348$ K.
- **General-linear.** $k = 2$, $h_1 = 2.0$ m, $(T_t)_1 = 318$ K, $(T_b)_2 = 348$ K.
- **Stepped.** $k = 2$, $h_j - h_{j-1} = 2$ m for the first case; $k = 20$, $h_j - h_{j-1} = 0.2$ m for the second case; $k = 200$, $h_j - h_{j-1} = 0.02$ m for the third case. The temperatures for the stepped cases can be read from Figure 6.17.
- **General three-zone.** $h_1 = 1.8$ m, $h_2 = 2.2$ m, $T_1 = 318$ K, $T_2 = 348$ K. Note that this distribution is equivalent to the continuous-linear temperature distribution described earlier.

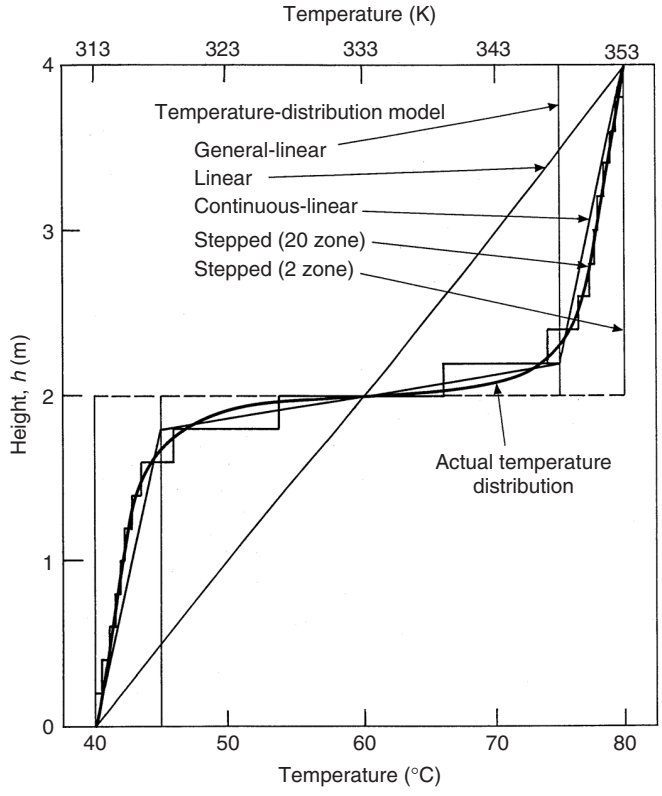

Figure 6.17 The realistic vertically stratified temperature distribution considered in the example, and some of the temperature-distribution models used to approximate it (linear, continuous-linear, general-linear, stepped with two zones, and stepped with 20 zones). The continuous-linear distribution shown is equivalent to a general three-zone distribution

Table 6.10 Specified general data for the example

• Temperatures (K)	
At TES top, $T(h = H)$	353
At TES bottom, $T(h = 0)$	313
Reference environment, T_o	283
• TES-fluid parameters	
Height, H (m)	4
Mass, m (kg)	10,000
Specific heat, c (kJ/kg K)	4.18

Results and Discussion

The results (see Table 6.11) demonstrate the following points for all temperature-distribution models considered:

- The TES energy and exergy contents differ significantly, the exergy values being more than an order of magnitude less than the energy values. This observation is attributable to the fact that

Table 6.11 Results for the stratification example

	Temperature-distribution model						Results from numerical integration
	Linear	General-linear	Stepped			Continuous-linear[a]	
			$k = 200$	$k = 20$	$k = 2$		
Temperatures (K)							
T_m	333.000	333.000	333.000	333.000	333.000	333.000	333.000
T_c	332.800	332.540	332.550	332.560	332.400	332.570	332.550
Energy values (MJ)							
E	2090.000	2090.000	2090.000	2090.000	2090.000	90.000	2090.000
E_m	2090.000	2090.000	2090.000	2090.000	2090.000	2090.000	2090.000
$E-E_m$	0.000	0.000	0.000	0.000	0.000	0.000	0.000
Exergy values (MJ)							
Ξ	172.500	181.800	181.400	181.000	186.700	80.700	181.400
Ξ_m	165.400	165.400	165.400	165.400	165.400	165.400	165.400
$\Xi-\Xi_m$	7.100	16.400	16.000	15.600	21.300	15.300	16.000
Percentage errors							
In values of T_e	+0.075	−0.030	0.000	+0.003	−0.045	+0.006	–
In values of Ξ	−4.900	+2.000	0.000	−0.200	+2.900	−0.400	–
In values of $\Xi-\Xi_m$	−55.600	+22.500	0.000	−2.500	+33.100	−4.400	–

[a]This case is also a general three-zone temperature-distribution model.

the stored thermal energy, although great in quantity, is at near-environmental temperatures, and therefore low in quality or usefulness.

- Values vary among the models for T_e, Ξ, and $\Xi - \Xi_m$, while values do not vary for T_m, E, E_m, and Ξ_m. The latter point is expected since the symmetry condition of Equation 6.127 holds for all model temperature distributions considered. As expected from Equation 6.123, $E = E_m$.

The effort required to evaluate the results in Table 6.11 and the accuracy of the results are different for each temperature-distribution model, as explained below:

- Accuracy can be measured by comparing the results for the model distributions with the results obtained by numerical integration (see Table 6.11). Percentage errors are given for the quantities in Table 6.11 that vary from model to model (i.e., for T_e, Ξ, and $\Xi - \Xi_m$), where

$$\% \text{ error} = \frac{(\text{Value}) - (\text{Numerical simulation value})}{(\text{Numerical simulation value})} 100 \tag{6.160}$$

  In Table 6.11, the percentage errors for T_e values are very small (ranging from −0.045% to +0.075%) and for Ξ values are fairly small (ranging from −4.9% to +2.9%), but, for values of $\Xi - \Xi_m$, are in some cases large (ranging from −55.6% to +33.1%).
- Calculational effort expended increases as the number of zones required in multizone distributions for acceptable approximations to the actual temperature distribution increases, and as the complexity of the calculations involved increases. Less calculational effort is required to obtain the values in Table 6.11 for all the different temperature-distribution models considered, than for the values obtained by numerical integration.

In the present example, the general three-zone model has an acceptable accuracy and yet is simple to use. Although the stepped models (with 20 or 200 zones) are more precise, they are more complex to apply. The poor correlations between the actual and linear temperature distributions, and

between the actual and stepped (with $k = 2$) distributions, cause these model distributions to provide results of significantly lower precision, although they are simpler to apply. Clearly, the selection of a particular distribution as a model involves a trade-off, and the three-zone temperature-distribution model appears to represent an appropriate compromise between high precision of results and an acceptable level of calculational effort.

6.8.6 *Increasing TES Exergy-Storage Capacity Using Stratification*

The increase in the exergy capacity of a thermal storage through stratification is described. A wide range of realistic storage-fluid temperature profiles is considered, and for each, the relative increase in exergy content of the stratified storage compared to the same storage when it is fully mixed is evaluated. It is shown that, for all temperature profiles considered, the exergy-storage capacity of a thermal storage increases as the degree of stratification, as represented through greater and sharper spatial temperature variations, increases. Furthermore, the percentage increase in exergy capacity is greatest for storages at temperatures near to the environment temperature, and decreases as the mean storage temperature diverges from the environment temperature (to either higher or lower temperatures).

Analysis

Thermal storages for heating and cooling capacity, having numerous temperature-distribution profiles, are considered. The general three-zone model, which, as discussed previously, is a suitable design-oriented temperature-distribution model for vertically stratified thermal storages, is utilized to evaluate storage energy and exergy contents. For each case, the ratio is evaluated of the exergy of the stratified storage Ξ to the exergy of the same storage when fully mixed Ξ_m. Using Equations 6.116b, 6.117b, and 6.125, this ratio can be expressed, after simplification, as

$$\frac{\Xi}{\Xi_m} = \frac{T_m/T_o - 1 - \ln(T_e/T_o)}{T_m/T_o - 1 - \ln(T_m/T_o)} \tag{6.161}$$

This ratio increases, from as low as unity when the storage is not stratified, to a value greater than one as the degree of stratification present increases. The ratio in Equation 6.161 is independent of the mass m and specific heat c of the storage fluid. The ratio is also useful as an evaluation, analysis, and design tool, as it permits the exergy of a stratified storage to be conveniently evaluated by multiplying the exergy of the equivalent mixed storage (a quantity straightforwardly evaluated) by the appropriate exergy ratio, where values for the exergy ratio can be determined separately (as is done here).

Several assumptions and approximations are utilized throughout this subsection:

- Storage horizontal cross-sectional area is taken to be fixed.
- The environmental temperature T_o is fixed at 20 °C for all cases (whether they involve thermal storage for heating or cooling capacity).
- Only one-dimensional gravitational (i.e., vertical) temperature stratification is considered.
- Only temperature distributions that are rotationally symmetric about the center of the storage, according to Equation 6.127, are considered. This symmetry implies that zone 2 is centered about the central horizontal axis of the storage, and that zones 1 and 3 are of equal size, that is, $x_1 = x_3 = (1 - x_2)/2$.

To model and then assess the numerous storage cases considered, two main relevant parameters are varied realistically:

- the principal temperatures (e.g., mean, maximum, minimum), and
- temperature-distribution profiles (including changes in zone thicknesses).

Specifically, the following characterizing parameters are varied to achieve the different temperature-distribution cases considered:

- The mixed-storage temperature T_m is varied for a range of temperatures characteristic of storages for heating and cooling capacity.
- The size of zone 2, which represents the thermocline region, is allowed to vary from as little as zero to as great as the size of the overall storage, that is, $0 \leq x_2 \leq 1$. A wide range of temperature profiles can thereby be accommodated, and two extreme cases exist: a single-zone situation with a linear temperature distribution when $x_2 = 1$, and a two-zone distribution when $x_2 = 0$.
- The maximum and minimum temperatures in the storage, which occur at the top and bottom of the storage, respectively, are permitted to vary about the mixed-storage temperature T_m by up to 15 °C.

Using the zone numbering system in Figure 6.16(a) and the symmetry condition introduced earlier, the following expressions can be written for the temperatures at the top and bottom of the storage, respectively:

$$T_3 = T_m + \Delta T_{st} \text{ and } T_0 = T_m - \Delta T_{st} \tag{6.162}$$

while the following equations can be written for the temperatures at the top and bottom of zone 2, respectively:

$$T_2 = T_m + \Delta T_{th} \text{ and } T_1 = T_m - \Delta T_{th} \tag{6.163}$$

where the subscripts "th" and "st" denote thermocline region (zone 2) and overall storage, respectively, and where

$$\Delta T \equiv |T - T_m| \tag{6.164}$$

According to the last bullet above, $0 \leq \Delta T_{th} \leq \Delta T_{st} = 15\,^{\circ}\text{C}$. Also, ΔT_{th} is the magnitude of the difference, on either side of the thermocline region (zone 2), between the temperature at the outer edge of zone 2 and T_m, while ΔT_{st} is the magnitude of the difference, on either side of the overall storage, between the temperature at the outer edge of the storage and T_m. That is,

$$\Delta T_{th} = \Delta T_1 = \Delta T_2 \text{ and } \Delta T_{st} = \Delta T_0 = \Delta T_3 \tag{6.165}$$

where the ΔT parameters in the above equations are defined using Equation 6.164 as follows:

$$\Delta T_j \equiv \left|T_j - T_m\right|, \text{ for } j = 0, 1, 2, 3 \tag{6.166}$$

Effects of Varying Stratification Parameters

- **Effect of varying T_m.** The variation of thermal-storage exergy with storage temperature for a mixed storage is illustrated in Figure 6.18. For a fixed storage total heat capacity (mc), storage exergy increases, from zero when the temperature T_m is equal to the environment temperature T_o, as the temperature increases or decreases from T_o. This general trend, which is illustrated here for a mixed storage, normally holds for stratified storages, since the effect on storage exergy of temperature is usually more significant than the effect of stratification.
- **Effect of varying minimum and maximum temperatures for a linear profile.** A linear temperature profile across the entire storage occurs with the three-zone model when $x_2 = 1$. Then, the upper and lower boundaries of zone 2 shift to the top and bottom of the storage, respectively,

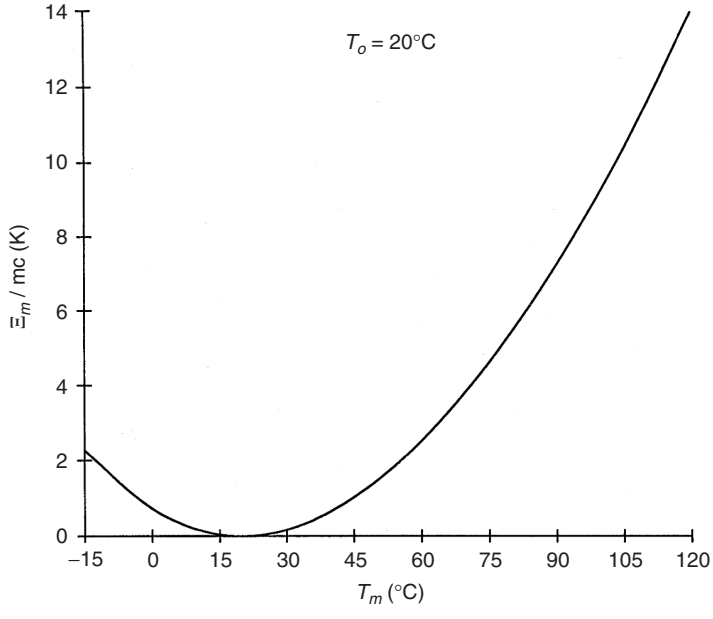

Figure 6.18 Variation with the mixed-storage temperature T_m of the modified exergy quantity Ξ_m/mc (where m and c are constant) for a mixed storage. When T_m equals the environment temperature $T_o = 20\,^\circ\text{C}$, $\Xi_m = 0$

and correspondingly the temperature deviation ΔT_{th} occurs at those positions. For a linear temperature profile, the ratio Ξ/Ξ_m is illustrated in Figures 6.19(a–c) for three temperature regimes, respectively:

– high-temperature thermal storage for heating capacity, that is, $T_m \geq 60\,^\circ\text{C}$;
– low-temperature thermal storage for heating capacity, that is, $20\,^\circ\text{C} \leq T_m \leq 60\,^\circ\text{C}$; and
– thermal storage for cooling capacity, that is, $T_m \leq 20\,^\circ\text{C}$.

The temperature range considered is above the environment temperature $T_o = 20°\text{C}$ for the first two cases, and below it for the third. Two key points are demonstrated in Figure 6.19. First, it is evident for all cases that, for a fixed mixed-storage temperature T_m, storage exergy content increases as the level of stratification increases (i.e., as ΔT_{th} increases). Secondly, the percentage increase in storage exergy, relative to the mixed-storage exergy at the same T_m, is greatest when $T_m = T_o$, and decreases both as T_m increases from T_o (see Figures 6.19a and b) and decreases from T_o (see Figure 6.19c). The main reason for this second observation relates to the fact that the absolute magnitude of the mixed exergy for a thermal storage is small when T_m is near T_o, and larger when T_m deviates significantly from T_o (see Figure 6.18). In the limiting case where $T_m = T_o$, the ratio Ξ/Ξ_m takes on the value of unity when $\Delta T_{th} = 0$ and infinity for all other values of ΔT_{th}. Hence, the relative benefits of stratification as a tool to increase the exergy-storage capacity of a thermal storage are greatest at near-environment temperatures, and less for other cases.

- **Effect of varying thermocline-size parameter x_2.** The variation of the ratio Ξ/Ξ_m with the zone-2 size parameter and the temperature deviation at the zone-2 boundaries, ΔT_{th}, is illustrated in Figure 6.20 for a series of values of the mixed-storage temperature T_m. For a fixed value of ΔT_{th} at a fixed value of T_m, the ratio Ξ/Ξ_m increases as the zone-2 size parameter x_2 decreases. This observation occurs because the stratification varies less smoothly and more sharp and pronounced as x_2 decreases.

- **Effect of varying temperature-distribution profile shape.** The temperature-distribution profile shape is varied, for a fixed value of T_m, primarily by varying values of the parameters x_2 and ΔT_{th} simultaneously. The behavior of Ξ/Ξ_m as x_2 and ΔT_{th} are varied for several T_m values is shown in Figure 6.20. For all cases considered, by varying these parameters at a fixed value of T_m (except for $T_m = T_o$), the ratio Ξ/Ξ_m increases, from a minimum value of unity at $x_2 = 1$ and $\Delta T_{th} = 0$, as x_2 decreases and ΔT_{th} increases. Physically, these observations imply that, for a fixed value of T_m, storage exergy increases as stratification becomes more pronounced, both by increasing the maximum temperature deviation from the mean storage temperature and by increasing the sharpness of temperature profile differences between storage zones.

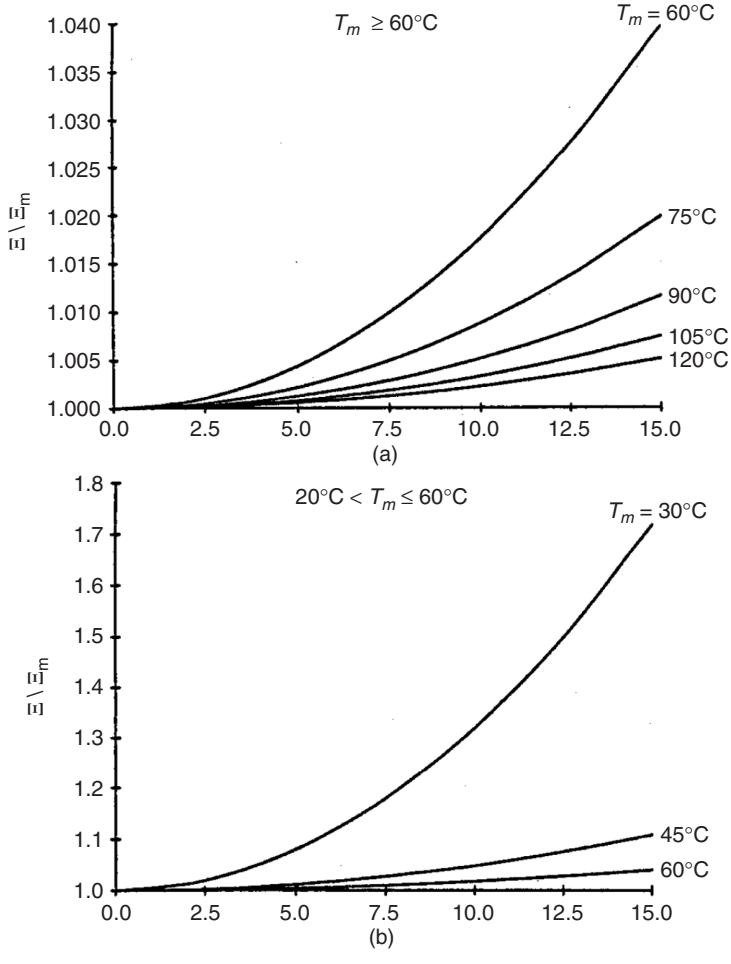

Figure 6.19 Illustration for three ranges of values of the mixed-storage temperature T_m (each corresponding to a different graph) of the variation of the ratio of the exergy values for stratified and fully mixed storages, Ξ/Ξ_m, with temperature deviation from T_m at the upper and lower boundaries of the thermocline zone (zone 2), ΔT_{th}. For all cases, a linear temperature profile is considered, that is, the zone-2 mass fraction is fixed at $x_2 = 1$. (a) High-temperature thermal storage for heating capacity, that is, $T_m \geq 60\,^{\circ}C$; (b) low-temperature thermal storage for heating capacity, that is, $20\,^{\circ}C \leq T_m \leq 60\,^{\circ}C$; (c) thermal storage for cooling capacity, that is, $T_m \leq 20\,^{\circ}C$

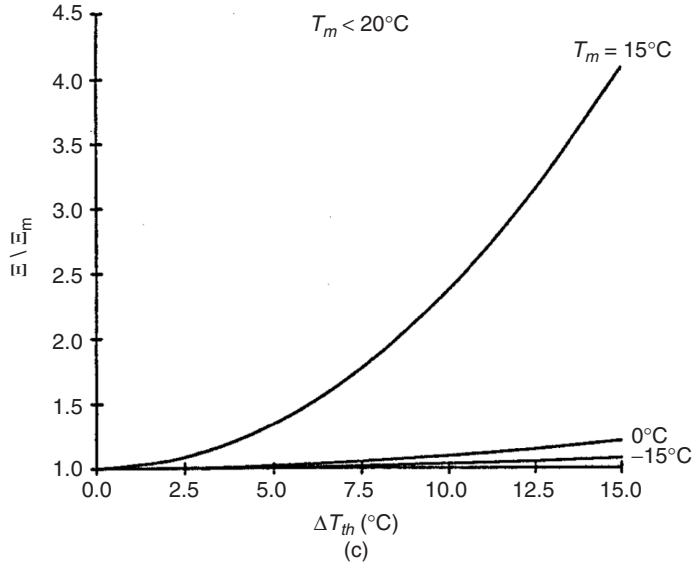

Figure 6.19 *(continued)*

6.8.7 *Illustrative Example: Increasing TES Exergy with Stratification*

In this example, several energy and exergy quantities relevant to the previous subsection are determined using the general three-zone model, for a thermal storage using water as the storage fluid and having a realistic stratified temperature distribution. The use of the data presented in this section as a design tool is also illustrated.

The actual distribution is taken to be that from the illustrative example in Section 6.8.5 for the general three-zone case. The temperature distribution is shown in Figure 6.17, along with the general three-zone model distribution used to approximate the actual distribution. Specified general data are listed in Table 6.10.

The results of the example (see Table 6.11) demonstrate that, for the case considered, the ratio $\Xi/\Xi_m = 180.7/165.4 = 1.09$. This implies that the exergy of the stratified storage is about 9% greater than the exergy of the mixed storage. In effect, therefore, stratification increases the exergy-storage capacity of the storage considered, relative to its mixed condition, by 9%.

Rather than determine values of the ratio Ξ/Ξ_m using the expressions in this section, values can be read from figures such as those in Figure 6.20 (although the case here of $T_m = 60°C$, $x_2 = 0.1$, and $\Delta T_{th} = 20°C$ falls slightly outside of the range of values covered in Figure 6.20 for the case of $T_m = 60°C$). Then, such diagrams can serve as design tools from which one can obtain a ratio that can be applied to the value of the exergy of the mixed storage to obtain the exergy of the stratified storage.

6.8.8 *Closure*

The temperature-distribution models described here (linear, stepped, continuous-linear, general-linear, basic three-zone, and general three-zone) facilitate the evaluation of energy and exergy contents of vertically stratified thermal storages. The selection of a particular distribution as a model involves a trade-off between result accuracy and calculational effort, and the three-zone models appear to provide the most reasonable compromise among these factors, and thus to be suitable as simple engineering aids for TES analysis, design, and optimization.

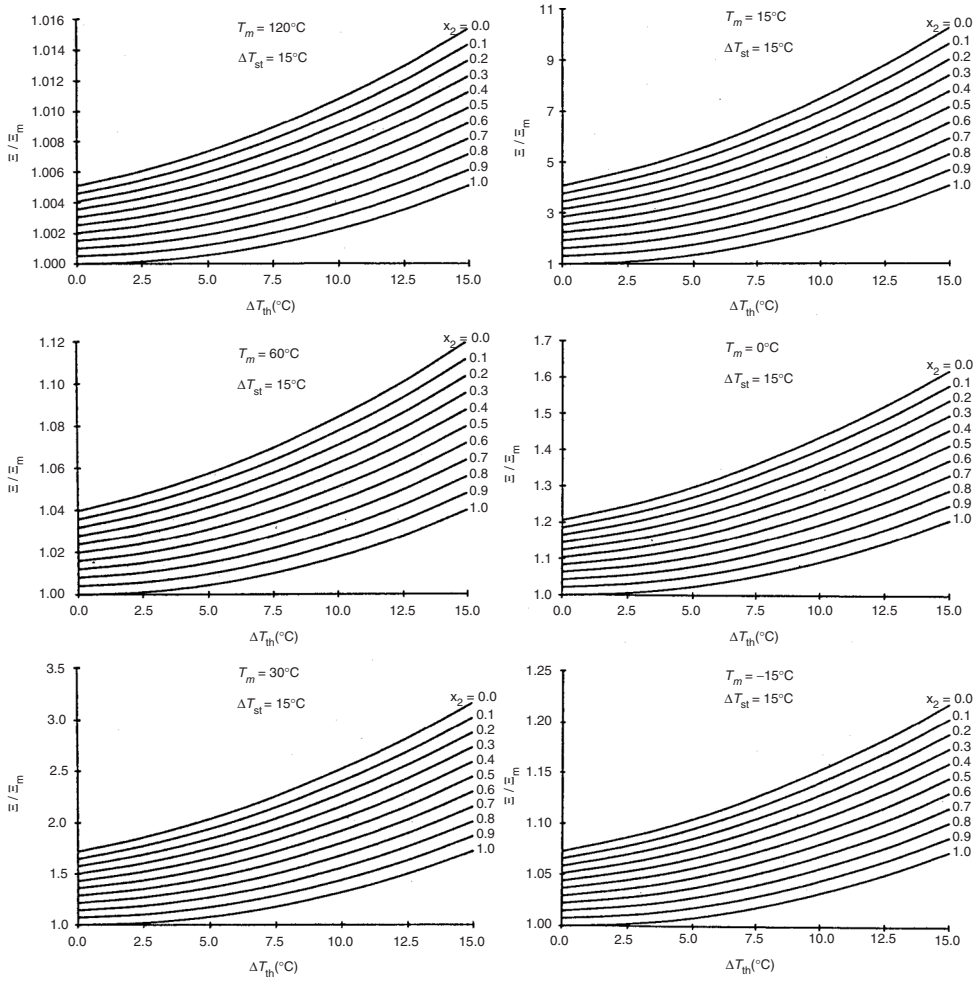

Figure 6.20 Illustration for a series of values of the mixed-storage temperature T_m (each corresponding to a different graph) of the variation of the ratio of the exergy values for stratified and fully mixed storages, Ξ/Ξ_m, with temperature deviation from T_m at the upper and lower boundaries of the thermocline zone (zone 2), ΔT_{th}, and with the zone-2 mass fraction x_2. The magnitude of the temperature deviation from T_m at the top and bottom of the storage, ΔT_{st}, is 15 °C for all cases

TES exergy values, unlike energy values, change due to stratification, giving a quantitative measure of the advantage provided by stratification. The examples considered illustrate how (i) the quantities of energy and exergy contained in a stratified TES differ, and (ii) the exergy content (or capacity) of a TES increases as the degree of stratification increases, even if the energy remains fixed. The use of stratification can therefore aid in TES design as it increases the exergy-storage capacity of a thermal storage.

6.9 Energy and Exergy Analyses of Cold TES Systems

An important application of TES is in facilitating the use of off-peak electricity to provide building heating and cooling. Recently, increasing attention has been paid in many countries to cold thermal

energy storage (CTES), an economically viable technology that has become a key component of many successful thermal systems. In many CTES applications, inexpensive off-peak electricity is utilized during the night to produce with chillers a cold medium, which can be stored for use in meeting cooling needs during the day when electricity is more expensive. CTES is applied mainly in building cooling, particularly for large commercial buildings that often need year-round cooling because of the heat released by occupants, lighting, computers, and other equipment. In most situations, CTES permits the mismatch between the supply and demand of cooling to be favorably altered (Dincer and Dost, 1996), leading to more efficient and environmentally benign energy use as well as reduced chiller sizes, capital and maintenance costs, and carbon dioxide and chlorofluorocarbon CFC emissions (Beggs, 1991).

To be economically justifiable, the annual costs needed to cover the capital and operating expenses for a CTES (and related systems) should be less than the costs for primary generating equipment supplying the same service loads and periods (Dincer, 1999). A CTES can lead to lower initial and operating costs for associated chillers when cooling loads are intermittent and of short duration. Secondary system capital costs may also be lower with CTES, for example, electrical service entrance sizes can sometimes be reduced because energy demand is lower.

Although CTES efficiency and performance evaluations are conventionally based on energy, energy analysis itself is inadequate for complete CTES evaluation because it does not account for such factors as the temperatures at which heat (or cold) is supplied and delivered. Exergy analysis overcomes some of these inadequacies in CTES assessments.

This section deals with the assessment using exergy and energy analyses of CTES systems, including sensible and/or latent storages, following earlier reports (Rosen *et al.*, (1999, 2000)). Several CTES cases are considered, including storages that are homogeneous or stratified and some that undergo phase changes. A full cycle of charging, storing, and discharging is considered for each case. This section demonstrates that exergy analysis provides more realistic efficiency and performance assessments of CTES systems than energy analysis, and conceptually is more direct since it treats cold as a valuable commodity. An example and case study illustrate the usefulness of exergy analysis in addressing cold thermal-storage problems.

6.9.1 Energy Balances

Consider a cold storage consisting of a tank containing a fixed quantity of storage fluid and a heat-transfer coil through which a heat-transfer fluid is circulated. Kinetic and potential energies and pump work are considered negligible. Energy balance for an entire cycle of a CTES can be written following Equation 6.3 in terms of "cold" as follows:

$$\text{Cold input} - [\text{Cold recovered} + \text{Cold loss}] = \text{Cold accumulation} \tag{6.167}$$

Here, "cold input" is the heat removed from the storage fluid by the heat-transfer fluid during charging; "cold recovered" is the heat removed from the heat-transfer fluid by the storage fluid; "cold loss" is the heat gain from the environment to the storage fluid during charging, storing, and discharging; and "cold accumulation" is the decrease in internal energy of the storage fluid during the entire cycle. Following Equation 6.3a, the overall energy balance for the simplified CTES system illustrated in Figure 6.21 becomes

$$(H_b - H_a) - [(H_c - H_d) + Q_l] = -\Delta E \tag{6.167a}$$

where H_a, H_b, H_c, and H_d are the enthalpies of the flows at points a, b, c, and d in Figure 6.21; Q_l is the total heat gain during the charging, storing, and discharging processes; and ΔE is the difference between the final and initial storage-fluid internal energies. The terms in square brackets in Equations 6.167 and 6.167a represent the net "cold output" from the CTES, and $\Delta E = 0$ if the CTES undergoes a complete cycle (i.e., the initial and final storage-fluid states are identical).

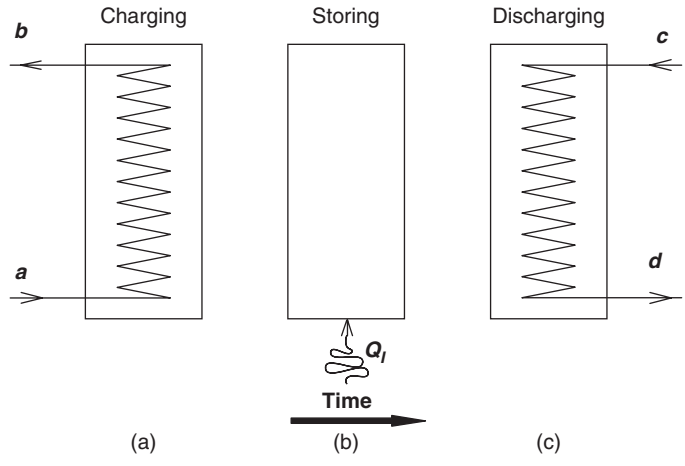

Figure 6.21 The three processes in a general CTES system: charging (a), storing (b), and discharging (c). The heat leakage into the system Q_l is illustrated for the storing process, but can occur in all three processes

The energy transfer associated with the charging fluid can be expressed as

$$H_b - H_a = m_a c_a (T_b - T_a) \tag{6.168}$$

where m_a is the mass flow of heat-transfer fluid at point a (and at point b), and c_a is the specific heat of the heat-transfer fluid, which is assumed constant. A similar expression can be written for $H_c - H_b$. The energy content of a storage which is homogeneous (i.e., entirely in either the solid or the liquid phase) is

$$E = m(u - u_o) \tag{6.169}$$

which, for sensible heat interactions only, can be written as

$$E = mc(T - T_o) \tag{6.169a}$$

where, for the storage fluid, c denotes the specific heat (assumed constant), m the mass, u the specific internal energy, and T the temperature. Also, u_o is u evaluated at the environmental conditions.

For a mixture of solid and liquid, the energy content of the solid and liquid portions can be evaluated separately and summed as follows:

$$E = m[(1 - F)(u_s - u_o) + F(u_t - u_o)] \tag{6.169b}$$

where u_s and u_t are the specific internal energies of the solid and liquid portions of the storage fluid, respectively, and F is the melted fraction (i.e., the fraction of the storage-fluid mass in the liquid phase).

For a storage fluid that is thermally stratified with a linear temperature profile in the vertical direction, the energy content can be shown with Equations 6.116b and 6.129 to be

$$E = mc\left(\frac{T_t + T_b}{2} - T_o\right) \tag{6.169c}$$

where T_t and T_b are the storage-fluid temperatures at the top and bottom of the linearly stratified storage tank, respectively.

The change in CTES energy content from the initial (i) to the final state (f) of a process can be expressed as in Equation 6.38.

6.9.2 Exergy Balances

An exergy balance for a CTES undergoing a complete cycle of charging, storing, and discharging can be written as in Equations 6.40 and 6.40a. The exergy content of a flow of heat-transfer fluid at state k (where $k = a, b, c,$ or d in Figure 6.21) can be expressed as in Equation 6.44. The exergy transfers associated with the charging and discharging of the storage by the heat-transfer fluid can be expressed by Equations 6.45 and 6.46, respectively.

The exergy loss associated with heat infiltration during the three storage periods can be expressed as in Equation 6.47a. The thermal exergy terms are negative for sub-environment temperatures, as is the case here for CTES, indicating that the heat transfer and the accompanying exergy transfer are oppositely directed. That is, the losses associated with heat transfer are due to heat infiltration into the storage when expressed in energy terms, but due to a cold loss out of the storage when expressed in exergy terms.

The exergy content of a homogeneous storage can be shown with Equation 6.116 to be

$$\Xi = m[(u - u_o) - T_o(s - s_o)] \tag{6.170}$$

where s is the specific entropy of the storage fluid and s_o is s evaluated at the environmental conditions. If only sensible heat interactions occur, Equation 6.170 can be written with Equation 6.119 as

$$\Xi = mc[(T - T_o) - T_o \ln(T/T_o)] \tag{6.170a}$$

For a mixture of solid and liquid, the exergy content can be written as

$$\Xi = m\{(1 - F)[(u_s - u_o) - T_o(s_s - s_o)] + F[(u_t - u_o) - T_o(s_t - s_o)]\} \tag{6.170b}$$

where s_s and s_t are the specific entropies of the solid and liquid portions of the storage fluid, respectively.

The exergy content of a storage that is linearly stratified can be shown with Equations 6.117b and 6.130 to be

$$\Xi = E - mcT_o\left[\frac{T_t(\ln T_t - 1) - T_b(\ln T_b - 1)}{T_t - T_b} - \ln T_o\right] \tag{6.170c}$$

The change in TES exergy content can be expressed as in Equation 6.43.

6.9.3 Energy and Exergy Efficiencies

For a general CTES undergoing a cyclic operation, the overall energy efficiency η can be evaluated as in Equation 6.32, with the word *energy* replaced by *cold* for understanding. Then, following Figure 6.21, the overall and charging-period energy efficiencies can be expressed as in Equations 6.48 and 6.52, respectively.

Energy efficiencies for the storing and discharging subprocesses can be written respectively as

$$\eta_2 = \frac{\Delta E_1 + Q_l}{\Delta E_1} \tag{6.171}$$

$$\eta_3 = \frac{H_c - H_d}{\Delta E_3} \tag{6.172}$$

where ΔE_1 and ΔE_3 are the changes in CTES energy contents during charging and discharging, respectively.

The exergy efficiency for the overall process can be expressed as in Equation 6.49, and for the charging, storing, and discharging processes, respectively, as in Equations 6.55, 6.61, and 6.67.

6.9.4 *Illustrative Example*

Cases Considered and Specified Data

Four different CTES cases are considered. In each case, the CTES has identical initial and final states, so that the CTES operates in a cyclic manner, continuously charging, storing, and discharging. The main characteristics of the cold storage cases are as follows:

- sensible heat storage, with a fully mixed-storage fluid;
- sensible heat storage, with a linearly stratified storage fluid;
- latent heat storage, with a fully mixed-storage fluid;
- combined latent and sensible heat storage, with a fully mixed-storage fluid.

The following assumptions are made for each of the cases:

- Storage boundaries are nonadiabatic.
- Heat gain from the environment during charging and discharging is negligibly small relative to heat gain during the storing period.
- The external surface of the storage tank wall is at a temperature 2 °C greater than the mean storage-fluid temperature.
- The mass flow rate of the heat-transfer fluid is controlled so as to produce constant inlet and outlet temperatures.
- Work interactions and changes in kinetic and potential energy terms, are negligibly small.

Specified data for the four cases are presented in Table 6.12 and relate to the diagram in Figure 6.21. In Table 6.12, T_b and T_d are the charging and discharging outlet temperatures of the heat-transfer fluid, respectively. The subscripts 1, 2, and 3 indicate the temperature of the storage fluid at the beginning of charging, storing, or discharging, respectively. Also, t indicates the liquid state and s indicates the solid state for the storage fluid at the phase-change temperature.

In addition, for all cases, the inlet temperatures are fixed for the charging-fluid flow at $T_a = -10$°C and for the discharging-fluid flow at $T_c = 20$ °C. For cases involving latent heat changes (i.e., solidification), $F = 10\%$. The specific heat c is 4.18 kJ/kg K for both the storage and heat-transfer fluids. The phase-change temperature of the storage fluid is 0 °C. The configuration of the storage tank is cylindrical with an internal diameter of 2 m and internal height of 5 m. Environmental conditions are 20 °C and 1 atm.

Table 6.12 Specified temperature data for the cases in the CTES example

Temperature (°C)	Case			
	I	II	III	IV
T_b	4.0	15	−1	−1
T_d	11.0	11	10	10
T_1	10.5	19/2[a]	0 (t)	8
T_2	5.0	17/−7[a]	0 (s)	−8
T_3	6.0	18/−6[a]	0 (t and s)	0 (t and s)

[a]When two values are given, the storage fluid is vertically linearly stratified and the first and second values are the temperatures at the top and bottom of the storage fluid, respectively.

Table 6.13 Energy and exergy quantities for the cases in the CTES example

Period or quantity	Energy quantities				Exergy quantities			
	I	II	III	IV	I	II	III	IV
Efficiencies (%)								
Charging (1)	100	100	100	100	51	98	76	77
Storing (2)	82	82	90	90	78	85	90	85
Discharging (3)	82	100	100	100	38	24	41	25
Overall	100	82	90	90	15	20	28	17
Input, recovered and lost quantities (MJ)								
Input	361.1	361.1	5237.5	6025.9	30.9	23.2	499.8	575.1
Recovered	295.5	295.5	4713.8	5423.3	4.6	4.6	142.3	94.7
Loss (external)	65.7	65.7	523.8	602.6	2.9	2.9	36.3	48.9
Loss (internal)	–	–	–	–	23.3	15.6	321.2	431.4

Results and Discussion

The results for the four cases are listed in Table 6.13, and include overall and subprocess efficiencies, input and recovered cold quantities, and energy and exergy losses. The overall and subprocess energy efficiencies are identical for Cases I and II, and for Cases III and IV. In all cases, the energy efficiency values are high. The different and lower exergy efficiencies for all cases indicate that energy analysis does not account for the quality of the "cold" energy, as related to temperature, and considers only the quantity of "cold" energy recovered.

The input and recovered quantities in Table 6.13 indicate the quantity of "cold" energy and exergy input to and recovered from the storage. The energy values are much greater than the exergy values because, although the energy quantities involved are large, the energy is transferred at temperatures only slightly below the reference-environment temperature, and therefore is of limited usefulness.

The cold losses during storage, on an energy basis, are entirely due to cold losses across the storage boundary (i.e., heat infiltration). The exergy-based cold losses during storage are due to both cold losses and internal exergy losses (i.e., exergy consumptions due to irreversibilities within the storage). For the present cases, in which the exterior surface of the storage tank is assumed to be 2 °C warmer than the mean storage-fluid temperature, the exergy losses include both external and internal components. Alternatively, if the heat-transfer temperature at the storage tank external surface is at the environment temperature, the external exergy losses would be zero and the total exergy losses would be entirely due to internal consumptions. If heat transfer occurs at the storage-fluid temperature, on the other hand, more of the exergy losses would be due to external losses. In all cases, the total exergy losses, which are the sum of the internal and external exergy losses, remain fixed.

The four cases demonstrate that energy and exergy analyses give different results for CTES systems. Both energy and exergy analyses account for the quantity of energy transferred in storage processes. Exergy analyses take into account the loss in quality of "cold" energy, and thus more correctly reflect the actual value of the CTES.

In addition, exergy analysis is conceptually more direct when applied to CTES systems because cold is treated as a useful commodity. With energy analysis, flows of heat rather than cold are normally considered. Thus, energy analyses become convoluted and confusing as one must deal with heat flows, while accounting for the fact that cold is the useful input and product recovered for CTES systems. Exergy analysis inherently treats any quantity that is out of equilibrium with the environment (be it colder or hotter) as a valuable commodity, and thus avoids the intuitive conflict in the expressions associated with CTES energy analysis. The concept that cold is a valuable commodity is both logical and in line with one's intuition when applied to CTES systems.

6.9.5 *Case Study: Thermodynamic Performance of a Commercial Ice TES System*

One type of CTES is ice storage, which has been increasingly utilized recently. In an ice thermal energy storage (ITES) system, off-peak electricity is utilized to create a large mass of ice, and during the day, this ice store is melted by absorbing the heat from buildings needing cooling (De Lucia and Bejan, 1990; Beggs, 1991). ITES is a proven technology applicable to any plant that has a chilled water system.

Numerous economic studies of ITES systems and their applications have been undertaken (Althof, 1989; Beggs, 1991; Fields and Knebels, 1991). Chen and Sheen (1993) developed a model for a CTES system that evaluates the component size for a eutectic salt storage system. The related computer simulation determines energy consumption, and performs a cost/benefit analysis to estimate the system payback period. Chen and Sheen also determined the best system operating strategies for varying weather conditions and electricity rates, particularly in Taiwan. Wood *et al*. (1994) investigated TES technical and economic aspects, and presented a techno-economic feasibility evaluation method for new technologies in the commercial sector using a pseudo-data analysis approach. Some (Badar *et al*., 1993; Domanski and Fellah, 1998) have applied thermoeconomic optimization techniques to TES systems that minimize the combination of entropy generation cost and annualized capital cost of the thermal component.

In this case study, which is based on an earlier analysis (Rosen *et al*., 2000), energy and exergy analyses of a commercial encapsulated ITES are performed. A full cycle, with charging, storing, and discharging stages, is considered. The case study demonstrates the usefulness of exergy analysis in thermodynamic assessments of ITES systems, provides insights into their performances and efficiencies, and shows that energy analysis leads to misleadingly optimistic statements of ITES efficiency.

Types and Operation of ITES Systems

By making ice at night for use in the day when it is needed to provide cooling, ITES systems take advantage of low off-peak electricity rates and often permit building chillers to be shut down or operated at reduced levels during the day. Consequently, owners can realize lower utility bills, and electrical utilities attain a reduction in peak demand, which can defer or avoid the need for new power plants. Ice storage systems are capable of providing the same quantity and quality of cooling as conventional chillers.

There are two main cases of ice storage systems, differing in the levels of electrical load shifting achieved. With a "full storage," the entire cooling load is shifted, eliminating chiller operation during peak hours. In a "partial storage," part of the load is met from a downsized chiller, and part from the storage. In both cases, the sizes of the chiller and of the storage depend on the total amount of cooling needed to meet the building load over the entire day. Sizing is the main factor differentiating ice storage from conventional air-conditioning, since in the latter case, the chiller must be larger to meet the peak cooling load, which normally occurs during the hottest part of the day.

Four main types of ITES systems are commonly used in commercial and industrial applications (Beckman and Gilli, 1984; Beggs, 1991): ice-on-coil, static ice tank, ice harvesting, and encapsulated ice store. The most common ITES type is the encapsulated ice store (Figure 6.22), which is considered in this case study. Encapsulated ITES systems consist of an insulated storage tank (normally constructed from either steel or concrete) that is filled with small plastic capsules containing deionized water and a nucleating agent (Carrier, 1990). Circulating around the capsules is a glycol/water brine solution. During charging, the brine solution is circulated through the tank at a sub-freezing temperature, causing the water in the capsules to freeze to form the ice store. To discharge the store when cooling is needed, the same brine solution is circulated through the tank but at a temperature above the freezing point of water. The ice in the capsules then melts, cooling the brine solution that is subsequently circulated to the air-conditioning unit.

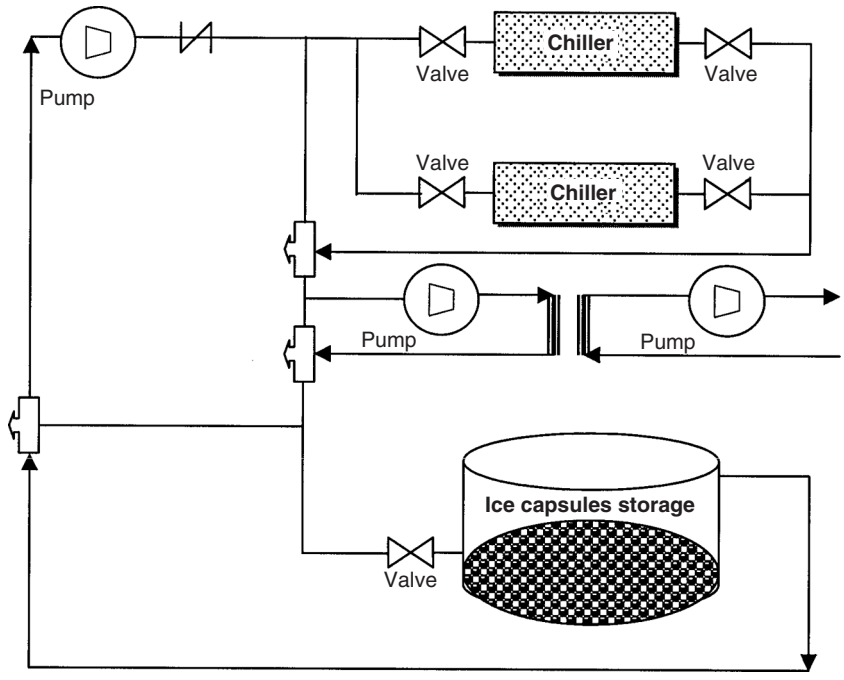

Figure 6.22 A schematic representation of an encapsulated ITES system

Description of ITES Considered and its Operation

The ITES system considered in this study (Figure 6.22) is designed to have the chiller operate continuously during the design day, and utilizes three operating modes (Carrier, 1990):

- **Charging.** The charging mode is the normal operating mode during no-load periods. The chiller cools the antifreeze solution to approximately $-4\,^{\circ}\mathrm{C}$. The antifreeze solution flows through the storage module, freezing the liquid water inside the encapsulated units. The circulating fluid increases in temperature (to a limit of $0\,^{\circ}\mathrm{C}$), and returns to the chiller to be cooled again. During charging, the building loop is isolated so that full flow is achieved through the storage module.
- **Chilling.** The chilling mode is the same as for a nonstorage (conventional) chiller system, with the entire building load being met directly by the chiller. The chiller operates at a warmer set point than for ice making, which results in an increased capacity and a higher coefficient of performance. In this mode, there is no flow through the storage module, and ice in the store is kept in reserve for use later in the day.
- **Chilling and discharging.** Chilling and discharging is the normal operating mode during daytime hours. The chiller and storage module share the cooling load, often in a series configuration. Systems are normally designed with the chiller downstream of the storage. Then, the storage module pre-cools the building return fluid before it is further cooled to the design supply temperature by the chiller. This sequence gives a higher effective storage capacity, since the exit temperature from the storage can be higher. The ice melting rate is controlled by modulating valves that cause some flow to bypass the storage module, usually to hold constant the blended fluid temperature downstream of the storage throughout discharging.

The design-day cooling load profile of a typical office building is considered here (Figure 6.23). The circles and squares in Figure 6.23 indicate the cooling load required for the building and the

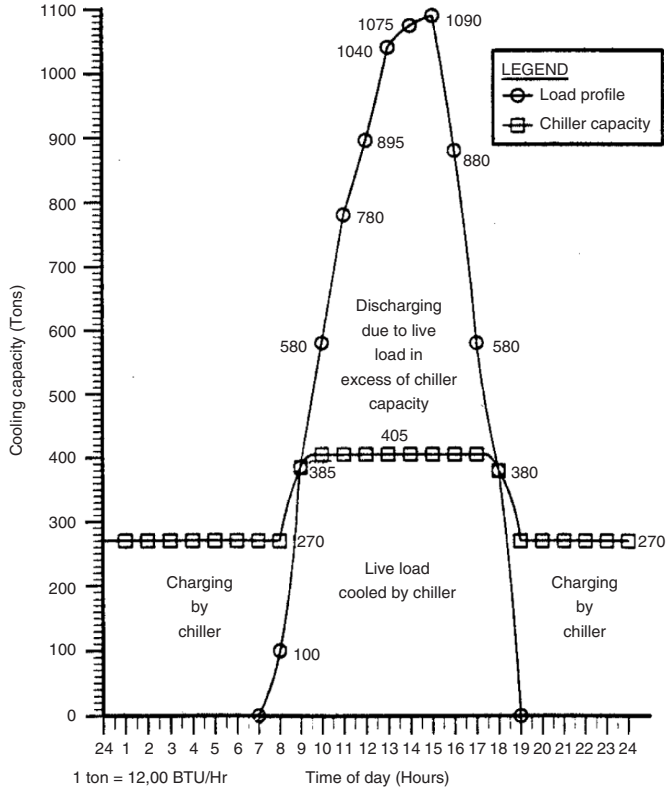

Figure 6.23 A load profile diagram for an encapsulated ITES system (see Rosen *et al*., 2000)

chiller loads, respectively. Data for the case, taken from Carrier (1990), is presented in Table 6.14 for a full 24-h cycle. The ITES is designed for the chiller to operate continuously during the day (i.e., partial storage operation is used). The ITES module has nonadiabatic storage boundaries with a total thermal resistance of $R_T = 1.98\,\text{m}^2\,\text{K/W}$. The specific heat of the heat-transfer fluid (a glycol-based antifreeze solution) is 3.22 kJ/kg K at $-6.6\,^\circ\text{C}$ and 3.60 kJ/kg K at $15.5\,^\circ\text{C}$, and the specific gravity is 1.13. The storage fluid (deionized water) has a freezing point of $0\,^\circ\text{C}$, a mass of 144,022 kg, and a density of $1000\,\text{kg/m}^3$. The storage module has a volume of $181.8\,\text{m}^3$, with $144.0\,\text{m}^3$ occupied by the storage fluid, and a surface area A of $241.6\,\text{m}^2$. The reference-environment conditions are $20\,^\circ\text{C}$ and 1 atm.

Thermodynamic Analysis

To reduce analysis complexity and to emphasize the significant factors in ice storage operation, it is assumed that the storage fluid remains isothermal at its melting point, fluids are frictionless, the pumping power is zero, and kinetic and potential energy terms are negligibly small. These assumptions neglect some of the irreversibilities in the encapsulated ITES system, notably those associated with the temperature gradients close to the freezing or thawing surfaces in the storage. The net effect of these assumptions is to increase the apparent exergy efficiencies, but probably not their relative values. Hence, the results should be valid in ordering the performances of competitive systems in an optimization process. The analysis generally follows the discussions

Table 6.14 Specified and evaluated data for the ITES case study

Hour	Process	Load (tons)			Melted fraction (%)	Efficiency (%)	
		Storage	Building	Chiller		Exergy	Energy
1	Charging	270	0	270	48.55	88.1	99.7
2	Charging	270	0	270	41.46	87.0	99.7
3	Charging	270	0	270	34.36	85.9	99.7
4	Charging	270	0	270	27.27	84.8	99.7
5	Charging	270	0	270	20.17	83.7	99.7
6	Charging	270	0	270	13.08	82.6	99.7
7	Charging	270	0	270	5.99	81.6	99.7
8	Charging	170	100	270	1.53	80.4	99.5
9	Storing	0	385	385	1.55	99.9	99.9
10	Discharging	175	580	405	6.12	66.0	99.7
11	Discharging	375	780	405	15.96	63.3	99.9
12	Discharging	490	895	405	28.83	59.9	99.9
13	Discharging	635	1040	405	45.53	58.5	99.9
14	Discharging	670	1075	405	63.15	57.1	99.9
15	Discharging	685	1090	405	81.16	55.7	99.9
16	Discharging	475	880	405	93.63	52.9	99.9
17	Discharging	175	580	405	98.21	63.9	99.7
18	Storing	0	380	380	98.22	99.9	99.9
19	Charging	270	0	270	91.13	93.5	99.7
20	Charging	270	0	270	84.03	92.6	99.7
21	Charging	270	0	270	76.94	91.8	99.7
22	Charging	270	0	270	69.84	90.9	99.7
23	Charging	270	0	270	62.74	90.1	99.7
24	Charging	270	0	270	55.65	89.3	99.7

earlier in this section. Also, losses due to heat gain from the environment, Q_l, are determined here as follows:

$$Q_l = \frac{A\Delta T}{R_T} \tag{6.173}$$

where ΔT is the difference between the storage-fluid and environmental temperatures, A is the surface area through which the heat is transferred, and R_T is the unit total thermal resistance of the storage module. Following Figure 6.21, the overall energy and efficiencies can be written with Equations 6.32 and 6.49 for the ITES module as it undergoes a cyclic operation over a 24-h period, by summing over the 24 h:

$$\eta = \frac{\text{Product cold recovered}}{\text{Cold input}} = \frac{\sum_{j=1}^{24} (H_c - H_d)_j}{\sum_{j=1}^{24} (H_b - H_a)_j} \tag{6.174}$$

$$\psi = \frac{\text{Exergy recovered}}{\text{Exergy input}} = \frac{\sum_{j=1}^{24} (\in_d - \in_c)_j}{\sum_{j=1}^{24} (\in_a - \in_b)_j} \tag{6.175}$$

Energy and exergy efficiencies for charging, storing, and discharging are similarly evaluated, following Section 6.9.3.

Results and Discussion

The overall energy and exergy efficiencies are 99.5% and 50.9%, respectively, and the hourly energy and exergy efficiencies are listed in Table 6.14. The hourly exergy efficiencies range from 80–94% and average 86% for the overall charging period, range from 53–66% and average 60% for the overall discharging period, and range from 99–100% for the overall storing period. The hourly energy efficiencies exceed 99% for all periods.

The marked differences in the energy and exergy efficiencies for the overall process and the subprocesses merit emphasis and explanation. The energy efficiencies are high, since they only account for heat gains from the environment, which are small. The exergy efficiencies are much lower since they account for the "usefulness" of the energy, which is related to the inlet and outlet temperatures and the mass flow rates of heat-transfer fluid. In the example, the charging fluid being at $-4\,^{\circ}C$, a much lower temperature than that of the environment, is a moderately high-quality cold flow. The cold flow recovered during discharging, however, is of much lower quality with a temperature much closer to that of the environment. Thus, the energy efficiencies, for each hour or for the entire cycle, are misleadingly high as they only account for energy recovery but neglect entirely the loss of quality of the flows. This quality loss is quantified with exergy analysis. Since the irreversibilities in an ITES process destroy some of the input exergy, ITES exergy efficiencies are always lower than the corresponding energy efficiencies.

Another interesting observation stems from the fact that exergy efficiencies provide a measure of how nearly a process approaches ideality, while energy efficiencies do not. Here, the energy efficiencies being over 99% for the overall process and all subprocesses erroneously imply that the ITES system is nearly ideal. The overall exergy efficiency of approximately 51%, as well as the subprocess exergy efficiencies, indicate that the ITES system is far from ideal, and has a significant margin for efficiency improvement. In this example, the same cooling capacity could be delivered from the ITES using about half of the input exergy if it were ideal. Thus, overall electrical use by the chillers could be greatly reduced while still maintaining the same cooling services. Such a reduction would reduce the necessary installed cooling power and electrical costs.

Further implications of the results follow:

- The fact that the exergy efficiencies are less than 100% implies that a mismatch exits between the quality of the thermal energy delivered by the ITES (and required by the cooling load) and the quality of the thermal energy input to the ITES. This mismatch, which is detectable through the temperature of the thermal energy flows across the ITES boundaries, is quantifiable with exergy analysis as the work potential lost during storage. The exergy loss, therefore, correlates directly with an additional use of electricity by the chillers than would occur without the exergy loss. When exergy efficiencies are 100%, there is no loss in temperature during storage.
- The nonideal exergy efficiencies imply that excessively high-quality thermal energy is supplied to the ITES than is required given the cooling load. Thus, exergy analysis indicates that lower quality sources of thermal energy could be used to meet the cooling load. Although economic and other factors must be taken into account when selecting energy resources, the exergy-based results presented here can assist in identifying feasible energy sources that have other desired characteristics (e.g., environmentally benign or abundant).

Consequently, the results demonstrate that a more perceptive measure of comparison than energy efficiency is needed if the true usefulness of an ITES is to be assessed and a rational basis for the optimization of its economic value established. Energy efficiencies ignore the quality (exergy) of the energy flows, and so cannot provide a measure of ideal performance. Exergy efficiencies provide more comprehensive and useful efficiency measures for practical ITES systems, and facilitate more rational comparisons of different systems. In addition, exergy analysis can assist in the optimization

of ITES systems, when combined with assessments of such other factors as resource-use reductions, environmental impact and emissions decreases, and economics.

6.9.6 Closure

Exergy analysis provides more meaningful and useful information than energy analysis about the efficiencies, losses, and performance for CTES systems. A prime justification for this view is that the loss of low temperature is accounted for in exergy – but not in energy-based performance measures. Furthermore, the exergy-based information is presented in a more direct and logical manner, as exergy methods provide intuitive advantages when CTES systems are considered. Consequently, exergy analysis can likely assist in efforts to optimize the design of CTES systems and their components, and to identify appropriate applications and optimal configurations for CTES in general engineering systems. Several additional key points can be drawn from this section: (i) exergy analysis can assist in selecting alternative energy sources for CTES systems, so that the potential role can be properly considered for CTES in meeting society's preferences for more efficient, environmentally benign energy use in various sectors; and (ii) the application of exergy analysis to CTES systems permits mismatches in the quality of the thermal energy supply and demand to be quantified, and measures to reduce or eliminate reasonably avoidable mismatches to be identified and considered. The material presented in this section for cold TES parallels that presented in the rest of this chapter for heat storage systems, although the advantages of the exergy approach appear to be more significant when CTES systems are considered due to manner in which "cold" is treated as a resource.

6.10 Exergy-Based Optimal Discharge Periods for Closed TES Systems

Since in many instances, energy-based performance measures can be misleading while exergy-based measures provide more realistic TES evaluations, exergy results can be useful in design and optimization activities. Some researchers (Bejan, 1978; Rosen, 1990) have attempted to obtain optimum design and operating parameters for sensible TES systems using exergy techniques. Bejan (1978) considered the charging process of a TES system. Krane (1987), considering the entire charging–discharging cycle, found that high-efficiency systems had charging–discharging time ratios of 1:4 or higher. It may not be possible to incorporate such charging–discharging time ratios into many TES applications. Optimal efficiencies and temperatures for the phase change in latent TES have also been investigated (Saborio-Aceves *et al*., 1994).

In this section, which follows an earlier report (Gunnewiek *et al*., 1993), the usefulness of using exergy-based measures in optimization and design is demonstrated for TES discharge processes. Analytical expressions are developed using energy and exergy methods for the storage-fluid temperature during discharging and the TES discharge efficiencies. Although in much of this chapter, pump work has been neglected with respect to thermal energy flows, one must account for work terms in optimization efforts. Thus pump work is accounted for in this section, and the optimum discharge period based on thermodynamic criteria is determined. An illustrative example is presented.

6.10.1 Analysis Description and Assumptions

A simple case is considered in which a sensible, closed, fully mixed TES undergoes a complete storage cycle where the final state of the TES is the same as the initial state. The TES system boundaries may be adiabatic or nonadiabatic, and the surroundings are at a constant temperature and pressure. Fluid flows are modeled as steady and one-dimensional. Kinetic and potential energy

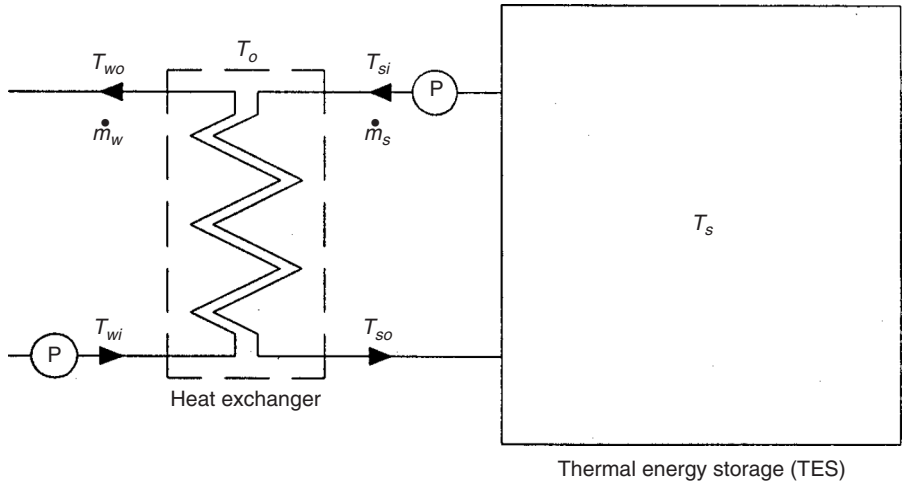

Figure 6.24 The closed TES system considered in evaluating optimal discharge periods

terms are considered negligible, as is the chemical component of exergy, because it does not contribute to the exergy transfers for a sensible TES system.

6.10.2 Evaluation of Storage-Fluid Temperature During Discharge

It is assumed that the recovery of thermal energy from the TES system is achieved with a heat exchanger (Figure 6.24). The heat-recovery rate may be written as

$$\dot{Q} = \dot{m}_s c_s (T_{si} - T_{so}) \tag{6.176}$$

where $\dot{m}_s$ and c_s are the mass flow rate and specific heat of the storage fluid, and T_{si} and T_{so} are the heat exchanger inlet and outlet storage-fluid temperatures, respectively.

Knowing the effectiveness ε of the heat exchanger, which is dependent on the heat-exchanger configuration and fluid flow conditions, and the minimum heat capacity rate C_{min} for the two fluids involved in the heat-transfer process, the heat-recovery rate may also be written as

$$\dot{Q} = C_{min} \varepsilon (T_{si} - T_{wi}) \tag{6.177}$$

Assuming that the temperature of the storage fluid entering the heat exchanger T_{si} is the same as the storage-fluid temperature T_s, and that the working-fluid temperature entering the heat exchanger T_{wi} is the same as the reference-environment temperature T_o, then it can be shown with Equations 6.176 and 6.177 that

$$T_{so} = T_s - \frac{C_{min}\varepsilon}{\dot{m}_s c_s}(T_s - T_o) \tag{6.178}$$

To evaluate the changing storage-fluid temperature during the discharge process, a mathematical model is introduced in which, for a finite time step of t^s, a mass of storage fluid at temperature T_s exits the TES while an equal mass of storage fluid at temperature T_{so} enters. The importance has recently been recognized of the time-step size used in the mathematical modeling and numerical simulation of TES systems (Fanny and Klein, 1988; Lightstone *et al*., 1988). The accuracy of the results is partially dependent on the time-step size and flow rates. A decrease in the time-step size increases the accuracy of the solution to a certain point. In one particular study (Lightstone *et al*., 1988), a decrease in a time step of 10 s resulted in no significant difference in the results.

Adiabatic TES Case

After each time step of the discharging period, the new storage-fluid temperature T_{sa} for a fully mixed TES with adiabatic boundaries can be expressed as

$$T_{sa} = \frac{(m - \dot{m}_s t^s)T_s + (\dot{m}_s t^s)T_{so}}{m} \tag{6.179}$$

where m is the mass of the storage fluid and is constant for a closed TES system. Using Equation 6.178, Equation 6.179 becomes

$$T_{sa} = T_s - \frac{C_{min}\varepsilon t^s}{mc_s}(T_s - T_o) \tag{6.179a}$$

Nonadiabatic TES Case

For a nonadiabatic TES with an overall heat-transfer coefficient U based on an outer-surface area A, the heat loss Q_l at any storage-fluid temperature T_s, for a finite time step t^s, is

$$Q_l = UAt^s(T_s - T_o) \tag{6.180}$$

and the TES energy content E_s is

$$E_s = mc_s(T_s - T_o) \tag{6.181}$$

Thus, after each finite time step during the discharging process, the new storage-fluid temperature T_{sn}, for a fully mixed TES with nonadiabatic boundaries, can be found with the following energy balance:

$$mc_s(T_{sn} - T_o) = mc_s(T_{sa} - T_o) - Q_l \tag{6.182}$$

After rearranging and substituting Equations 6.179a and 6.180, it can be shown that

$$T_{sn} = T_s - \frac{C_{min}\varepsilon t^s}{mc_s}(T_s - T_o) - \frac{UAt^s}{mc_s}(T_s - T_o) \tag{6.183}$$

Note that Equation 6.183 expresses the new storage-fluid temperature after a finite time step for any fully mixed, closed TES with adiabatic or nonadiabatic boundaries.

6.10.3 Discharge Efficiencies

Energy Efficiency

The heat Q_3 recovered from a TES during the ith finite time step $t_s(i)$ can be written as

$$Q_3(i) = \dot{m}_s c_s t^s(i)[T_{sn}(i) - T_{so}(i)] \tag{6.184}$$

Equation 6.184 does not account for the work required to recover the heat. If pump work is considered, the net energy recovered from the TES system may be written as $Q_3(i) - \dot{W}t^s(i)$, where $\dot{W}$ is the shaft power used by the pump, and the discharge energy efficiency after n time steps is defined as

$$\eta = \sum_{i=1}^{n} \frac{Q_3(i) - \dot{W}t^s(i)}{E_s(i = 0)} \tag{6.185}$$

Here $E_s(i = 0)$ is the initial energy content of the storage, when the storage-fluid temperature is T_s. Note that the energy discharge efficiency is 100% when heat transfer is ideal and the TES is perfectly insulated.

Exergy Efficiency

The thermal exergy X_3 recovered from the TES during time step i can be written as

$$X_3(i) = \dot{m}_s c_s t^s(i) \left[(T_{sn}(i) - T_{so}(i)) - T_o \ln \frac{T_{sn}(i)}{T_{so}(i)} \right] \tag{6.186}$$

Accounting for pump work, the net exergy recovered is $X_3(i) - \dot{W} t^s(i)$ and the discharge exergy efficiency can be written as

$$\psi = \sum_{i=1}^{n} \frac{X_3(i) - \dot{W} t^s(i)}{\Xi_s(i=0)} \tag{6.187}$$

where $\Xi_s(i=0)$ is the initial exergy content of the TES, expressible as

$$\Xi_s = mc_s[(T_s - T_o) - T_o \ln(T_s/T_o)] \tag{6.188}$$

6.10.4 Exergy-Based Optimum Discharge Period

From a thermodynamic perspective, the optimum discharge period for a TES is that corresponding to the maximum discharge efficiency. The authors feel that the optimum discharge period is more meaningfully determined using exergy rather than energy efficiencies, because exergy analysis considers the quality or usefulness of storage-fluid energy, which is dependent on the fluid and ambient temperatures, and recognizes the difference in usefulness of pump work and recovered heat, whereas energy analysis treats these two energy forms as equal.

It is noted that the optimum discharge period here, which is constrained to being based solely on thermodynamic criteria, may not in general coincide with the optimum period when factors other than thermodynamics (e.g., economics, environmental impact) are taken into account.

6.10.5 Illustrative Example

Consider an active solar space-heating system having a sensible, fully mixed TES that is charged during daylight hours and discharged at night. The storage medium, water, has a mass of $m = 10{,}000\,\text{kg}$, a constant specific heat of $c_s = 4.18\,\text{kJ/kg K}$, and a temperature at the beginning of the discharge period of $T_s = 353\,\text{K}$. Heat transfer between the storage fluid and working fluid (air, with $c_w = 1.007\,\text{kJ/kg K}$) occurs in a heat exchanger with a "number of transfer units" of $NTU = 2.5$, an effectiveness of $\varepsilon = 0.7$, and mass flow rates of $\dot{m}_s = 0.22$ and $\dot{m}_w = 1.2\,\text{kg/s}$. The temperature of the reference environment is $T_o = 293\,\text{K}$. A time step of $t^s = 600\,\text{s}$ is used.

Energy and exergy discharge efficiencies are evaluated as a function of discharge period duration for several cases. Figure 6.25 compares storages having adiabatic and nonadiabatic boundary conditions, that is, $UA = 0$ and 0.15 kW/K, when the pump shaft power is $\dot{W} = 0.745\,\text{kW}$. Figure 6.26 considers the influence of pump shaft power ($\dot{W} = 0$ and $0.745\,\text{kW}$) for a nonadiabatic TES ($UA = 0.15\,\text{kW/K}$).

In Figure 6.25, the top two curves show energy efficiencies for adiabatic and nonadiabatic storages, and the bottom two curves show the corresponding exergy efficiencies. The difference in discharge efficiencies for adiabatic and nonadiabatic TES systems is attributable to heat losses, which reduce the amount of heat that can be recovered in the heat-transfer process. Two points of significance are noted in the differences between the energy and exergy efficiency curves. First, the maximum exergy and energy discharge efficiencies differ and occur at different times, for example, for the nonadiabatic TES, the maximum exergy efficiency (28.7%) occurs at 13.5 h, while the maximum energy efficiency (72.1%) occurs at 57.3 h. Secondly, the net exergy recovered from a TES becomes negative (and consequently, the exergy discharge efficiency becomes negative) before the maximum energy discharge efficiency is attained.

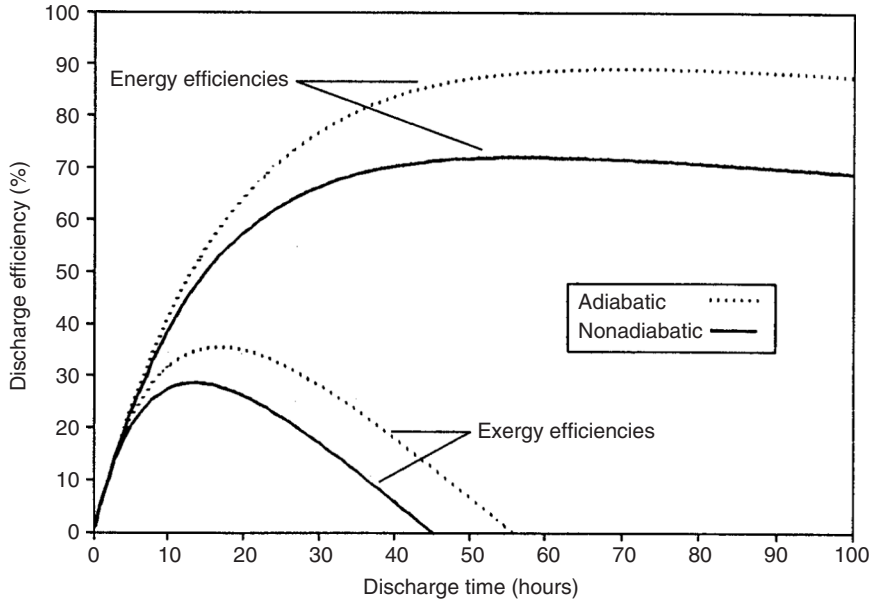

Figure 6.25 Discharge efficiencies, accounting for pump work, for adiabatic and nonadiabatic TES systems

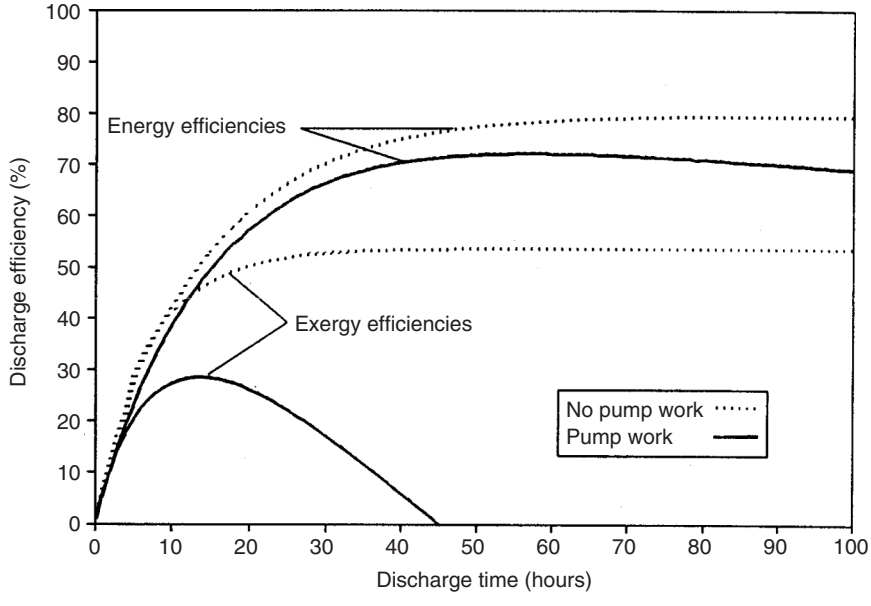

Figure 6.26 Discharge efficiencies for nonadiabatic TES systems with and without pump work

In Figure 6.26, it can be seen that if pump shaft power is considered negligible, maximum discharge efficiencies are higher for both energy and exergy analysis, relative to when the pump shaft power is considered nonzero. Also, with negligible pump shaft power, the maximum net energy recovery is not diminished by continued operation of the heat-exchanger pump. In addition, Figure 6.26 demonstrates that thermal energy and thermal exergy differ, depending on the temperatures involved, while pump shaft power is equivalent in energy and exergy terms. Hence in Figure 6.26, the difference between the exergy and energy efficiencies is much greater for the cases with pump work than without.

6.10.6 Closure

Using energy and exergy discharge efficiencies and a method for evaluating the changing storage-fluid temperature for the discharge process of a closed, fully mixed, sensible TES system, optimal discharge periods can be evaluated based on thermodynamic considerations. The results show that the difference between the results of energy and exergy analyses is significant, and that the impact of pump work on the optima can be important. The authors feel that, since exergy is a measure of the quality or usefulness of energy, exergy performance measures are more meaningful than energy performance measures, and should be considered in the evaluation of the optimum discharge period for TES systems and in related design activities.

6.11 Exergy Analysis of Solar Ponds

Solar ponds provide an interesting option for simultaneously collecting and storing solar energy and are viable in some regions (e.g., those with readily available land, much sunshine, little snow, and access to inexpensive salt – NaCl or bittern). The technology was developed in Israel in the 1960s. Solar ponds are usually large and deep, and sized to provide community heating. The pond acts as a sensible TES that can supply thermal energy for many applications. The ability to collect and store solar energy makes the solar pond somewhat akin to some passive solar energy technologies (e.g., trombe walls).

A solar pond (see Figure 6.27) differs from an ordinary pond or lake in one key way. In the latter, solar radiation warms the water and increases its buoyancy, causing it to rise to the surface where it loses heat to the atmosphere. This phenomenon is inhibited in a solar pond by dissolving salt into its bottom layer, making that water too dense to rise, even when hot. Thus, solar energy reaching the bottom of the pond is trapped, unlike the water in an ordinary pond that remains at nearly atmospheric temperature. The salt concentration increases with depth, forming a saline concentration gradient. The added salt also inhibits natural convection, allowing the cooler water on top to act as insulation and reduce evaporation. Salt water can be heated to high temperatures, even above the boiling point of fresh water. Solar ponds also differ in other ways from the ordinary ponds: solar ponds contain clear water to increase solar radiation penetration as much as possible, and the pond bottom is darkened to increase solar radiation absorption. Thermal energy is discharged from the solar pond as hot brine.

The three regions or zones of a typical solar pond can be seen in Figure 6.27 and have the following characteristics:

- The top region is the surface zone or upper convective zone (UCZ). This zone contains a homogeneous layer of low-salinity brine or fresh water. This zone is fed with fresh water of a density near to the density of fresh water in the upper part to maintain the cleanliness of the pond and replenish lost water due to evaporation.
- The middle region is the gradient zone or nonconvective zone (NCZ) or insulation zone. This zone acts as a thermally insulating layer. It contains a salinity gradient, implying water nearer the surface is less concentrated than water below it. That is, the brine density of the salty water in this

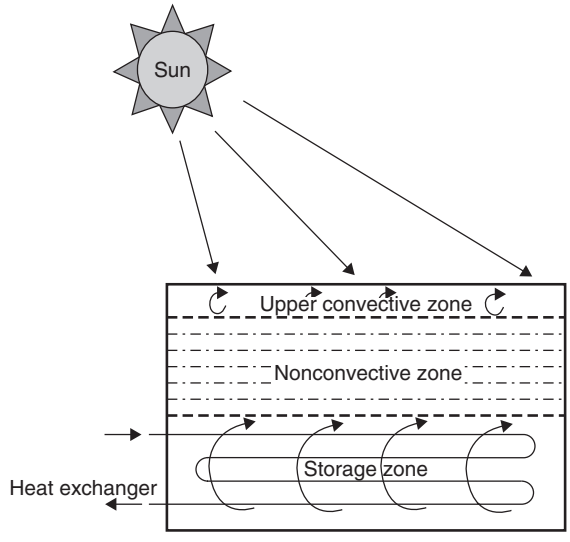

Figure 6.27 Illustration of a solar pond

zone gradually increases toward the lower convective zone (LCZ). Hence, there is no convection in the gradient zone even when the lower zone is heated since the hotter, saltier water at the bottom of the gradient remains denser than the less salty water above it. The NCZ performs an important function in a solar pond: it allows solar radiation to penetrate into the storage zone but inhibits heat (long-wave thermal radiation) from escaping. This function is possible in part because water is opaque to infrared radiation.

- The lower region is the LCZ or heat storage zone (HSZ). This zone contains homogeneous, concentrated salty water that can be either convecting or thermally stratified. Much of the incident solar energy is absorbed and stored in this zone. This is because water transmits solar radiation well and infrared radiation poorly. Hence, solar energy that reaches and is absorbed in this zone can escape via conduction only. The thermal conductivity of water is moderately low and, if the gradient zone has substantial thickness, heat escapes upward from the lower zone slowly. The LCZ has the highest temperature, so the strongest thermal interactions occur between this zone and the adjacent insulated bottom and side walls.

Solar ponds are relatively simple devices that operate straightforwardly, require little maintenance (e.g., they need cleaning to maintain water transparency), and have long lifetimes. The pumps and piping used to maintain the salt gradient are not complex. The performance of a solar pond depends on its thermal-storage capacity, construction and maintenance, and the thermophysical properties of its components (especially the storage fluid) (Karakilcik *et al*., 2006a, b). Solar ponds do not typically require backup systems because their high heat capacity and large thermal mass normally allow them to buffer periods of reduced solar intensity.

Various investigations of solar ponds have been reported, including modeling to facilitate examinations of performance, efficiency, and operation. The case study described here draws heavily on results reported previously (Karakilcik and Dincer, 2008).

6.11.1 Experimental Solar Pond

In this case study, we examine an experimental solar pond located in Adana, Turkey at Cukurova University (35°18′ E longitude, 36°59′ N latitude). Temperature distributions, energy and exergy

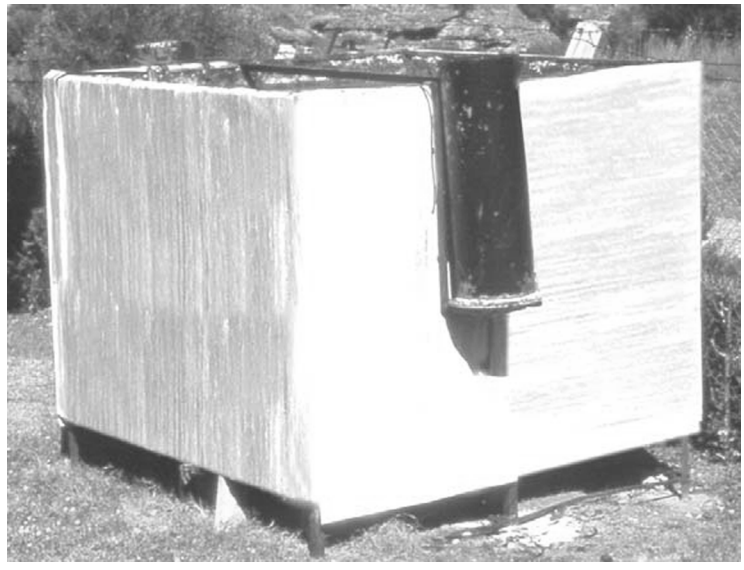

Figure 6.28 A photo of experimental solar pond

losses, and efficiencies are measured or determined. The data allow pond performance to be obtained experimentally for 11 representative months (all but June). Significant factors affecting performance are described, for example, incident solar radiation, zone thicknesses, wall shading, and insulation.

The experimental solar pond considered in this case study (Figure 6.28) is 1.5 m deep and has a square horizontal profile of side lengths 2 m. The UCZ, NCZ, and HSZ thicknesses are 0.1 m, 0.6 m, and 0.8 m, respectively. The salt-water solution contains a NaCl reagent and fresh water. A salt gradient exists in the zones, with the pond water having a density of 1000–1045 kg/m^3 in the UCZ, 1045–1170 kg/m^3 in the NCZ and 1170–1200 kg/m^3 in HSZ. The bottom and the side walls of the pond are plated with 5-mm thick iron sheets, and contain a layer of glass wool insulation 50 mm thick. The solar pond has a steel base 0.5 m above the ground, which is somewhat insulated with 20 mm thick wood slats. The inner and outer side walls are covered with anti-corrosion paint. Figure 6.29 illustrates the inner zones of the solar pond and Figure 6.30 illustrates solar radiation entering the pond and the shading area by its south sidewall. The UCZ, NCZ, and HSZ thicknesses of the salt gradient solar pond are seen in Figure 6.30 to be X_1, $X_2 - X_1$, and $X_3 - X_2$, respectively. Other property data for the solar pond parts and surroundings are listed in Table 6.15.

6.11.2 Data Acquisition and Analysis

Data Acquisition

The experimental unit used to obtain data is described in detail elsewhere, along with the experimental method and measurements (Karakilcik and Dincer, 2008; Karakilcik *et al*., 2006a, b). The inner zones of the experimental unit (Figure 6.30) consist of three zones (eight saline water layers). The UCZ is 10 cm thick. The NCZ consists of six layers each of 10 cm thickness and having different density. The HSZ is 80 cm thick. Some details on data follow:

- Temperatures are sensed at heights from the bottom of the pond of 0.05, 0.30, 0.55, 0.70, 0.80, 1.05, 1.35, and 1.50 m, and, from the bottom of the pond downward into the insulated bottom,

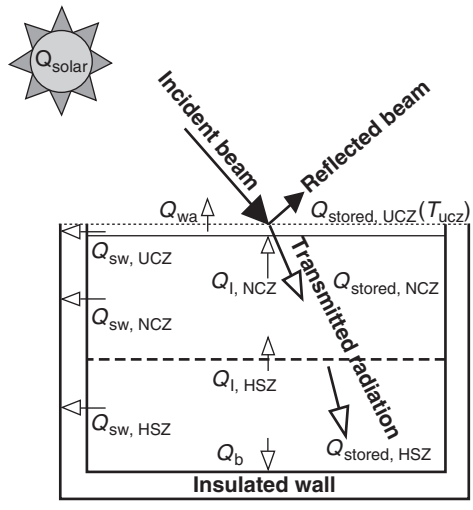

Figure 6.29 Illustration of all heat transfers in experimental solar pond

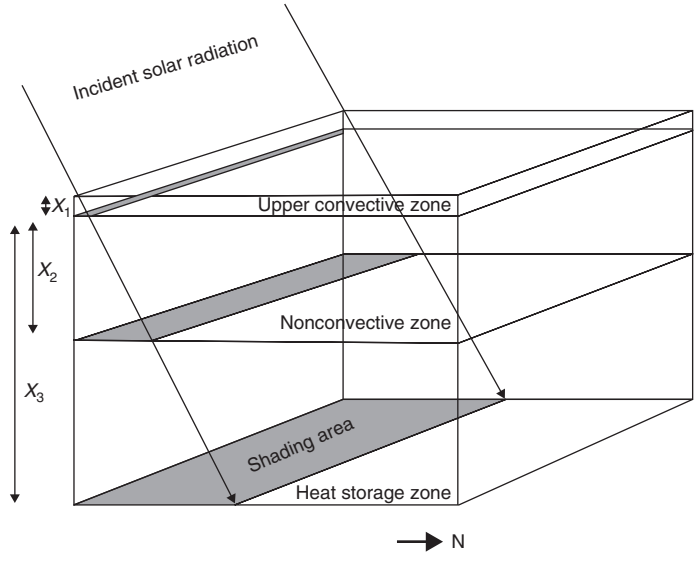

Figure 6.30 Illustration of the three zones in the experimental solar pond

at 15 and 45 mm, and for heights from the bottom of the side wall of 0, 0.35, 0.65, 0.75, 1.00, and 1.35 m.

- Inner and wall temperatures of the pond are measured on an hourly basis during the day.
- Temperatures at the inner zones and insulated sidewall of the pond are measured by sensors with a range of $-65\,^{\circ}\mathrm{C}$ to $+155\,^{\circ}\mathrm{C}$, and with an accuracy of $\pm 0.1^{\circ}\mathrm{C}$ for the temperature range of $0\,^{\circ}\mathrm{C}$ to $120\,^{\circ}\mathrm{C}$. The sensors consist of 1N4148 semiconductor devices with coaxial cables lengths of 17 to 20 m.

Table 6.15 Selected properties of materials comprising and surrounding experimental solar pond

Property	Storage substance		Experimental container		Surroundings
	Brine	Water	Insulation	Painted wall	Air
Density (kg/m^3)	1185	998	200	7849	1.16
Specific heat (kJ/kg/K)	–	4.182	0.670	0.460	1.007
Thermal conductivity (kJ/m/K/h)	–	2.160	0.143	21.20	0.0947

Source: (Karakilcik, 2006a, b).

- Solar energy data are obtained using a pyranometer, and hourly and daily average air temperatures are obtained from a local meteorological station.
- The temperature-distribution profiles and other data are obtained using a data acquisition system (Karakilcik and Dincer, 2008).

Data Analysis

To understand the thermal performance of a solar pond, the rates of absorption of the incident solar radiation by zone and the temperature distributions of its regions need to be determined. Part of the solar radiation incident on the solar pond is absorbed, part is reflected at the surface, and the remaining part is transmitted (see Figure 6.29). Most of the incident radiation is transmitted through the layers and part reaches the HSZ where it is converted to heat and stored.

The absorption by the salty water solutions changes with concentration of the solution. The fluid in the UCZ has uniform and low salinity (like seawater). Concentration and temperature both increase linearly with pond depth in the NCZ, while the fluid is stratified due in the LCZ to its high salinity and correspondingly varying density.

In this analysis, the pond and its three zones are separated into 30 inner layers or zones. The temperatures of the layers vary temporally and depend on various factors, such as incident solar radiation, transmission and absorption characteristics (by layer), pond dimensions, structure and insulation, shading, solar pond fluid thermophysical properties (e.g., thermal conductivity), and surrounding climate. Analysis of an experimental solar pond is generally complicated due to variations in these factors.

Temperatures

To determine heat losses from the solar pond, experimental temperature distributions with pond height are obtained for the inner zones (see Table 6.16 and Figure 6.31). The temperatures at points in each zone are measured during the months and the monthly average temperatures are determined.

Table 6.16 Mean monthly temperatures (in °C) of solar pond zones and surroundings

	January	February	March	April	May	July	August	September	October	November	December
Upper convective zone (UCZ)	10	12	14	18	27	33	34	33	28	20	18
Nonconvective zone (NCZ)	14	15	19	22	36	42	43	41	32	22	20
Heat storage zone (HSZ)	17	18	22	28	40	52	55	50	41	28	23
Surroundings	10	11	14	18	22	28	28	26	21	16	11

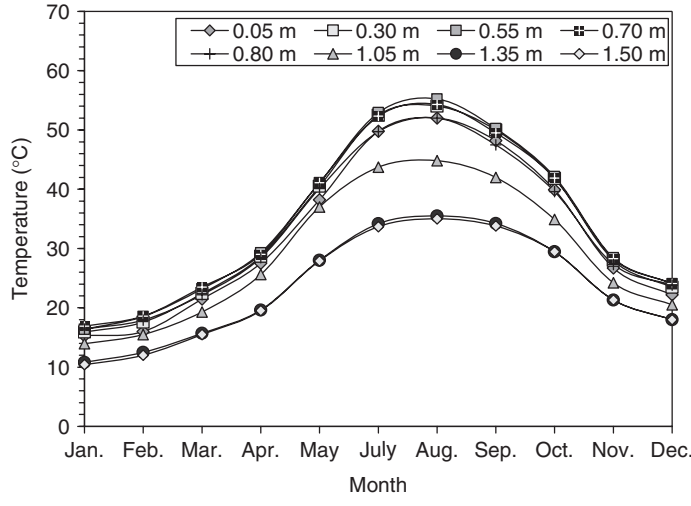

Figure 6.31 Monthly temperature distributions at various heights of the solar pond

Zone temperatures are clearly seen to vary with month, as the surrounding temperature and incoming solar radiation vary significantly monthly. Specifically, the temperature of each zone reaches a maximum in August and a minimum in January. These maximum and minimum temperatures, respectively, are 35 °C and 10 °C for the UCZ, 45 °C and 14 °C for the NCZ, and 55 °C and 17 °C for the HSZ. Generally, the temperatures of the zones increase with incident solar flux.

Brine Density Gradient

The vertical variation of brine density in the solar pond is illustrated in Figure 6.32 for each month. The monthly differences are likely attributable to the warmer conditions in summer, and are related

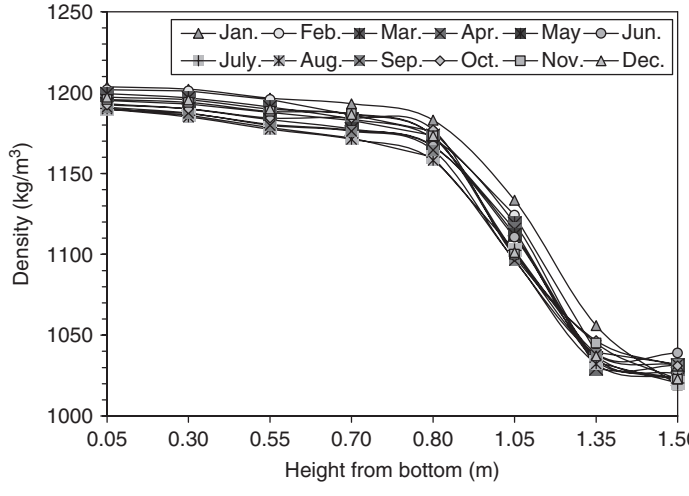

Figure 6.32 Density variation of water in the solar pond

to the absorption and reflection of incident solar radiation at the pond surface, surface heat losses to air, and the thermophysical properties of brine. As expected, increasing temperature reduces the density more in the summer months. The increase in saline density for the UCZ and the NCZ is caused by evaporation of water at the upper region. These changes can be reduced by continuously adding fresh water to the top of the pond. Significant changes are observed in the UCZ and the NCZ when salt gradient protection systems for cleaning purposes are not used.

6.11.3 Energy and Exergy Assessments

Energy Flows, Efficiencies, and Losses

Energy flows in the inner zones of the pond are illustrated in Figure 6.29. The thermal performance of the solar pond depends on incident solar radiation, shading and reflection, transmission and absorption, as well as heat flows to the surroundings and across the zones. The net energy stored in the zones is determined by using the property data in Table 6.15. Heat losses significantly affect performance; these are significant at the pond surface, but are kept very small by insulation from the sides and bottom.

The sunlit area and temperature of the zones, especially the HSZ, are affected by wall shading. The average sunny area and shaded areas, respectively, are determined to be 3.93 m^2 and 0.07 m^2 for the UCZ, 3.13 m^2 and 0.87 m^2 for the NCZ, and 2.63 m^2 and 1.37 m^2 for the HSZ.

The net average values of solar radiation incident on the zone sunny area during January, May, and August, respectively, are 439, 2077, and 2042 MJ for the UCZ, 352, 1662, and 1634 MJ for the NCZ, and 193, 914, and 899 MJ for the HSZ. Most of the incident solar radiation is transmitted to the NCZ through the UCZ, although some is absorbed in the NCZ. Furthermore, much of the incident solar radiation is transmitted from the NCZ to the HSZ. Little incident solar radiation is reflected from the NCZ to the UCZ. The majority of the incident radiation reaches the HSZ from the NCZ. This transmitted solar radiation from the NCZ is absorbed in the HSZ, while little of the incident solar radiation is reflected from the HSZ to the upper zones.

The energy stored in each of the zones is shown in Figure 6.33. For instance, the respective quantities of energy stored for January and August are 4 and 93 MJ in the UCZ, 311 and 225 MJ

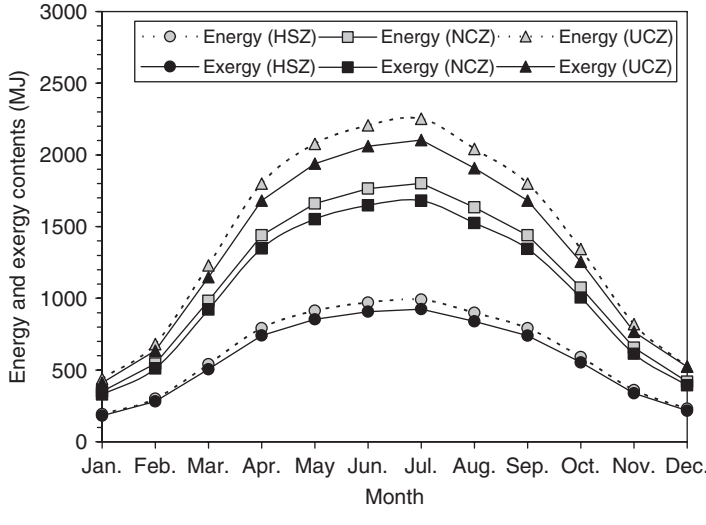

Figure 6.33 Monthly variation of energy and exergy contents of the solar pond zones

in the NCZ, and 19 and 253 MJ in the HSZ. Most of the energy is stored in the HSZ, which is responsible for the greatest heat loss.

Zone energy efficiencies are shown in Figure 6.34. The UCZ efficiencies vary from 0.9% to 4.5% for January and August, respectively. The NCZ energy efficiencies vary from 3.2% to 13.8% for January and August, respectively, while the HSZ efficiencies vary from 9.7% to 28.1% for January and August, respectively. Although the UCZ receives the greatest incident solar radiation, it exhibits the lowest zone efficiencies, mainly because of its small thickness and large surface heat losses to the surrounding air. The low UCZ efficiency is also attributable to shading. Shading significantly decreases the performance of the NCZ and the HSZ.

The performance of the solar pond as a TES depends upon the total radiation reaching its zones. In summer, much of the incident solar radiation is absorbed by the HSZ and little is reflected from the pond bottom wall. Increasing shading area from the top to the bottom of the pond reduces the solar radiation transmitted. In a solar pond, efficiencies are low since the stored energy is much smaller than the incident solar radiation on the zone surfaces. Energy losses from heat transfer to air from the UCZ reduce energy efficiency. Little of the incident solar radiation is stored in the pond and the UCZ efficiency has little impact on the overall performance of the pond compared to the NCZ. The efficiencies are dependent on the temperatures of the brine and surrounding air. The monthly temperature variations between the zones affect the diffusion of salt molecules from the pond bottom and heat losses.

To better understand the true magnitudes of thermodynamic efficiencies and losses for the solar pond and to potentially improve performance, exergy analysis is useful. This is the topic of the next section.

Exergy Flows, Efficiencies, and Losses

By clarifying and correcting many of the weaknesses of energy analysis of solar pond systems, exergy analysis is useful for analysis, design, and improvement. For instance, exergy analysis assesses meaningful efficiencies and losses. Corresponding exergy flows for the energy flows in Figure 6.29 for each of the zones in the pond can be determined. Also, energy and exergy efficiencies are compared for the three pond zones. Here, the exergy of the solar radiation is expressed assuming a surface temperature for the sun of 6000 K, using an expression proposed by Petala (2003).

Monthly energy and exergy contents for the pond zones, determined using average temperatures in Table 6.16, are shown in Figure 6.33. The energy and exergy contents follow the solar irradiation annual profile, with the lowest exergy contents observed in January and the highest in July. The energy contents exceed the corresponding exergy contents. Energy is conserved, so the only energy losses are heat emissions to the surroundings. Exergy can also be lost to the surrounding but it is also destroyed in each zone due to irreversibilities and processes like mixing fluids of different temperatures. The temperature of the surroundings affects energy and exergy losses significantly since both involve losses to the ambient air.

Monthly variations in exergy input, exergy recovered and exergy destruction and losses for the zones are provided in Table 6.17 (except for June when maintenance was performed on the data acquisition system). The exergy recovered and the exergy destruction and losses sum to the exergy input. The exergy input for all zones is greatest in July when incoming solar irradiation is greatest, and the other exergy terms vary somewhat in proportion to the exergy input.

Exergy accumulation is assumed not to occur in the UCZ, since it is less than 1%. Exergy accumulation is also assumed negligible for the NCZ. The exergy recovered in the UCZ is transferred to the NCZ. The exergy recovered from the UCZ varies from 392 MJ in January to 1682 MJ in July. Similarly, exergy recovered in the NCZ is transferred to the HSZ. The exergy recovered from the NCZ varies from 18 MJ in January to 958 MJ in July. In the HSZ, exergy is stored rather than recovered, permitting solar ponds to perform daily or seasonal storage. Much less exergy is stored in the HSZ than the exergy input and the exergy destruction and losses. The exergy recovered from the NCZ varies from 170 MJ in January to 743 MJ in July.

Table 6.17 Mean monthly exergy parameters (in MJ) for solar pond zones

	January	February	March	April	May	July	August	September	October	November	December
Input											
UCZ	417	644	1161	1700	1976	2168	1982	1740	1300	783	506
NCZ	335	517	931	1363	1588	1748	1601	1404	1049	629	408
HSZ	188	291	525	768	885	959	869	767	573	350	224
Recovered or stored*											
UCZ	329	511	920	1348	1553	1682	1525	1345	1005	614	393
NCZ	188	291	525	768	885	958	869	766	573	350	224
HSZ	17	27	53	89	141	204	218	181	133	57	28
Loss**											
UCZ	88	133	241	352	423	486	457	395	295	169	113
NCZ	147	226	406	595	703	790	732	638	476	279	184
HSZ	171	264	472	679	744	755	651	586	440	293	196

*Values for HSZ are stored exergy and for UCZ and NCZ are recovered exergy.
**Includes exergy destruction and waste exergy emission.

Monthly energy and exergy efficiencies for the zones of the solar pond are presented in Figure 6.34. The exergy efficiencies are lower than the energy efficiencies for each pond zone. The differences between energy and exergy efficiencies are smaller in winter than summer. The efficiencies for the HSZ are higher than the corresponding efficiencies for the UCZ and NCZ. The pond inner zones store more exergy in the summer than the winter. The exergy destruction and losses significantly affect the performance and detract from system efficiency.

6.11.4 Potential Improvements

The energy and exergy analyses using experimental data reported in this case study of a solar pond has demonstrated that performance is affected strongly by the variation of temperature with

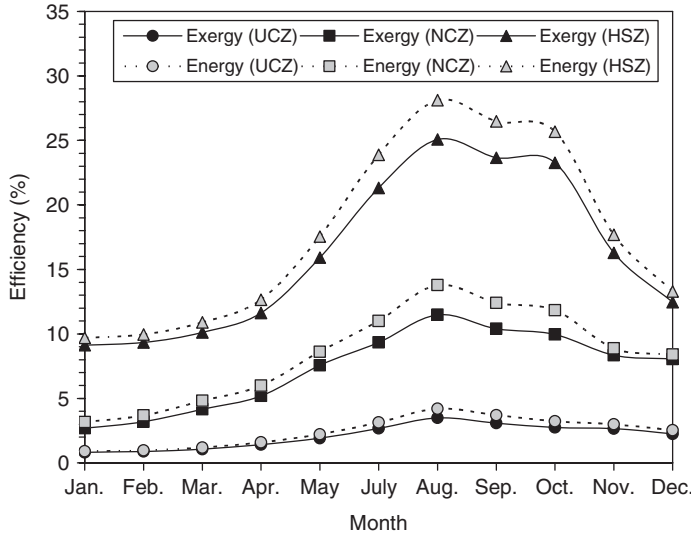

Figure 6.34 Monthly variation of energy and exergy efficiencies of the solar pond zones

depth, especially the LCZ temperature, and that the temperature of the zones is affected by incident radiation, zone thickness, shading, and thermal losses.

To increase the pond efficiency, several modifications could be considered:

- Heat losses and solar radiation reflection from upper zone should be reduced, as should shading and thermal losses from the bottom and side walls.
- Zone thicknesses should be modified where practical. This modification would also enhance the stability of the pond.
- Energy and exergy efficiencies and losses of the pond zones should be applied to help determine the best operating state.

6.12 Concluding Remarks

This chapter has demonstrated that the use of exergy analysis is very important in developing a good understanding of the thermodynamic behavior of TES systems, and for rationally assessing, comparing, and improving their efficiencies.

Methods identified by exergy analysis as having high improvement potential for TES systems are only limited by the creativity and knowledge of engineers and designers, and can include:

- reducing thermal losses (heat leakage from hot TES systems and heat infiltration to cold TES systems) by improving insulation levels and distributions;
- avoiding temperature degradation by using smaller heat-exchanger temperature differences, ensuring that heat flows of appropriate temperatures are used to heat cooler flows, and increasing heat-exchanger efficiencies;
- avoiding mixing losses by retaining and taking advantage of thermal stratification; and
- reducing pumping power by using more efficient pumps, reduced-friction heat-transfer fluids, and appropriate heat-recovery threshold temperatures.

The authors feel that the development is required of standard TES evaluation methodologies which take into account the thermodynamic considerations discussed in this chapter. By accounting for these considerations, meaningful methodologies can be developed for assessing the comparative value of alternative storages. In particular, the use of exergy analysis (and related concepts) is important because it clearly takes into account the loss of availability and temperature of heat in storage operations, and hence it more correctly reflects the thermodynamic and economic value of the storage operation.

Without methodologies capable of providing perceptive measures of technical, and ultimately of competitive economic performance, the development of better technology will be unscientific and disorganized, and open to subjective assessments of accomplishment. The development of better assessment methodologies will ensure effective use of energy resources by providing the basis for identifying the more productive directions for development of TES technology, and identifying the better systems without the lengthy and inefficient process of waiting for them to be sorted out by competitive economic success in the marketplace.

Nomenclature

A	surface area
c	specific heat
c_p	specific heat at constant pressure
c_v	specific heat at constant volume
C	heat capacity rate
e	specific energy

E	energy
f	fraction; mean height fraction
F	fraction of storage-fluid mass in liquid phase
h	specific enthalpy; specific base enthalpy; height (relative to TES bottom)
H	enthalpy; TES fluid height
i	time-step increment
I	exergy consumption due to irreversibilities
ke	specific kinetic energy
m	mass
N	moles
NTU	number of transfer units
pe	specific potential energy
P	absolute pressure
Q	heat
R	thermal resistance
s	specific entropy
S	entropy
t	time
T	temperature
u	specific internal energy
U	internal energy; overall heat-transfer coefficient
v	specific volume
V	volume
W	shaft work
x	mass fraction
X	thermal exergy (i.e., the exergy associated with heat Q)
y	mole fraction

Greek Symbols

α	constant parameter
ε	specific flow exergy; heat-exchanger effectiveness
$\in$	flow exergy
η	energy efficiency
θ	parameter
μ	chemical potential
ζ	specific exergy
Ξ	exergy
$\prod$	entropy production
ρ	density
τ	exergetic temperature factor
ϕ	zone temperature distribution
ψ	exergy efficiency

Subscripts

a	inlet flow during charging; adiabatic; parameter
amb	ambient
b	outlet flow during charging; bottom; parameter

c	injected during charging period; charging; inlet flow during discharging
d	recovered during discharging period; discharging; outlet flow during discharging
e	exit; equivalent
f	final
i	initial; ith constituent; inlet
j	zone
jk	number of zones
min	minimum
kin	kinetic component
l	loss
m	mixed
n	nonadiabatic
net	net
o	environmental state; chemical exergy; outlet
oo	dead state
p	product
ph	physical component
pot	potential component
r	region of heat interaction
s	solid state; storage fluid
st	storage (overall)
t	threshold; top; liquid state
T	total
th	thermocline zone (zone 2)
w	working fluid
1	charging period
2	storing period
3	discharging period

Superscripts

.	rate with respect to time
–	mean
′	modified case
A	case A
B	case B; basic three-zone model
C	case C; continuous-linear model
D	case D
G	general-linear model
L	linear model
s	step
S	stepped model
T	general three-zone model

Acronyms

ATES	aquifer thermal energy storage
CTES	cold thermal energy storage
ITES	ice thermal energy storage
TES	thermal energy storage

References

Adebiyi, G.A., Hodge, B.K., Steele, W.G., Jalalzedeh-Aza, A. and Nsofor, E.C. (1996). Computer simulations of a high temperature thermal energy storage system employing multiple families of phase-change storage materials, *Journal of Energy Resources Technology* 118, 102–111.

Ahern, J.E. (1980). *The Exergy Method of Energy System Analysis*, Wiley, New York.

Ahrendts, J. (1980). Reference states, *Energy-The International Journal* 5, 667–678.

Alefeld, G. (1990). What are thermodynamic losses and how to measure them? *A Future for Energy*: *Proc. of the Florence World Energy Research Symposium*, Firenze, Italy, pp. 271–279.

Althof, J. (1989). Economic feasibility of thermal storage, *Heating/Piping/Air Conditioning* September, 159–163.

Badar, M.A., Zubair, S.M. and Al-Farayedhi, A.A. (1993). Second-law-based thermoeconomic optimization of a sensible heat thermal energy storage system, *Energy* 18, 641–649.

Baehr, H.D. and Schmidt, E.F. (1963). Definition und berechnung von brennstoffexergien (Definition and calculation of fuel exergy), *Brennst-Waerme-Kraft* 15, 375–381.

Barbaris, L.N., Hooper, F.C. and Rosen, M.A. (1988). The relationship between storage period duration and measures of the overall performance of sensible thermal energy storages, *Proceedings of the International Conference on Applied Geothermal Energy and Thermal Energy Storage*, France, pp. 723–727.

Bascetincelik, A., Ozturk, H.H., Paksoy, H.O. and Demirel, Y. (1998). Energetic and exergetic efficiency of latent heat storage system for greenhouse heating, *Renewable Energy* 16, 691–694.

Beckman, G. and Gilli, P.V. (1984). *Thermal Energy Storage*, Springer-Verlag, New York.

Beggs, C. (1991). The economics of ice thermal storage, *Building Research and Information* 19, 342–355.

Bejan, A. (1978). Two thermodynamic optima in the design and operation of thermal energy storage systems, *Journal of Heat Transfer* 100, 708–712.

Bejan, A. (1982). Thermal energy storage, Chapter 8, In: *Entropy Generation through Heat and Fluid Flow*, Wiley, New York, pp. 158–172.

Bejan, A. (1995). *Entropy Generation Minimization: The Method of Thermodynamic Optimization of Finite-Size Systems and Finite-Time Processes*, CRC Press, Boca Raton, Florida.

Bjurstrom, H. and Carlsson, B. (1985). An exergy analysis of sensible and latent heat storage, *Heat Recovery Systems* 5, 233–250.

Bosnjakovic, F. (1963). Bezugszustand der exergie eines reagiernden systems (Reference states of the exergy in a reacting system, *Forschung Im Ingenieurwesen* 20, 151–152.

Brosseau, P. and Lacroix, M. (1998). Numerical simulation of a multi-layer latent heat thermal energy storage system, *International Journal of Energy Research* 22, 1–15.

Carrier (1990). *Encapsulated Ice Store*, USA.

Chase, M.W., Davies, C.A., Downey, J.R., *et al*., eds. (1985). *JANAF Thermochemistry Tables*, 3rd edition, American Chemical Society and American Inst. of Physics, Washington, DC.

Chen, C.S. and Sheen, J.N. (1993). Cost benefit analysis of a cooling energy storage system, *IEEE Transactions on Power Systems* 8 (4), 1504–1510.

Costa, M., Buddhi, D. and Oliva, A. (1998). Numerical simulation of a latent heat thermal energy storage system with enhanced heat conduction, *Energy Conversion and Management* 39, 319–330.

Crane, P., Scott, D.S. and Rosen, M.A. (1992). Comparison of exergy of emissions from two energy conversion technologies, considering potential for environmental impact, *International Journal of Hydrogen Energy* 17, 345–350.

De Lucia, M. and Bejan, A. (1990). Thermodynamics of energy storage by melting due to conduction or natural convection, *ASME Journal of Solar Energy Engineering* 112, 110–116.

Dincer, I. (1999). Evaluation and selection of energy storage systems for solar thermal applications, *International Journal of Energy Research* 23, 1017–1028.

Dincer, I. and Dost, S. (1996). A perspective on thermal energy storage systems for solar energy applications, *International Journal of Energy Research* 20, 547–557.

Dincer, I., Dost, S. and Li, X. (1997a). Performance analyses of sensible heat storage systems for thermal applications, *International Journal of Energy Research* 21, 1157–1171.

Dincer, I., Dost, S. and Li, X. (1997b). Thermal energy storage applications from an energy saving perspective, *International Journal of Global Energy Issues* 9, 351–364.

Dincer, I. and Rosen, M.A. (2007). *Exergy: Energy, Environment and Sustainable Development*, Elsevier, Oxford, UK.

Domanski, R. and Fellah, G. (1998). Thermoeconomic analysis of sensible heat, thermal energy storage systems, *Applied Thermal Engineering* 18 (8), 693–704.

Edgerton, R.H. (1982). *Available Energy and Environmental Economics*, D.C. Heath, Toronto.

Fanny, A.H. and Klein, S.A. (1988). Thermal performance comparisons for solar hot water systems subjected to various collector and heat exchanger flow rates, *Solar Energy* 40, 1–11.

Fields, W.M.G. and Knebel, D.E. (1991). Cost effective thermal energy storage, *Heating/Piping/Air Conditioning*, July, 59–72.

Gaggioli, R.A. (1983). Second law analysis to improve process and energy engineering, In *Efficiency and Costing: Second Law Analysis of Processes* (ed. R.A. Gaggioli), Vol. 235, ACS Symposium Series, American Chemical Society, Washington, DC, pp. 3–50.

Gaggioli, R.A. and Petit, P.J. (1977). Use the second law first, *Chemtech* 7, 496–506.

Gretarsson, S.P., Pedersen, C.O. and Strand, R.K. (1994). Development of a fundamentally based stratified thermal storage tank model for energy analysis calculations, *ASHRAE Transactions* 100, 1213–1220.

Gunnewiek, L.H., Nguyen, S. and Rosen, M.A. (1993). Evaluation of the optimum discharge period for closed thermal energy storages using energy and exergy analyses, *Solar Energy* 51, 39–43.

Gunnewiek, L.H. and Rosen, M.A. (1998). Relation between the exergy of waste emissions and measures of environmental impact, *International Journal of Environment &Pollution* 10, 261–272.

Hafele, W. (ed.) (1981). Energy, negentropy, and endowments, Chapter 21, In *Energy in a Finite World: A Global Systems Analysis*, Ballinger, Toronto, pp. 693–705.

Hahne, E. (1986). Thermal energy storage: some views on some problems, *Proceedings of the 8th International Heat Transfer Conference*, San Francisco, pp. 279–292.

Hahne, E., Kubler, R. and Kallewit, J. (1989). The evaluation of thermal stratification by exergy, In *Energy Storage Systems* (ed. B. Kilkis and S. Kakac), Kluwer, Dordecht, pp. 465–485.

Hevert, H.W. and Hervert, S.C. (1980). Second law analysis: an alternative indicator of system efficiency, *Energy-The International Journal* 5, 865–873.

Homan, K.O., Sohn, C.W. and Soo, S.L. (1996). Thermal performance of stratified chilled water storage tanks, *HVAC and R Research* 2 (2), 158–170.

Hooper, F.C., Barbaris, L.N. and Rosen, M.A. (1988). An engineering approach to the evaluation of the performance of stratified thermal energy storages, *Proceedings of the International Conference on Applied Geothermal Energy and Thermal Energy Storage*, Versailles, France, pp. 155–160.

Hoyer, M.C., Walton, M., Kanivetsky, R. and Holm, T.R. (1985). Short-term aquifer thermal energy storage (ATES) test cycles, St. Paul, Minnesota, U.S.A., *Proceedings of the 3rd International Conference on Energy Storage for Building Heating and Cooling*, Toronto, Canada, pp. 75–79.

Ismail, K.A.R., Leal, J.F.B. and Zanardi, M.A. (1997). Models of liquid storage tanks, *Energy-The International Journal* 22, 805–815.

Ismail, K.A.R. and Stuginsky, R. (1999). A parametric study on possible fixed bed models for PCM and sensible heat storage, *Applied Thermal Engineering* 19, 757–788.

Jansen, J. and Sorensen B. (1984). *Fundamentals of Energy Storage*, Wiley, New York.

Jenne, E.A. (ed.) (1992). *Aquifer Thermal Energy (Heat and Chill) Storage*, Pacific Northwest Lab, Richland, WA.

Karakilcik, M. and Dincer, I. (2008). Exergetic performance analysis of a solar pond. *International Journal Thermal Sciences* 47, 93–102.

Karakilcik, M., Dincer, I. and Rosen, M.A. (2006a). Performance investigation of a solar pond. *Applied Thermal Engineering* 26, 727–735.

Karakilcik, M., Kiymac, K. and Dincer, I. (2006b). Experimental and theoretical temperature distributions in a solar pond. *International Journal of Heat and Mass Transfer* 49, 825–835.

Keenan, J.H., Chao, J. and Kayle, J. (1992). *Gas Tables International Version. Properties of Air Products of Combustion and Component Gases Compressible Flow Functions*, Krieger, Florida.

Kestin, J. (1980). Availability: the concept and associated terminology, *Energy-The International Journal* 5, 679–692.

Kleinbach, E.M., Beckman, W.A. and Klein, S.A. (1993). Performance study of one-dimensional models for stratified thermal storage tanks, *Solar Energy* 50, 155–166.

Kotas, T.J. (1995). *The Exergy Method of Thermal Plant Analysis*, reprint edition, Krieger, Florida.

Kotas, T.J., Raichura, R.C. and Mayhew, Y.R. (1987). Nomenclature for exergy analysis, In *Second Law Analysis of Thermal Systems* (ed. M.J. Moran E. Sciubba), ASME, New York, pp. 171–176.

Krane, R.J. (1985). A second law analysis of a thermal energy storage system with Joulean heating of the storage element, *Paper 85-WA/HT-19, ASME Winter Annual Meeting*, 17-21 Nov., Miami.

Krane, R.J. (1987). A second law analysis of the optimum design and operation of thermal energy storage systems, *International Journal of Heat and Mass Transfer* 30, 43–57.

Krane, R.J. and Krane, M.J.M. (1991). The optimum design of stratified thermal energy storage systems, *Proceedings of the International Conference on the Analysis of Thermal and Energy Systems*, Greece, pp. 197–218.

Laouadi, A. and Lacroix, M. (1999). Thermal performance of a latent heat energy storage ventilated panel for electric load management, *International Journal of Heat and Mass Transfer* 42, 275–286.

Lightstone, M., Hollands, K.G.T. and Hassani, A.V. (1988). Effect of plume entrainment in the storage tank on calculated solar energy performance, *Energy Solutions for Today*: *Proceedings of the 14*th *Annual Conference of Solar Energy Society of Canada*, Canada, pp. 236–241.

Lucca, G. (1990). The exergy analysis: role and didactic importance of a standard use of basic concepts, terms and symbols, *A Future For Energy*: *Proceedings of the Florence World Energy Research Symposium*, Firenze, Italy, pp. 295–308.

Maloney, D.P. and Burton, J.R. (1980). Using second law analysis for energy conservation studies in the petrochemical industry, *Energy-The International Journal* 5, 925–930.

Mathiprakasam, B. and Beeson, J. (1983). Second law analysis of thermal energy storage devices, *Proceedings of the AIChE Symposium Series, National Heat Transfer Conference*, Seattle, Washington, DC.

Mavros, P., Belesiotis, V. and Haralambopoulos, D. (1994). Stratified energy storage vessels-characterization of performance and modeling of mixing behavior, *Solar Energy* 52, 327–336.

Moran, M.J. (1989). *Availability Analysis: A Guide to Efficient Energy Use*, ASME, New York.

Moran, M.J. (1990). Second law analysis. What is the state of the art? A future for energy, *Proceedings of the Florence World Energy Research Symposium*, Firenze, Italy, pp. 249–260.

Moran, M.J. and Keyhani, V. (1982). Second law analysis of thermal energy storage systems, *Proceedings of the 7*th *International Heat Transfer Conference* Vol. 6, Munich, pp. 473–478.

Moran, M.J. and Shapiro, H.N. (2000). *Fundamentals of Engineering Thermodynamics*, 4th edition, Wiley, Toronto.

Morris, D.R., Steward, F.R., and Szargut, J. (1988). *Exergy Analysis of Thermal, Chemical and Metallurgical Processes*, Springer-Verlag, New York.

Nelson, J.E.B., Balakrishnan, A.R. and Murthy, S.S. (1999). Experiments on stratified chilled water tanks, *International Journal of Refrigeration* 22 (3), 216–234.

Petala, R. (2003). Exergy of undiluted thermal radiations. *Solar Energy* 74, 469–488.

Rodriguez, L.S.J. (1980). Calculation of available-energy quantities, in *Thermodynamics: Second Law Analysis* (ed. R.A. Gaggioli), American Chemical Society, Washington, DC, pp. 39–60.

Rosen, M.A. (1990). Evaluation of the heat loss from partially buried, bermed heat storage tanks, *International Journal of Solar Energy* 9, 147–162.

Rosen, M.A. (1991). On the importance of temperature in performance evaluations for sensible thermal energy storage systems, *Proceedings of the Bienniel Congress International Solar Energy Society* (ed. M.E. Arden, S.M.A. Burley and M. Coleman), Vol. 2, Part II, Pergamon, New York, pp. 1931–1936.

Rosen, M.A. (1992a). Evaluation of energy utilization efficiency in Canada using energy and exergy analyses, *Energy-The International Journal* 17, 339–350.

Rosen, M.A. (1992b). Appropriate thermodynamic performance measures for closed systems for thermal energy storage, *ASME Journal of Solar Energy Engineering* 114, 100–105.

Rosen, M.A. (1998a). A semi-empirical model for assessing the effects of berms on the heat loss from partially buried heat storage tanks, *International Journal of Solar Energy* 20, 57–77.

Rosen, M.A. (1998b). The use of berms in thermal energy storage systems: energy-economic analysis, *Solar Energy* 63 (2), 69–78.

Rosen, M.A. (1999a). Second law analysis: approaches and implications, *International Journal of Energy Research* 23 (5), 415–429.

Rosen, M.A. (1999b). Second-law analysis of aquifer thermal energy storage systems, *Energy-The International Journal* 24, 167–182.

Rosen, M.A. and Dincer, I. (1997a). On exergy and environmental impact, *International Journal of Energy Research* 21, 643–654.

Rosen, M.A. and Dincer, I. (1997b). Sectoral energy and exergy modeling of Turkey, *ASME Journal of Energy Resources Technology* 119, 200–204.

Rosen, M.A. and Dincer, I. (1999a). Thermal storage and exergy analysis: the impact of stratification, *Transactions of CSME* 23 (1B), 173–186.

Rosen, M.A. and Dincer, I. (1999b). Exergy analysis of waste emissions, *International Journal of Energy Research* 23 (13), 1153–1163.

Rosen, M.A., Dincer, I. and Pedinelli, N. (2000). Thermodynamic performance of ice thermal energy storage systems, *ASME Journal of Energy Resources Technology* 122 (4), 205–211.

Rosen, M.A. and Hooper, F.C. (1991a). A general method for evaluating the energy and exergy contents of stratified thermal energy storages for linear-based storage fluid temperature distributions, *Proceedings of the 17th Annual Conference of the Solar Energy Society of Canada*, Toronto, pp. 182–187.

Rosen, M.A. and Hooper, F.C. (1991b). Evaluating the energy and exergy contents of stratified thermal energy storages for selected storage-fluid temperature distributions, *Proceedings of the Biennial Congress of International Solar Energy Society*, Denver, pp. 1961–1966.

Rosen, M.A. and Hooper, F.C. (1992). Modeling the temperature distribution in vertically stratified thermal energy storages to facilitate energy and exergy evaluation, in *Thermodynamics and the Design, Analysis and Improvement of Energy Systems*, AES-Vol 27/HTD-Vol. 228 (ed. R.F. Boehm), American Society of Mechanical Engineers, New York, pp. 247–252.

Rosen, M.A. and Hooper, F.C. (1994). Designer-oriented temperature-distribution models for vertically stratified thermal energy storages to facilitate energy and exergy evaluation, *Proceedings of the 6th International Conference on Thermal Energy Storage*, Espoo, Finland, pp. 263–270.

Rosen, M.A., Hooper, F.C. and Barbaris, L.N. (1988) Exergy analysis for the evaluation of the performance of closed thermal energy storage systems, *ASME Journal of Solar Energy Engineering* 110, 255–261.

Rosen, M.A. and Horazak, D.A. (1995). Energy and exergy analyses of PFBC power plants, Chapter 11, In *Pressurized Fluid Bed Combustion* (ed. M. Alvarez-Cuenca and E.J. Anthony), Chapman & Hall, London, pp. 419–448.

Rosen, M.A., Nguyen, S. and Hooper, F.C. (1991). Evaluating the energy and exergy contents of vertically stratified thermal energy storages, *Proceedings of the 5th International Conference on Thermal Energy Storage*, Scheveningen, The Netherlands, pp. 7.4.1–7.4.6.

Rosen, M.A., Pedinelli, N. and Dincer, I. (1999) Energy and exergy analyses of cold thermal storage systems, *International Journal of Energy Research* 23 (12), 1029–1038.

Rosen, M.A. and Scott, D.S. (1987). On the sensitivities of energy and exergy analyses to variations in dead-state properties, In *Analysis and Design of Advanced Energy Systems*, AES-Vol. 3-1, ASME, New York, pp. 23–32.

Rosen, M.A. and Scott, D.S. (1998). Comparative efficiency assessments for a range of hydrogen production processes, *International Journal of Hydrogen Energy* 23, 653–659.

Rosen, M.A. and Tang, R. (1997). Increasing the exergy storage capacity of thermal storages using stratification, In *Proceedings of the ASME Advanced Energy Systems Division*, AES-Vol. 37 (ed. M.L. Ramalingam, J.L. Lage, V.C. Mei and J.N. Chapman), ASME, New York, pp. 109–117.

Rosenblad, G. (1985). Quality loss from seasonal storage of heat in rock, magnitude and evaluation, *Proceedings of the 3rd International Conference on Energy Storage for Building Heating and Cooling*, Toronto, pp. 594–599.

Saborio-Aceves, S., Nakamura, H. and Reistad, G.M. (1994). Optimum efficiencies and phase change temperature in latent heat storage systems, *Journal of Energy Resources Technology* 116, 79–86.

Sussman, M.V. (1980). Steady-flow availability and the standard chemical availability, *Energy-The International Journal* 5, 793–804.

Sussman, M.V. (1981). Second law efficiencies and reference states for exergy analysis, *Proceedings of the 2nd World Congress Chemical Engineering*, *Canadian Society of Chemical Engineers*, Montreal, pp. 420–421.

Szargut, J. (1967). Grenzen fuer die anwendungsmoeglichkeiten des exergiebegriffs (Limits of the applicability of the exergy concept), *Brennstoff-Waerme-Kraft* 19, 309–313.

Taylor, M.J. (1986). Second law optimization of a sensible heat thermal energy storage System with a distributed storage element, MS Thesis, Department of Mechanical and Aerospace Engineering, University of Tennessee, Knoxville.

Wepfer, W.J. and Gaggioli, R.A. (1980). Reference datums for available energy, in *Thermodynamics: Second Law Analysis*, Vol. 122 (ed. R.A. Gaggioli), ACS Symposium Series, American Chemical Society, Washington, DC, pp. 77–92.

Wood, L.L., Miedema, A.K. and Cates, S.C. (1994). Modeling the technical and economic potential of thermal energy storage systems using pseudo-data analysis, *Resource and Energy Economics* 16, 123–145.

Yoo, H., Kim, C-J. and Kim, C. (1998). Approximate analytical solutions for stratified thermal storage under variable inlet temperature, *Solar Energy* 66, 47–56.

Study Questions/Problems

6.1 What is exergy and how is it different from energy?

6.2 What are the different types of exergy?

6.3 Describe the significance of the reference environment in exergy analysis.

6.4 The mean summer temperature in a particular location is 26 °C and the mean winter temperature is −2 °C. What would be an appropriate reference-environment temperature for assessing the performance of a diurnal TES in winter? What would be an appropriate reference-environment temperature for assessing the performance of a diurnal TES in spring? What would be an appropriate reference-environment temperature for assessing the performance of a seasonal TES that collects heat during the summer and utilizes it during the winter?

6.5 What is the exergy transfer associated with a heat transfer of 1000 kJ at 400 K, in a reference environment at 300 K?

6.6 What is the exergy flow rate associated with a flow of electrical power of 1000 kW? Does the answer depend on the reference environment?

6.7 What is the exergy flow rate associated with a mass flow rate of water of 25 kg/s at 2 atm and 360 K, in a reference environment at 290 K and ambient pressure?

6.8 What are the two main types of exergy losses? Do they have energy-based counterparts?

6.9 Describe the steps involved in performing an exergy analysis of a TES system.

6.10 What is the energy loss for a TES in which 1000 kJ of thermal energy is injected during charging and 700 kJ of thermal energy is recovered during discharging? What is the energy efficiency of the TES?

6.11 For the previous question, if the thermal energy is injected at 90 °C and recovered at 55 °C, and if the reference-environment temperature is 10 °C, what would be the exergy loss and the exergy efficiency of the TES? Estimate the breakdown of the exergy loss into exergy associated with waste heat emission and exergy loss due to internal exergy destruction.

6.12 Identify and compare several possible TES energy efficiencies. Repeat this task for TES exergy efficiencies. Then, compare and contrast the energy and exergy efficiencies.

6.13 How does stratification improve the exergy efficiency of a TES?

6.14 Describe at least four causes of loss of stratification in a TES.

6.15 If the heat loss from a TES during a period of operation is 20 kJ during charging, 80 kJ during storing, and 10 kJ during discharging, what is the heat loss from the TES during the overall period?

6.16 The exergy associated with surface heat losses from a TES is 200 kJ, but the overall exergy loss for the TES is 450 kJ. Explain why these values are not the same.

6.17 A closed TES undergoes a charging process in which heat is transferred to it from a stream of 4000 kg of water which enters at 70 °C and leaves at 55 °C. Heat is recovered from the storage

by a stream of 2500 kg of water entering at 20 °C and leaving at 40 °C. Determine for the TES, the energy input, the energy recovered, the energy lost, and the energy efficiency. Also, determine for the TES, the exergy input, the exergy recovered, the exergy lost, and the exergy efficiency. Compare the answers and explain the differences between the energy and exergy parameters. Assume an appropriate reference-environment condition.

6.18 A closed TES undergoes a charging process in which heat is transferred to it from a stream of fluid which enters at 80 °C and leaves at 40 °C, and heat is recovered from the storage by a stream of fluid entering at 20 °C. Could the heat-recovery fluid exit at a temperature above 80 °C? Could the heat-recovery fluid exit at a temperature above 40 °C but below 80 °C? The reference-environment temperature is 15 °C. Justify your answers.

6.19 If the exergy efficiency is equal to the energy efficiency for a closed TES which receives a heat flow during charging at a certain temperature, what must be the relation between the charging and discharging temperatures?

6.20 For an aquifer TES storing heating capacity, a threshold temperature below which heat is not recovered is sometimes applied. Is the energy of exergy efficiency of the ATES more affected by the application of this threshold? Explain why the exergy efficiency is only slightly affected by the threshold application.

6.21 As an underground water resource, there are concerns about the quality of waters in aquifers. Discuss the potential for contamination of aquifer water if it is used for thermal energy storage. Also, investigate environmental and other regulations that exist in your jurisdiction related to the use of aquifer as underground thermal energy storages.

6.22 Does thermal stratification increase or decrease the exergy efficiency of a TES containing a fixed quantity of energy? Does thermal stratification increase or decrease the energy efficiency of the TES? Justify your answers.

6.23 Determine the exergy content of a water storage which is stratified with an upper temperature of 60 °C and a lower temperature of 40 °C, assuming the stepped temperature-distribution model with two steps applies. The mass of water in the storage is 200 kg and the reference-environment temperature is 20 °C.

6.24 Determine the exergy content of a water storage which is stratified with an upper temperature of 40 °C and a lower temperature of 20 °C, assuming the linear temperature-distribution model applies. The mass of water in the storage is 200 kg and the reference-environment temperature is 20 °C.

6.25 Determine the exergy content of a water storage in the previous question after a long period of time has passed and the storage fluid becomes fully mixed, assuming no heat is lost from the TES. The mass of water in the storage is 200 kg and the reference-environment temperature is 20 °C.

6.26 What is the main weakness of the linear temperature distribution model for vertical themal stratification in a TES?

6.27 Heat storages can exhibit vertical thermal stratification. Can cold storages be thermally stratified? Justify your answer.

6.28 What types of physical and other methods can be used to maintain thermal stratification of a TES? Discuss how they work. Explain how they contribute to increasing the exergy content of a TES.

6.29 To provide an equivalent amount of storage of cooling capacity, how does the volume of an ice-based cold TES compare to the volume of a liquid water-based cold TES? Justify your answer.

6.30 What is the thermocline in a TES?

6.31 Explain why the thermocline is important for retaining exergy in a vertically stratified TES.

6.32 Determine the cooling capacity of an ice TES of $3\,m^3$ volume which undergoes only latent heat changes at $0\,^\circ C$. Then determine the cooling capacity of a water CTES of $3\,m^3$ volume which undergoes only sensible heat changes between $3\,^\circ C$ and $9\,^\circ C$. Compare the two answers.

6.33 Why is it important to consider pump work when evaluating the energy and exergy efficiencies for a TES system? Does the inclusion of pump work have a greater effect on the energy efficiency or the exergy efficiency?

6.34 For an insulated TES, describe the behavior of the energy efficiency with discharge period when pump work is accounted for and when it is neglected.

6.35 Describe the three zones of a solar pond.

6.36 Is energy and exergy stored in all zones of a solar pond? Explain.

6.37 Where in a solar pond is the fluid density the greatest?

Appendix: Glossary of Selected Exergy-Related Terminology

This glossary identifies exergy-related terminology from the literature that is of relevance to the TES discussions in this chapter. Most exergy terminology has only recently been adopted, and is still evolving. Often more than one name is assigned to the same quantity, and more than one quantity to the same name. Only exergy-related definitions are given for terms having multiple meanings. The glossary is based in part on previously developed broader glossaries (Kotas *et al*., 1987; Kotas, 1995; Kestin, 1980).

Available Energy. See exergy

Available Work. See exergy

Availability. See exergy

Base Enthalpy. The enthalpy of a compound (at T_o and P_o) evaluated relative to the stable components of the reference environment (i.e., relative to the dead state).

Chemical Exergy. The maximum work obtainable from a substance when it is brought from the environmental state to the dead state by means of processes involving interaction only with the environment.

Dead State. The state of a system when it is in thermal, mechanical, and chemical equilibrium with a conceptual reference environment (having intensive properties of pressure P_o, temperature T_o, and chemical potential μ_{ioo} for each of the reference substances in their respective dead states).

Degradation of Energy. The loss of work potential of a system which occurs during an irreversible process.

Dissipation. See exergy consumption.

Effectiveness. See second-law efficiency.

Energy Analysis. A general name for any technique for analyzing processes based solely on the first law of thermodynamics. Also known as *first-law analysis*.

Energy Efficiency. An efficiency determined using ratios of energy. Also known as *thermal efficiency or first-law efficiency*.

Energy Grade Function. The ratio of exergy to energy for a stream or system.

Entropy Creation. See entropy production.

Entropy Generation. See entropy production.

Entropy Production. A quantity equal to the entropy increase of an isolated system (associated with a process) consisting of all systems involved in the process. Also known as *entropy creation or entropy generation*.

Environment. See reference environment.

Environmental State. The state of a system when it is in thermal and mechanical equilibrium with the reference environment, that is, at pressure P_o and temperature T_o of the reference environment.

Essergy. See exergy. Derived from essence of energy.

Exergetic Temperature Factor. A dimensionless function of the temperature T and environmental temperature T_o given by $(1 - T_o/T)$.

Exergy. (1) A general term for the maximum work potential of a system, stream of matter or a heat interaction in relation to the reference environment as the datum state. Also known as available energy, availability, essergy, technical work capacity, usable energy, utilizable energy, work capability, work potential, or xergy. (2) The unqualified term *exergy* or *exergy flow* is the maximum amount of shaft work obtainable when a steady stream of matter is brought from its initial state to the dead state by means of processes involving interactions only with the reference environment.

Exergy Analysis. An analysis technique in which process performance is assessed by examining exergy balances. A type of second-law analysis.

Exergy Consumption. The exergy consumed or destroyed during a process due to irreversibilities within the system boundaries. Also known as *dissipation*, *irreversibility*, or *lost work*.

Exergy Efficiency. A second-law efficiency determined using ratios of exergy.

External Irreversibility. The portion of the total irreversibility for a system and its surroundings occurring outside the system boundary.

First-Law Analysis. See energy analysis.

First-Law Efficiency. See energy efficiency.

Ground State. See reference state.

Internal Irreversibility. The portion of the total irreversibility for a system and its surroundings occurring within the system boundary.

Irreversibility. (1) An effect, making a process nonideal or irreversible. (2) See exergy consumption.

Negentropy. A quantity defined such that the negentropy consumption during a process is equal to the negative of the entropy creation. Its value is not defined, but is a measure of order.

Nonflow Exergy. The exergy of a closed system, that is, the maximum net usable work obtainable when the system under consideration is brought from its initial state to the dead state by means of processes involving interactions only with the environment.

Physical Exergy. The maximum amount of shaft work obtainable from a substance when it is brought from its initial state to the environmental state by means of physical processes involving interaction only with the environment. Also known as *thermomechanical exergy*.

Rational Efficiency. A measure of performance for a device given by the ratio of the exergy associated with all outputs to the exergy associated with all inputs.

Reference Environment. An idealization of the natural environment which is characterized by a perfect state of equilibrium, that is, absence of any gradients or differences involving pressure, temperature, chemical potential, kinetic energy, and potential energy. The environment constitutes a natural reference medium with respect to which the exergy of different systems is evaluated.

Reference State. A state with respect to which values of exergy are evaluated. Several reference states are used, including environmental state, dead state, standard environmental state, and standard dead state. Also known as ***ground state*** .

Reference Substance. A substance with reference to which the chemical exergy of a chemical element is calculated. Reference substances are often selected to be common, valueless environmental substances of low chemical potential.

Resource. A material found in nature or created artificially in a state of disequilibrium with the environment.

Restricted Equilibrium. See thermomechanical equilibrium.

Second-Law Analysis. A general name for any technique for analyzing process performance based solely or partly on the second law of thermodynamics. Abbreviated as SLA.

Second-Law Efficiency. A general name for any efficiency based on a second-law analysis (e.g., exergy efficiency, effectiveness, utilization factor, rational efficiency, task efficiency). Often loosely applied to specific second-law efficiency definitions.

Task Efficiency. See second-law efficiency.

Technical Work Capacity. exergy.

Thermal Efficiency. See energy efficiency.

Thermal Exergy. The exergy associated with a heat interaction, that is, the maximum amount of shaft work obtainable from a given heat interaction using the environment as a thermal energy reservoir.

Thermomechanical Exergy. See physical exergy.

Thermomechanical Equilibrium. Thermal and mechanical equilibrium.

Unrestricted Equilibrium. Complete (thermal, mechanical, and chemical) equilibrium.

Usable and Useful Energy. See exergy.

Utilizable Energy. See exergy.

Utilization Factor. See second-law efficiency.

Work Capability. See exergy.

Work Potential. See exergy.

Xergy. See exergy.